National Library of Canada
Collections Development Branch

Canadian Theses on
Microfiche Service

Bibliothèque nationale du Canada
Direction du développement des collections

Service des thèses canadiennes
sur microfiche

NOTICE

The quality of this microfiche is heavily dependent upon the quality of the original thesis submitted for microfilming. Every effort has been made to ensure the highest quality of reproduction possible.

If pages are missing, contact the university which granted the degree.

Some pages may have indistinct print especially if the original pages were typed with a poor typewriter ribbon or if the university sent us a poor photocopy.

Previously copyrighted materials (journal articles, published tests, etc.) are not filmed.

Reproduction in full or in part of this film is governed by the Canadian Copyright Act, R.S.C. 1970, c. C-30. Please read the authorization forms which accompany this thesis.

THIS DISSERTATION
HAS BEEN MICROFILMED
EXACTLY AS RECEIVED

AVIS

La qualité de cette microfiche dépend grandement de la qualité de la thèse soumise au microfilmage. Nous avons tout fait pour assurer une qualité supérieure de reproduction.

S'il manque des pages, veuillez communiquer avec l'université qui a conféré le grade.

La qualité d'impression de certaines pages peut laisser à désirer, surtout si les pages originales ont été dactylographiées à l'aide d'un ruban usé ou si l'université nous a fait parvenir une photocopie de mauvaise qualité.

Les documents qui font déjà l'objet d'un droit d'auteur (articles de revue, examens publiés, etc.) ne sont pas microfilmés.

La reproduction, même partielle, de ce microfilm est soumise à la Loi canadienne sur le droit d'auteur, SRC 1970, c. C-30. Veuillez prendre connaissance des formules d'autorisation qui accompagnent cette thèse.

LA THÈSE A ÉTÉ
MICROFILMÉE TELLE QUE
NOUS L'AVONS REÇUE

Ottawa, Canada
K1A 0N4

NL-339 (Rev. 8/80)

PARTIAL-RESPONSE TRANSMISSION SYSTEMS

by

Muya Wachira

Thesis submitted to the School of Graduate Studies,
University of Ottawa, in partial fulfilment of
the requirements for the degree of
Master of Applied Science

Department of Electrical Engineering
University of Ottawa
Ottawa, Ontario
February, 1979

© Muya Wachira, Ottawa, Canada, 1979.

ABSTRACT

After a description of the concepts of partial-response signalling (PRS) with a special emphasis on Class I and IV, the autocorrelation function of a three-level Class I PRS system is derived. From this the power spectral density is obtained. This derivation presents an alternative way of finding the spectrum to the existing one.

The design and implementation of a three-level partial-response signalling system is presented. A practical transmission system operates in an interference environment, but the interference problem for PRS has not been well studied in the available literature. The probability of error performance, as a function of signal-to-noise (interference) ratio in an additive white gaussian noise and various interference environments, is calculated and measured. The performance is first evaluated in the case of either sinusoidal interference alone or square-wave interference alone corrupting the desired signal. An expression, in the form of an integral, giving the performance of the system when the desired signal is corrupted by both gaussian noise and sinusoidal interference is derived and the experimental results reported. The effect of more than one interferer is also considered.

After a brief review of quadrature partial-response signalling (QPRS) and eight-phase shift keying (8-ϕPSK), a succinct comparison of these two methods is made. It appears that in linear applications, QPRS might be more cost effective, but its performance is more degraded if bandlimiting precedes a saturated-mode travelling-wave tube TWT in the RF amplifier. A number of manufacturers have developed digital radio systems using these two techniques. The major characteristics of these systems are presented in two tables.

RESUME

Après une description des concepts de la signalisation à réponse partielle (SRP), soulignant la Classe I et la Classe IV, la fonction d'autocorrélation d'un système SRP de la Classe I utilisant un signal de trois niveau est dérivée. A partir de cette fonction, la densité spectrale de la puissance est obtenue. Cette dérivation représente une méthode alternative d'obtenir le spectre d'un signal à réponse partielle.

L'élaboration et la mise en oeuvre d'un système de signalisation à réponse partielle de trois niveaux sont présentées. Un système pratique de transmission doit pouvoir fonctionner dans un environnement de brouillage, mais cependant le problème du brouillage relié aux signaux SRP n'a pas été étudié en détail comme nous le révèle la littérature courante sur ce sujet. Ainsi, la probabilité d'erreur en fonction du rapport signal-bruit (signal-brouillage) est calculée et mesurée en relation à divers environnements de brouillage et de bruit gaussien additif. La performance est tout d'abord évaluée dans le cas de simple brouillage sinusoidal ou de brouillage d'onde carrée qui perturbe le signal désiré. Une expression, sous forme d'une intégrale, donnant la performance du système quand le signal désiré est perturbé par du bruit gaussien aussi que du brouillage sinusoidal, est dérivée est les résultants mesurés sont rapportés. L'effet de plus d'une source de brouillage est également considéré.

Suivant une brève revue de la signalisation à réponse partielle en quadrature (SRPQ) et de la signalisation octovalente à phase manipulée

(SOPM), une comparaison concise de ces deux méthodes est alors présentée. En relation aux applications linéaires, il s'ensuit que la SRPQ soit plus économique mais cependant, sa performance subit le plus de dégradation si le filtrage de bande précède un tube à ondes progressives saturé dans un amplificateur à fréquence radio. Un certain nombre de compagnies manufacturières ont développé des systèmes radio de type numérique utilisant l'une ou l'autre de ces deux techniques. Les caractéristiques principales de ces systèmes sont présentées sous forme de deux tableaux.

ACKNOWLEDGEMENTS

The author would like to extend his sincere gratitude to the many people who helped him directly or indirectly, technically or otherwise, in making this work a success.

Thanks are due to his supervisor, Professor Willem Steenaart, for his useful suggestions, encouragement, and understanding during the entire programme.

No thanks can express the author's indebtedness to his thesis supervisor, Dr. Kamilo Feher, for his ever present counselling, numerous constructive criticisms, and for indefatigably motivating him (despite threats to his neck) throughout the course of the research.

The invaluable help of Mr. Rawlee Scott with some of the hardware, and the useful discussions with Mr John Huang of Spar Technology Limited are gratefully acknowledged.

Perhaps the most important contribution was by the other graduate students (especially Mr. André Brind'Amour) who wholeheartedly stood by him and created an ambiance conducive to studying. Their help, comments, criticisms, arguments, quarrels, and discussions shall be long remembered.

Finally, since it appears to be customary to thank one's spouse, girlfriend etc., the author, not wishing to

be an exception, would like to thank his future wife for not meeting him while this work was in progress, thus maintaining interference below the acceptable level.

TABLE OF CONTENTS

	Page
ABSTRACT	ii
RESUME	iii
ACKNOWLEDGEMENTS	v
TABLE OF CONTENTS	vi
LIST OF FIGURES	viii
LIST OF TABLES	xii
LIST OF SYMBOLS AND ABBREVIATIONS	xiii
CHAPTER ONE	
INTRODUCTION	1
CHAPTER TWO	
PARTIAL-RESPONSE SIGNALLING IN BASEBAND	9
2.1 Introduction	9
2.2 The impulse response approach	12
2.2.1 Binary and Multilevel PAM systems	12
2.2.2 The PRS concept	17
2.2.3 3-level Class I PRS (the duobinary) scheme	18
2.2.4 Class IV PRS scheme	26
2.2.5 Generalisation of PRS	33
2.3 Digital implementation	39
2.3.1 Class I	39
2.3.2 Class IV	48
2.4 PRS systems with a pseudo-random binary sequence (PRBS) input	54
2.4.1 PRBS sequences	54
2.4.2 The autocorrelation and p.s.d. of a PRS sequence formed from a PRBS sequence	56
CHAPTER THREE	
QUADRATURE PARTIAL RESPONSE SIGNALLING	69
3.1 Modulation systems using PRS	69
3.2 The QPRS method	70
3.3 Principles of eight-phase modulation	76
3.4 Comparison of 8-ϕ PSK and QPRS systems	80
CHAPTER FOUR	
PERFORMANCE OF PRS SYSTEMS	86
4.1 Introduction	86
4.2 Performance in an AWGN environment	87
4.3 Interference in PRS systems	104
4.3.1 Square-wave interference	105
4.3.2 Sinusoidal interference	109
4.3.2 Combined noise and interference	114

Page

CHAPTER FIVE
AN EXPERIMENTAL PRS SYSTEM 117
5.1 The encoder 117
5.2 The decoder 122
5.3 The QPRS system 125
5.4 Measurement techniques and test results 131

CHAPTER SIX
CONCLUSION 151

APPENDIX I 154
APPENDIX II 158
APPENDIX III 160
APPENDIX IV 162

REFERENCES 164

LIST OF FIGURES

Figure		Page
1-1	A block diagram of a digital communication system.	2
1-2	(a) A unipolar nonreturn-to-zero signal. (b) A polar return-to-zero signal.	3
2-1	(a) Ideal Nyquist filter transfer function. (b) Phase function of an ideal Nyquist filter. (c) Impulse response of the Nyquist filter-Nyquist pulse.	13
2-2	Sinusoidal roll-off spectral shaping. (a) Transfer functions. (b) Impulse responses.	17
2-3	Transfer function of a 3-level Class I PRS scheme transmitting at f_s symbols per second.	19
2-4	The impulse response of a 3-level Class I PRS filter.	21
2-5	Signalling with duobinary pulses.	22
2-6	Transfer function of a Class IV PRS scheme transmitting f_s symbols per second.	26
2-7	The impulse response and its components, for modified duobinary.	29
2-8	Signalling with modified duobinary pulses.	30
2-9	Generalised PRS signal generation and decoding	35
2-10	A Class I PRS precoder.	40
2-11	A general Class I correlative encoder.	41
2-12	Duobinary encoder (with precoder).	45
2-13	The duobinary conversion.	47
2-14	Experimental eye diagram for duobinary.	48
2-15	Modified duobinary encoder (with a precoder).	49
2-16	Conversion of a binary waveform into a modified duobinary waveform.	52
2-17	Experimental eye diagram for modified duobinary signal.	53

		Page
2-18.	A 15-stage maximal length shift register.	55
2-19	Graphic evaluation of $R(\tau)$ for $\tau \varepsilon (0, T)$.	59
2-20	Evaluation of $R(\tau)$ for $\tau \varepsilon (T, 2T)$.	60
2-21	Graphic evaluation of $R(\tau)$ for $\tau \varepsilon ((n-1)T, nT)$, $3 \leq n \leq 13$.	61
2-22	Autocorrelation function of a duobinary sequence. (a) with a PRBS input. (b) with a random binary input.	63
2-23	Differentiation of $R(\tau)$ to get impulses.	65
2-24	Autocorrelation functions and power spectra for a duobinary system with (a) PRBS input of length 15 (b) random input for a data rate of 64 kb/s	68
3-1	A simplified block diagram of a QPRS modulator.	71
3-2	RF signal state diagram for QPRS.	72
3-3	A simplified block diagram of a QPRS demodulator.	73
3-4	Bit error rate characteristics of various modulation techniques.	75
3-5	8-phase PSK (a) generation (b) phase positions and their bit designations.	77
3-6	Coherent detection of an 8- ϕsignal.	78
4-1	Polybinary signalling levels.	88
4-2	Error zones when kth level is transmitted.	90
4-3	Error zones for when kth level is transmitted for M-1 even. (a) k is even. (b) k is odd.	91
4-4	Error zones for when the kth level is transmitted, for M-1 odd. (a) k is even. (b) k is odd.	95
4-5	Probability of error versus signal-to-noise ratio in dB.	102

		Page
4-6	(a) Time-domain representation of a random binary pattern. (b) P.d.f. of an interfering square wave or random binary binary pattern.	106
4-7	Example of a Class I PRS signal.	107
4-8	P(e) versus SIR for square-wave interference.	109
4-9	(a) Time-domain representation of a sinusoid. (b) P.d.f. of a sinusoid.	110
5-1	Combination of precoding and correlative level coding to save one delay unit.	118
5-2	Circuit diagram of a duobinary encoder.	
5-3	The duobinary waveform resulting from a binary NRZ input.	120
5-4	Circuit diagram of a modified duobinary encoder.	121
5-5	Time-domain waveform for a Class IV PRS encoder.	121
5-6	Input/output transfer characteristics for (a) duobinary decoder (b) modified duobinary decoder.	122
5-7	A three-level PRS decoder (Class I or Class IV).	123
5-8	Comparator input/output transfer characteristics.	124
5-9	Circuit diagram of a 3-level Class I decoder.	126
5-10	Serial-to-parallel converter with timing diagram.	127
5-11	90° phase-shifting network.	128
5-12	The circuit diagram of the QPRS modulator.	129
5-13	A circuit for a parallel-to-serial converter and its timing diagram.	130
5-14	A circuit diagram of the whole demodulator.	132
5-15	Bench equipment for the system performance evaluation.	134
5-16	(a) Eye diagram for a duobinary system. (b) Eye diagram for a modified duobinary system.	135
5-17	Power spectral density for a binary NRZ signal.	136

		Page
5-18	Power spectral density for a 3-level Class I PRS signal (unfiltered).	136
5-19	Power spectral density for a filtered 3-level Class I PRS signal.	137
5-20	Power spectral density for a Class IV PRS signal.	137
5-21	Laboratory test set-up for the measurement of the probability of error.	139
5-22	P(e) versus SNR in an AWGN environment for a 3-level PRS system.	141
5-23	P(e) versus SIR in a square-wave interference environment only for a 3-level PRS system.	142
5-24	P(e) performance in a sinusoidal interference only environment for an NRZ signal.	144
5-25	P(e) performance of a PRS signal in a sinusoidal interference only environment.	145
5-26	Performance of a PRS system in the presence of both sinusoidal interference (30 kHz) and gaussian noise, for various interference levels.	147
5-27	The effect of two interfering sinusoidals on the performance of a PRS system when AWGN is also present.	148
5-28	Comparison of square-wave and sinusoidal interferences in the presence of AWGN.	150

LIST OF TABLES

Table		Page
I	Levels of Class IV PRS corresponding to pairs of bits	30
II	System parameters for low- and medium-capacity radios	84
III	System parameter for high-capacity radios	85

LIST OF SYMBOLS AND ABBREVIATIONS

$\{a_n\}$	Binary sequence
A	Amplitude
AWGN	Additive white gaussian noise
$\{b_n\}$	Precoded (binary) sequence
b/s	Bits per second
b/s/Hz	Bits per second per Hertz
BER	Bit error rate
B_n	Noise bandwidth
BNR	Bell-Northern Research
CCIR	Comité Consultatif International de Radio
C/N	Carrier power-to-noise power ratio
CNR	Carrier-to-noise ratio in dB
dB	decibel
dBm	decibel relative to one milliwatt
DOC	Department of Communications
e	Euler's number - 2.71828
E_b/N_0	Energy per bit-to-noise density ratio
erf(x)	Error function $\frac{2}{\sqrt{\pi}} \int_0^x e^{-t^2} dt \leq 1$
erfc(x)	Complementary error function $\frac{2}{\sqrt{\pi}} \int_x^\infty e^{-t^2} dt \leq 2$

f	Frequency in Hz
$\mathcal{F}$	Fourier transform
$\mathcal{F}^{-1}$	Inverse Fourier transform
f_{br}	Bit-rate frequency
FCC	Federal Communications Commission
f_s	Signalling frequency
$h(t)$	Impulse response
$H(f)$	Network transfer function
Hz	Hertz
i	Integer
I	Interference power
IF	Intermediate frequency
ISI	Intersymbol interference
ITU	International Telecommunications Union
j	$\sqrt{-1}$ Imaginary number
k	Boltzmann constant (= - 228.6 dBW/Hz-K)
	Summing integer
K	Kelvin
LHS	Left-hand side
ln(x)	Natural logarithm of x
m	Integer

M	$= 2^n$ number of phases in an M-ary PSK signal
MLD	Maximum likelihood detection
MSK	Minimum (frequency) shift keying
MT	Matched Transmission
n	Number of bits per symbol
N	$= 2^n - 1$ period of an n-stage maximal length shift register sequence
N	Noise power
NEC	Nippon Electric Company
N_{rms}	Rms voltage of noise
p	a priori probability (e.g. probability of a mark)
PAM	Pulse amplitude modulation
PCM	Pulse code modulation
pdf	Probability density function
P(e)	Probability of error
$\{P_n\}$	Partial-response signalling sequence
PRBS	Pseudo-random binary sequence
PRS	Partial-response signalling
P/S	Parallel-to-serial
p(x)	pdf of the variable x
Q(x)	Area under the gaussian curve $\frac{1}{\sqrt{2\pi}}\int_0^x e^{-u^2} du \leq \frac{1}{2}$

QAM	Quadrature amplitude modulation
QPRS	Quadrature partial-response signalling
QPSK	Quadrature phase-shift keying
R_b	Bit rate
RF	Radio frequency
RHS	Right-hand side
$R(\tau)$	Autocorrelation function
RZ	Return-to-zero
S	Signal power
$S_a(x)$	Sampling function = $\frac{\sin x}{x}$
S/I	Signal-to-interference power ratio
SIR	Signal-to-interference ratio in dB
sin c(x)	= $\frac{\sin \pi x}{\pi x}$
S/N	Signal-to-noise power ratio
SNR	Signal-to-noise ratio in dB
S/P	Serial-to-parallel
S_{rms}	Rms voltage of the signal
SSB	Single-sideband
STR	Symbol timing recovery
s(t)	Input signal
t	Time variable
T	Symbol interval

	- Time delay
T1	Noth American standard rate of 1.544 Mb/s
TTL	Transistor-transistor logic
TWT	Travelling wave tube
$u(t)$	Heaviside unit step function
V	Peak value of a signal
α	Fractional excess Nyquist bandwidth
$\delta(t)$	Dirac delta function or unit impulse function
σ	Standard deviation
	- Rms value of noise voltage
ω	Angular frequency in radians, $= 2\pi f$
ω_c	Carrier (angular) frequency
π	Ratio of the circumference of a circle to its diameter, $\approx 22/7$.
$\oplus$	Modulo-2 sum
$\sum_i$	Summation over i

CHAPTER ONE

INTRODUCTION

The object of a transmission system is to relay information from one point to another as fast and as accurately as possible. This would be but a small feat if only one such system were to exist (hence infinite bandwidth), as much power as desired could be employed, and if extraneous signals such as noise and interference were not present. To the chagrin of the communications engineer however, this is not the case. Several methods have been devised to make transmission of information in such non-ideal conditions feasible. These methods include multiplexing, modulation techniques, signal processing such as coding, and various detection schemes.

The advantages of digital communications are well known [1, 2, 3]. The basic constituents of a digital communication system are shown in Fig. 1-1. The data source produces a sequence of digits which represents the information to be transmitted. In binary data communication these (binary) digits are termed "bits". The transmitter transforms the input digits into electrical waveforms suitable for transmission through the channel. The channel is the physical medium which interconnects the transmitter and the receiver. It may consist of a pair of wires as in a telephone connexion, a coaxial cable, a radio link, a microwave system, or a satellite link. In passing through the channel, the transmitted signal will be attenuated, distorted, and corrupted by various types of noise. The receiver attempts to recover the transmitted waveform from the signal coming

from the channel. However, due to noise and distortion, the receiver sometimes makes errors in deciding which data sequences were sent. To minimise errors, the waveforms must be chosen so as not to be confused by the receiver.

In synchronous communication, each digit has a time slot of T-seconds allocated for its transmission. For binary input, a "MARK" (also called a "one") is usually represented by a square pulse of amplitude A and duration t_b-seconds whereas a "SPACE" (or a "zero") is represented by the absence of a pulse. Such a signal is called a

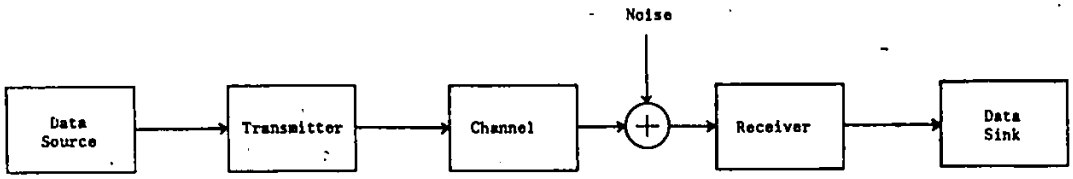

Figure 1-1. A block diagram of a digital communication system.

"unipolar" signal. If the duration of the pulse (t_b) is equal to the bit interval, T-sec, then the signal is said to be "nonreturn-to-zero" (NRZ), otherwise it is return-to-zero (RZ). An example of a unipolar nonreturn-to-zero signal appears in Fig. 1-2(a). It is often desirable to have the bits represented by square pulses of opposite polarities -

a 1 by a positive pulse and a 0 by a negative pulse - as shown in Fig. 1-2(b). RZ pulses have a broader spectrum than NRZ pulses; thus for identical bit rates, they require more bandwidth [4]. For this reason, they are seldom used in data transmission. For the same peak-to-peak value of the signal, it is not difficult to see that the unipolar signal has twice as much power as (3dB more power than) the polar signal. Polar signals are therefore more frequently encountered, in transmission systems, than unipolar ones.

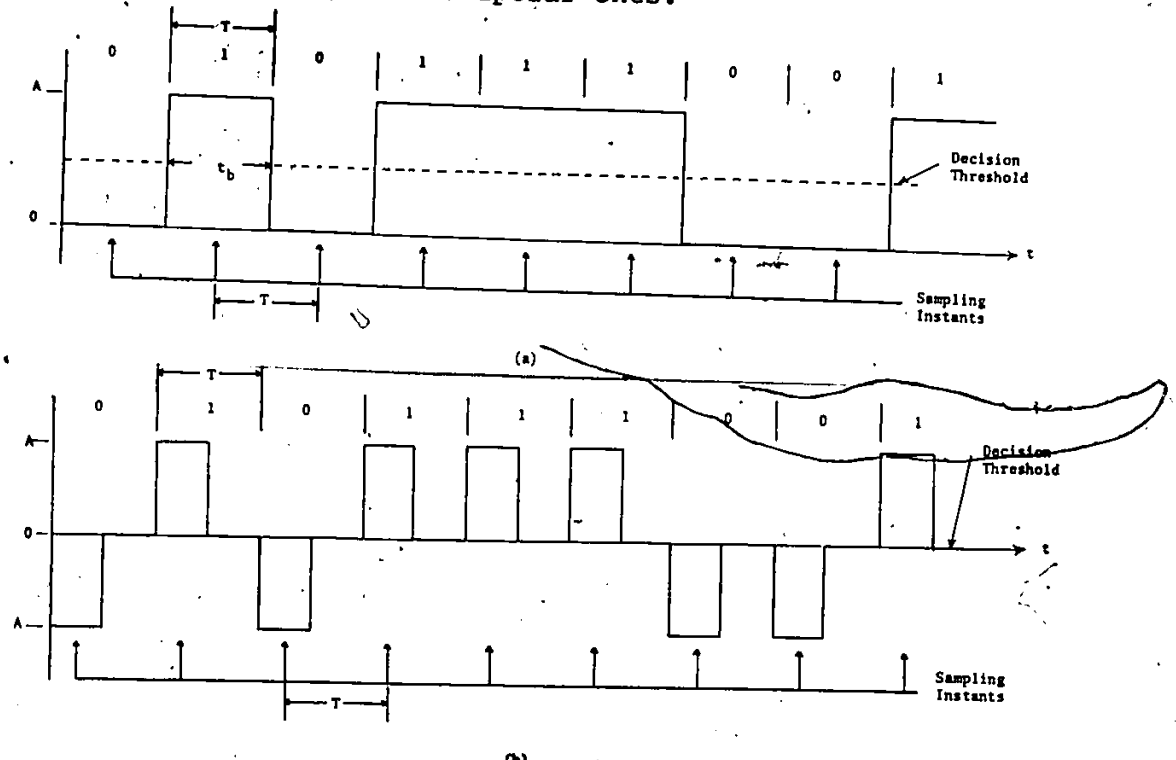

Figure 1-2. (a) A unipolar nonreturn-to-zero signal. (b) A polar return-to-zero signal.

The receiver consists essentially of a device which samples the incoming signal at regularly spaced intervals of T-sec, followed by a

threshold comparator (also called a slicer) with the decision threshold suitably chosen. In most applications the threshold is set half way between the MARK and SPACE levels.

Sometimes the transmitter may assign waveforms, not to single bits but to groups of bits. Each waveform assigned to a group of bits is usually called a "symbol". Signalling speed is then expressed in symbols per second or "bauds". If each symbol represents n bits say, then the baud rate must be multiplied by n to get the data rate in bits per second (b/s). If the format of symbols is binary then bits per second and bauds are equivalent. For synchronous communication with a symbol spacing of T_s seconds, the symbol rate is given by

$$f_s = 1/T_s \qquad (1\text{-}1)$$

where f_s is the symbol rate in bauds.

In the old days when users of the spectrum were few in number, bandwidth used to be almost free - "yours for the taking" - and power used to be precious. Today power is more easily produced but bandwidth is becoming more precious as the spectrum becomes more congested. This congestion is due to the increased number of users each with more information to transmit. Also there has been a recent tendency to transmit in a digital manner. (Digital systems require more bandwidth than analogue ones unless sophisticated modulation and signal processing techniques are used. However, this makes the system very complex and prohibitively expensive.) Spectrum economy in data

transmission is hence becoming mandatory, and spectrally efficient techniques are called for. Such techniques must maximise the transmitted data rate in a given bandwidth. A term that is frequently encountered in connexion with such techniques is the "bandwidth (spectral) efficiency", which is defined as the ratio of the data rate to the bandwidth, and is expressed in bits per second per hertz (b/s/Hz). By specifying the limits of the transmitted out-of-band interference, regulatory bodies, such as FCC[1], DOC[2], and CCIR[3], effectively specify the minimum bandwidth efficiency of digital systems. It is also desirable to achieve the bandwidth efficiency needed with as low average signal power as possible. This is to say that in a noisy environment the bandwidth efficiency should be attained with the minimum practical average signal-to-noise ratio (S/N) possible. (Energy per bit-to-noise density ratio - E_b/N_0 - is sometimes used instead of S/N.)

Whereas the performance of an analogue system is specified mainly by the signal-to-noise ratio, for digital systems, performance is measured by the error rate. For this purpose, symbol error rate, bit error rate (BER), and probability of error are often used. Bit (symbol) error rate is defined as the ratio of the number (N_e) of bits (symbols) in error in a time interval t_e to the total number (N_{te}) of bits (symbols) transmitted in that time interval, i.e.

---

1 Federal Communications Commission (USA)
2 Department of Communication (Canada)
3 Comité Consultatif International de Radio (Organised under the auspices of International Telecommunications Union, ITU.)

$$BER = N_e/N_{te} = N_e/R_b t_e \qquad (1\text{-}2)$$

where R_b is the bit (symbol) rate of the source.
The probability of bit (symbol) error, P(e), is the probability that any bit is incorrectly received. For a large number of transmitted bits, the BER approximates P(e), or P(e) is the limit of BER as N_{te} approaches infinity. Commercially available BER analysers usually use a minimum N_e of about 100.

A good digital system is thus one that is bandwidth efficient, i.e. it transmits more b/s/Hz in the available bandwidth, and achieves a low probability of error with as low an E_b/N_0 ratio as possible, in an interference environment. Other factors, such as hardware simplicity, cost, reliability, and maintainability, must also be taken into account.

Partial-response signalling (PRS) or correlative level coding is a method that combines relatively good bandwidth efficiency with low hardware complexity. Partial response is a scheme in which the channel response to a single symbol extends, in a known fashion, over more than one symbol interval; hence the partial-response channel is a channel with finite memory. In simpler terms, the basic idea behind PRS (explained more fully in the next chapter) is the correlation between adjacent bits in a bit stream, hence the name correlative level coding [5]. It is this bit dependency that achieves spectral reshaping. It is possible to redistribute the energy such that very little is located at

low frequencies, and to introduce spectral nulls at different points. An added advantage of correlative level coding schemes is their inherent error-detecting capability.

Historically, Lender was the first to introduce the correlative coding scheme which he called the duobinary scheme for data transmission [5] and later extended it to the polybinary [6]. Kretzmer introduced the term partial-response signalling and categorised PRS into several classes [7, 8]. Gerrish and Howson [9] discussed precoding for PRS systems with multilevel inputs. Smith [10] proposed an improvement of the duobinary performance in the presence of gaussian noise by using null-zone detection, which makes use of the inherent redundancy of PRS. Kobayashi and Tang [11] extended this to a more general soft decision scheme called the ambiguity-zone detection. By noting an analogy between correlative level coding and convolutional coding, Kobayashi [12] and Forney [13] have shown the applicability of the maximum-likelihood decoding to PRS, thereby improving the performance considerably. Harashima and Miyakawa [14] introduced the matched-transmission (MT) technique and showed that PRS is a special case of MT. Kabal and Pasupathy [15] presented a unified study of PRS and compared several PRS schemes.

Because of its bandwidth efficiency PRS is being used where high bit efficiencies are required. It not only finds application in high-speed data transmission but also in magnetic recording systems [16].

PRS promises to become a widely-used method be it in transmission of data over private wires or switched telephone circuits, short- and long-haul voice communications, magnetic recording or high-speed data

transmission. Work on PRS has been reported in several countries including the USA, Japan, Canada, Italy, the USSR, the United Kingdom, Germany, Hungary and Australia to mention a few.

This thesis covers certain details of PRS that are not well documented in the literature or that can only be found in widely scattered sources. It reports on a practical implementation of a baseband partial-response signalling system and the evaluation of its performance. Also included is a guideline to a design of a quadrature partial-response signalling (QPRS) modem. The modem is intended as an improvement of the present QPSK systems operating at 1.544 Mb/s, by increasing the bit rate to 3 Mb/s using the same bandwidth. In Chapter Two, the concept of partial-response signalling is described fully. In Chapter Three, the quadrature partial-response modulation method is presented and compared with eight-phase shift keying (8-ϕPSK) modulation technique. Several digital microwave systems employing either of these two methods are presented in two tables. The interference problem has not been well analysed in the available literature. An analysis of the performance of a PRS system in an additive white gaussian noise (AWGN) environment, a square wave interference environment, a sinusoidal interference environment, and finally an environment with both gaussian noise and sinusoidal interference is attempted in Chapter Four. The hardware implementation of a baseband PRS system and a paper design of a QPRS system are presented in Chapter Five. Measurement techniques and the results obtained are also presented. Finally in Chapter Six future research points and possible extensions of this work are suggested.

CHAPTER TWO

PARTIAL-RESPONSE SIGNALLING IN BASEBAND

2.1 Introduction

Partial-response signalling is a method of signalling which uses a controlled amount of intersymbol interference to achieve a higher bandwidth efficiency. In binary data transmission, three-level PRS attains (or even slightly exceeds) the Nyquist signalling rate of 2 b/s/Hz of baseband bandwidth by allowing intersymbol interference to create three levels that must be detected at the receiver instead of the two original levels. PRS thus has the same capacity as a binary system using a brickwall (rectangular) filter, but with realisable (gradually rolling-off) and perturbation-tolerant filters. The levels in a PRS system are correlated and it is this correlation property that offers efficient bandwidth compression for a given bit rate or conversely higher bit rates for a given bandwidth. Furthermore, the correlation properties facilitate transmission error detection at the receiver without the necessity of introducing redundant bits in the original data stream [5].

Before the advent of partial-response signalling 15 years ago, the only way to achieve higher bit rates than binary was memoryless multilevel pulse amplitude modulation (PAM) signalling. In this type of signalling the symbol rate is reduced by using more than two levels per symbol. M levels per symbol are used (M-ary signals), reducing the symbol rate by a factor of n relative to binary, where

$$n = \log_2 M \qquad (2\text{-}1)$$

Each symbol represents n bits of information and for a given bandwidth the M-ary signal has a speed of transmission n times higher than that of binary.

For any M-level signal, the increase in signal-to-noise ratio required at the receiver for the same error rate as the binary is approximately

$$20 \log_{10}(M-1)\text{dB}. \qquad (2\text{-}2)$$

Correlative level coding is now briefly compared with multilevel PAM techniques in terms of speed per unit bandwidth, error performance, and complexity of equipment. For the sake of simplicity quarternary PAM and duobinary[1] (3-level Class I) are compared. Both these techniques offer a bandwidth compression by a factor of 2 compared to binary i.e., they both have the same speed per unit bandwidth (2 b/s/Hz). However the PRS signal has three levels while the PAM signal has four levels. Hence in terms of signal-to-noise ratio penalty relative to binary (equation (2-2)), PRS has a 3.5 dB advantage over four-level PAM.

In the duobinary system each level or symbol represents one bit as

---

1 It is assumed here that practical binary and other PAM systems use an α of 1(α is defined in the next section).

opposed to 2 bits/symbol in the quarternary PAM. In other words the symbol rate of PRS is the same as the binary while that of 4-level PAM is half that of the binary. This makes PRS less tolerant to imperfections in the filter characteristics [17]. On the other hand 1 bit/symbol implies that an error in one symbol results in only one bit in error whereas the 2 bits/symbol system can result in two bits in error when one symbol is in error.

Quarternary levels are formed by pairing successive bits, but PRS levels result from addition of successive adjacent bits. Thus in 4-level PAM any level transitions may occur in two successive digit-time slots, but for PRS only transitions between adjacent signalling levels are possible. Hence, intersymbol interference (ISI) in terms of horizontal eye opening is much larger in the quarternary PAM than in 3-level PRS [18].

Whereas error detection in the duobinary is possible without introducing redundant bits, in the 4-level PAM, error detection is only possible by introducing redundant bits in the original bit stream, causing a reduction in the actual information bit rate.

Also, equipment implementation of quarternary PAM is more complex than that of 3-level PRS. The latter has comparable complexity to that of binary systems. (Equipment complexity is closely related to cost, reliability, and maintainability, therefore it is an important consideration for a commercial system.)

The most well-known classes of PRS [7] are: Class I PRS or polybinary of which duobinary is the simplest example; and Class IV or modified duobinary. Class V has been used but to a lesser extent.

These classes will be stressed throughout the rest of this chapter. PRS can be produced by passing a binary sequence through a simple digital filter as will be described in a later section. An analogue filter approximating the required filter function may also be used.

2.2 The Impulse Response Approach

The impulse response, h(t), of a channel is defined as the output response of the channel to a single impulse $\delta(t)$ (i.e., a pulse of vanishingly narrow width but of finite energy) at the input of that channel. If the channel transfer function is H(f), the impulse response is given by

$$h(t) = \int_{-\infty}^{\infty} H(f) e^{j2\pi ft} df \qquad (2-3)$$

2.2.1 Binary and Multilevel PAM Systems

The design of classical binary and multilevel PAM systems is based on the concept of intersymbol interference (ISI). This is one of the possible system impairments due to imperfect channels. Most digital receivers consist essentially of a sampling device which samples the incoming signal at regularly spaced intervals of T-seconds. Ideally the sampled amplitude should consist of a value from only one impulse response - the present one. If the response of the channel to an impulse spreads beyond its alloted time slot T, it may well be that previous and future responses have non-zero amplitudes at the sampling instant. These constitute intersymbol interference.

Classical or Nyquist-type binary or multilevel PAM systems are designed so as to eliminate ISI. Nyquist showed that to transmit

digital data at a rate of $f_s(=1/T)$ symbols per second without ISI, the minimum required bandwidth is $f_s/2$ Hz [4, 17]. This minimum bandwidth $f_s/2 = 1/2T$ Hz, where T is the symbol duration, is also known as Nyquist bandwidth. The above can be stated otherwise. The maximum possible theoretical rate that can be transmitted, without intersymbol interference, through an ideal low-pass filter having a cut-off frequency of $f_s/2(=1/2T)$Hz is $f_s(=1/T)$ symbols per second. Thus the maximum spectrum utilisation is 2 symbols/s/Hz. The transfer function of an ideal Nyquist filter together with its impulse response are shown in Fig. 2-1.

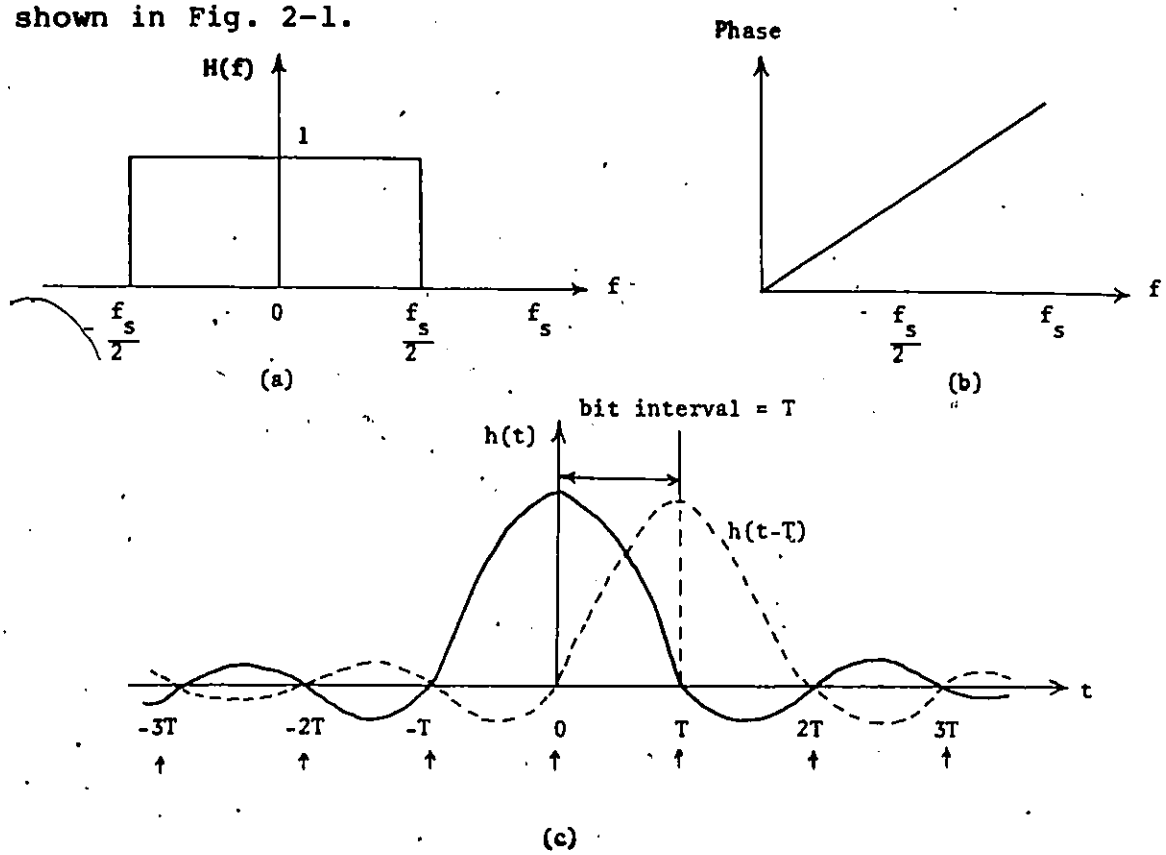

Figure 2-1. **(a) Ideal Nyquist filter transfer function.**
(b) Phase function of an ideal Nyquist filter.
(c) Impulse response of the Nyquist filter - Nyquist pulse.

The transfer function is given by

$$H(f) = \begin{cases} 1 < 0 \ , & |f| < f_s/2 \\ 0 \ , & \text{elsewhere} \end{cases} \qquad (2\text{-}4)$$

The impulse response is obtained from (2-3)

$$h(t) = \int_{\frac{-f_s}{2}}^{\frac{f_s}{2}} e^{j2\pi ft} df = f_s \frac{\sin \pi f_s t}{\pi f_s t} \qquad (2\text{-}5)$$

or

$$h(t) = \frac{1}{T} \frac{\sin \pi t/T}{\frac{\pi t}{T}}$$

Note that although h(t) spreads beyond its alloted time slot T, it passes through zero at the other sampling instants and hence the interference between successive symbols is nil.

This system has, however, no practical application. The sharp cut-off of the filter is unrealisable as it would call for infinite delay and no phase distortion. Besides, the relatively large overshoots of h(t), which fall off as 1/t, would cause excessive ISI if any deviations from the ideal situation occured, such as pulse rate, filter cut-off frequency, or timing offset in the sampler.

To accommodate more practical filters Nyquist derived the famous theorem on vestigial symmetry which assures gradual cut-off of the

low-pass characteristic but no ISI. This theorem states that if H(f) is real and has odd symmetry about the nominal cut-off frequency $f_s/2$(or 1/2T)Hz, then the corresponding impulse-response h(t) is an even time function and h(iT) = 0 for all nonzero integer values of i [4, 19]. Hence data can be transmitted at f_s(or 1/T) symbols/sec without intersymbol interference. These filters are called <u>equivalent Nyquist filters</u>. A class of equivalent Nyquist filters that is extensively used is that where H(f) has a sinusoidal roll-off centred at $f_s/2$ Hz. The transfer function is given by

$$H(f) = \begin{cases} T, & 0 \leq |f| \leq \frac{1}{2T}(1-\alpha) \\ \frac{T}{2}\left\{1-\sin\frac{\pi T}{\alpha}\left(f-\frac{1}{2T}\right)\right\}, & \frac{1}{2T}(1-\alpha) \leq |f| \leq \frac{1}{2T}(1+\alpha) \\ 0, & \text{elsewhere} \end{cases} \quad (2\text{-}6)$$

where α is the fractional bandwidth used in excess of the minimum Nyquist bandwidth, ($\alpha \in [0,1]$). $\alpha = 0$ represents the ideal Nyquist filter as given by (2-4), while $\alpha = 1$ (100% roll-off) means that the total bandwidth is twice the minimum Nyquist bandwidth.

The corresponding impulse response is easily shown to be [Appendix I]

$$h(t) = \frac{\sin \frac{\pi t}{T}}{\frac{\pi t}{T}} \frac{\cos \alpha \frac{\pi t}{T}}{1 - \frac{4\alpha^2 t^2}{T^2}} \qquad (2\text{-}7)$$

Some of the transfer functions, corresponding to several values of α, and the resulting impulse responses are shown in Fig. 2-2[17].

It will be noticed that for all values of α, h(t) attains maximum amplitude at t=0, and has zeros at regularly spaced T-second intervals, consequently no intersymbol interference at the sampling instants. The case of α = 1, variously known as "full-cosine", "raised-cosine", or "100% roll-off", has a response h(t) with additional zeros in the middle of the intervals and has little oscillation. Hence, it is not sensitive to variations in the signalling rate or offset in sampling instant, and does not need as careful phase equalisation as the other cases [17 p. 50, 4 p. 57]. However,it can only accommodate 1 symbol/s/Hz. As α decreases bandwidth efficiency increases. However, the response becomes more oscillatory and thus more sensitive to perturbations in timing. Also, phase equalisation beecomes more difficult. For practical purposes, filters with α of 0.15 to 1.0 are often used.

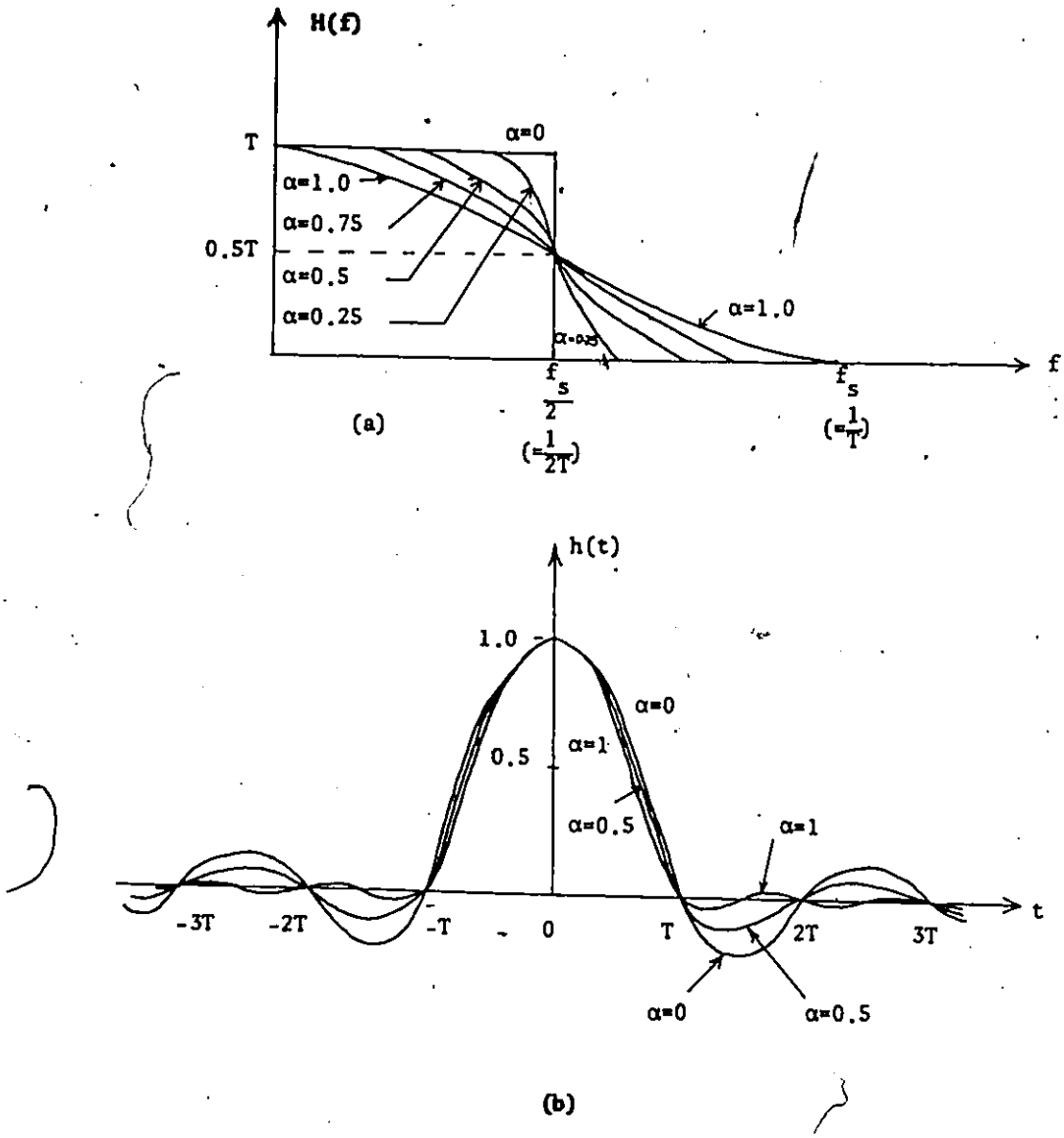

Figure 2-2. **Sinusoidal roll-off spectral shaping.**
(a) Transfer functions (only positive frequencies shown).
(b) Impulse responses.

2.2.2 The PRS Concept

It was seen that in order to have no significant ISI and without the need of very high precision in timing of the sampling instants, the baseband channel requires twice the minimum Nyquist bandwidth. Although zero-memory multilevel PAM systems may be used to increase

spectrum utilisation, this results in an increased number of levels, hence poor error performance owing to the increased sensitivity to noise. One of the salient characteristics of multilevel PAM schemes is that the levels are chosen independently. By introducing correlation between the levels, Lender [5] showed that it was possible to realise the theoretical symbol rate of f_s symbols/s in a bandwidth of $f_s/2$ Hz. That is to say that 2 symbols/s/Hz may be achieved by using physically realisable filters. These are the so-called partial-response filters. The roll-off is gradual and not discontinuous. Nyquist's criterion of elimination of ISI is violated and intersymbol interference exists between neighbouring symbols. In PRS, the impulse response is such that there is significant ISI in the samples of the received waveform at the output of the baseband channel. Reduction in bandwidth and shaping of the spectrum is realised by allowing considerable, albeit well defined, amounts of intersymbol interference between neighbouring signal elements. This intersymbol interference (since it is known) can be eliminated at the receiver using suitable techniques. For example if binary data are used at the input, the PRS filter converts the data into a three-level signal, but it is possible to reconstruct the original binary data from the three-level signal at the receiver since the amount of ISI is known.

2.2.3 3-Level Class I Partial-Response Signalling (the Duobinary) scheme

The transfer function of a duobinary channel is given by

$$H(f) = \begin{cases} 2 \cos \pi \frac{f}{f_s}, & 0 \leq |f| \leq f_s/2 \\ 0, & \text{elsewhere} \end{cases} \qquad (2\text{-}8)$$

This transfer function is depicted in Fig. 2-3.

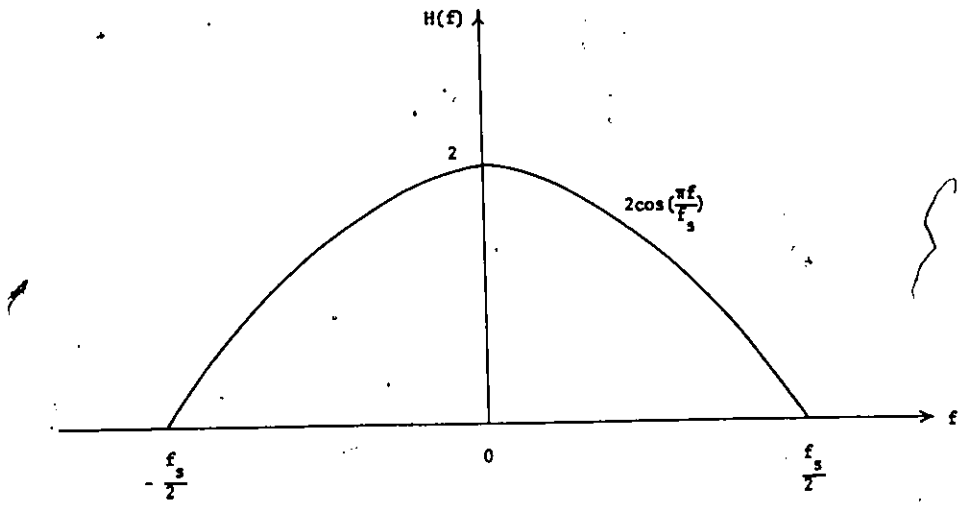

Figure 2-3. Transfer function of a 3-level Class I PRS scheme transmitting at f_s symbols per second.

The corresponding impulse response is

$$h(t) = \int_{-\infty}^{\infty} A(f)e^{j2\pi ft}df = \int_{\frac{-f_s}{2}}^{\frac{f_s}{2}} 2\cos\left(\frac{\pi f}{f_s}\right)e^{j2\pi ft}df$$

$$= \int_{\frac{-f_s}{2}}^{\frac{f_s}{2}} \left(e^{j\frac{\pi f}{f_s}} + e^{-j\frac{\pi f}{f_s}}\right)e^{j2\pi ft}df = \int_{\frac{-f_s}{2}}^{\frac{f_s}{2}} \left(e^{j\pi f(2t+\frac{1}{f_s})} + e^{j\pi f(2t-\frac{1}{f_s})}\right)df$$

$$= \left[\frac{e^{j\pi f(2t+\frac{1}{f_s})}}{j\pi(2t+\frac{1}{f_s})} + \frac{e^{j\pi f(2t-\frac{1}{f_s})}}{j\pi(2t-\frac{1}{f_s})}\right]_{\frac{-f_s}{2}}^{\frac{f_s}{2}}$$

$$= f_s\left[\frac{\sin\pi(f_s t+\frac{1}{2})}{\pi(f_s t+\frac{1}{2})} + \frac{\sin\pi(f_s t-\frac{1}{2})}{\pi(f_s t-\frac{1}{2})}\right]$$

Since $f_s = 1/T$,

$$h(t) = f_s \text{sinc } f_s(t+\tfrac{T}{2}) + f_s \text{sinc } f_s(t-\tfrac{T}{2}) \qquad (2\text{-}9)$$

where $\text{sinc}(x) = \frac{\sin\pi x}{\pi x}$

By elementary manipulations (2-9) may be simplified to

$$h(t) = \frac{4}{\pi} f_s \left[\frac{\cos \pi f_s t}{1-4f_s^2 t^2}\right] \qquad (2\text{-}10)$$

It may be observed from (2-9) that the impulse response h(t) is a superposition of two identical sinc(f_st) responses; one delayed by T seconds from the other. The impulse response and its two components, given by (2-9), are shown in Fig. 2-4.

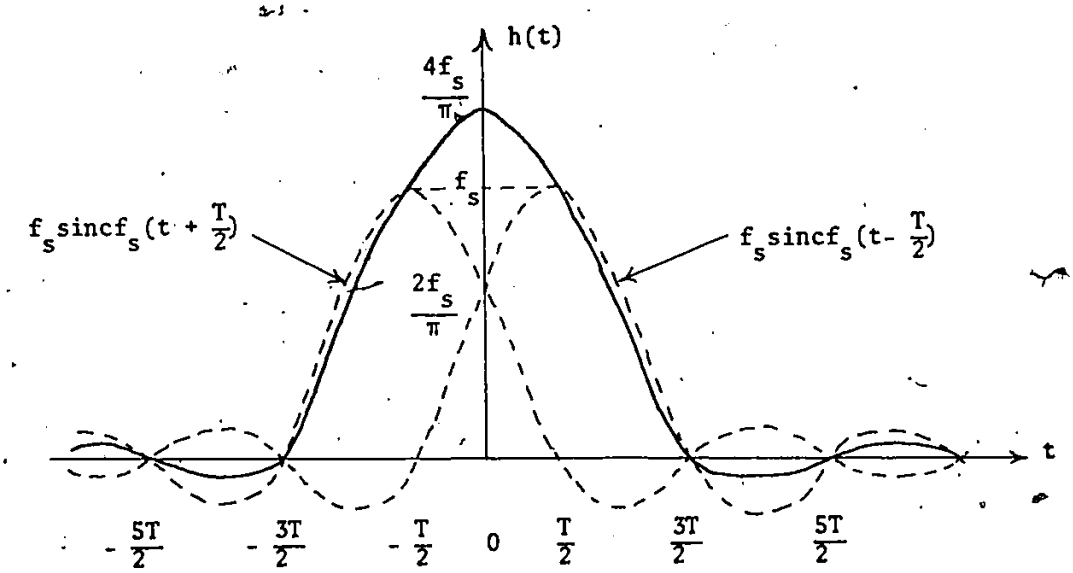

Figure 2-4. The impulse response of a 3-level Class I PRS filter.

The impulse response has zeros at $t = \pm(2n+1)T/2$, $n = 1,2,3,\ldots$ as opposed to the Nyquist one (Fig. 2-1) which had zeros at $t = \pm nT$, $n = 1,2,3,\ldots$ Also, $h(\pm T/2) = f_s$. Hence, if signalling is performed with this impulse, h(t), at rate of $f_s(=1/T)$, with the sampling instants chosen to be $\pm n\,T/2$, the resulting signal will have three possible

values at the sampling instant. If the binary '1's and '0's are represented by pulse and no pulse respectively, the three possible values will be 0, f_s, and $2f_s$ depending on the adjacent bits. [When neither pulse is present, the amplitude is zero; when only one pulse is present, the amplitude is f_s, and when both pulses are present, the amplitude becomes $2f_s$.] If binary '1's and '0's are represented by positive pulse and negative pulse respectively, then the possible values are $-f_s$, 0, and $+f_s$. The value of the envelope of the pulse train at $t = \pm T/2$ is due to the sum of two adjacent pulses only. This is shown in Fig. 2-5.

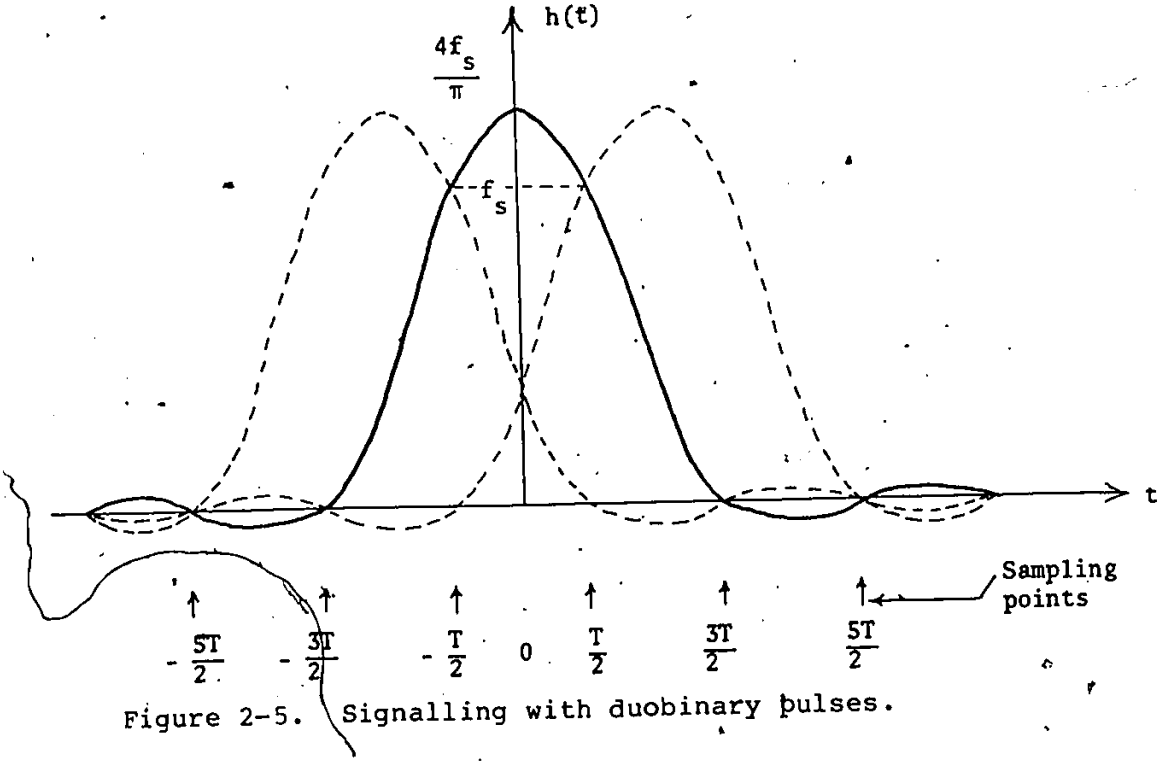

Figure 2-5. Signalling with duobinary pulses.

This can be thought of as introducing a controlled amount of ISI, which in this case, comes only from the preceding symbol. Since the

transmitted symbol depends on the present bit and the preceding bit, the channel can be considered as having 'memory'. PRS systems have also been referred to as "finite-memory systems".

Let $\{a_n\}$ represent the binary sequence, such that $a_n = 0$ or 1; and let q_n be the sampled value of the noise at the receiver. Letting p_n be the sample value of the received waveform,

$$p_n = f_s a_n + f_s a_{n-1} + q_n \qquad (2\text{-}11)$$

If at the sampling time, a_{n-1} has already been correctly detected, then the detector removes the term $f_s a_{n-1}$ from p_n:

$$g_n = p_n - f_s a_{n-1} = f_s a_n + q_n \qquad (2\text{-}12)$$

Subtracting $f_s a_{n-1}$ from p_n eliminates the intersymbol interference of the (n-1)th element that was introduced at the transmitter. Thus g_n depends only on the wanted bit a_n and the noise component; hence a_n can be recovered from g_n. This detection process is sometimes referred to as nonlinear decision feedback equalisation. One of its drawbacks is that the detection of each symbol depends on the correct detection of the preceding one. If a_{n-1} is incorrectly detected, a_n is also likely to be in error. Hence, errors tend to propagate or occur in bursts. However, in practice, for binary inputs, these error bursts have lengths of no more than three or four bits. For binary inputs, this represents an

increase in signal-to-noise ratio requirements of about 0.2-0.5 dB.

To avoid error propagation, Lender [5,6] devised a simple method known as precoding. The signal is coded in such a way that each received symbol is detected independently, without the need for compensating for the previous bit. That is, the precoder compensates the input sequence for the channel memory.

The original binary sequence $\{a_n\}$ is transformed into another sequence $\{b_n\}$ such that

$$b_n = a_n \oplus b_{n-1} \tag{2-13}$$

where $\oplus$ represents modulo-2 addition of the binary digits. Equation (2-13) could also be written as

$$a_n = b_n \oplus b_{n-1}$$

The sequence b_n is then transmitted in the channel the same way a_n was, i.e. in (2-11)

$$p_n = f_s b_n + f_s b_{n-1} + q_n$$

For simplicity assume there is no noise, such that

$$p_n = f_s(b_n + b_{n-1}) \tag{2-14}$$

Suppose that $a_n = 0$; then $b_n = b_{n-1}$ and according to (2-14), $p_n = 2f_s b_n$. If a positive pulse for '1' and a negative pulse for '0' are used, then p_n will be either $2f_s$ or $-2f_s$. If $a_n = 1$, b_n becomes the reverse of b_{n-1} and p_n is always 0. Thus it appears that the decoding rule is

$$a_n = 0 \text{ if } p_n = \pm 2f_s$$

$$a_n = 1 \text{ if } p_n = 0. \qquad (2\text{-}15)$$

If pulse/no pulse transmission was adopted for '1' and '0' respectively however, the decoding rule would be

$$a_n = 0 \text{ if } p_n = 0 \text{ or } 2f_s$$

$$a_n = 1 \text{ if } p_n = f_s \qquad (2\text{-}16)$$

It is important to note that in both cases [(2-15) and (2-16)], a '0' is always represented by the two extreme levels, while a '1' is represented by the middle level.

If noise is present, detection will be by means of two threshold comparators with decision thresholds set at f_s and $-f_s$ for (2-15) and $f_s/2$, $-f_s/2$ for (2-16). Alternatively for the case leading to (2-15) a rectifier followed by a single threshold comparator may be used.

Since no knowledge of any other sample except p_n is required, no error propagation will result. Hence, the use of a differential encoding process at the transmitter, instead of a differential decoding process at the receiver, eliminates the possibility of generating error bursts.

2.2.4 Class IV Partial-Response Signalling Scheme

For Class IV (also known as modified duobinary), the required transfer function, which is quasi band-pass, is

$$H(f) = \begin{cases} j2\sin(2\pi\frac{f}{f_s}), & |f| < f_s/2 \\ 0, & \text{elsewhere} \end{cases} \qquad (2\text{-}17)$$

as is shown in Fig. 2-6.

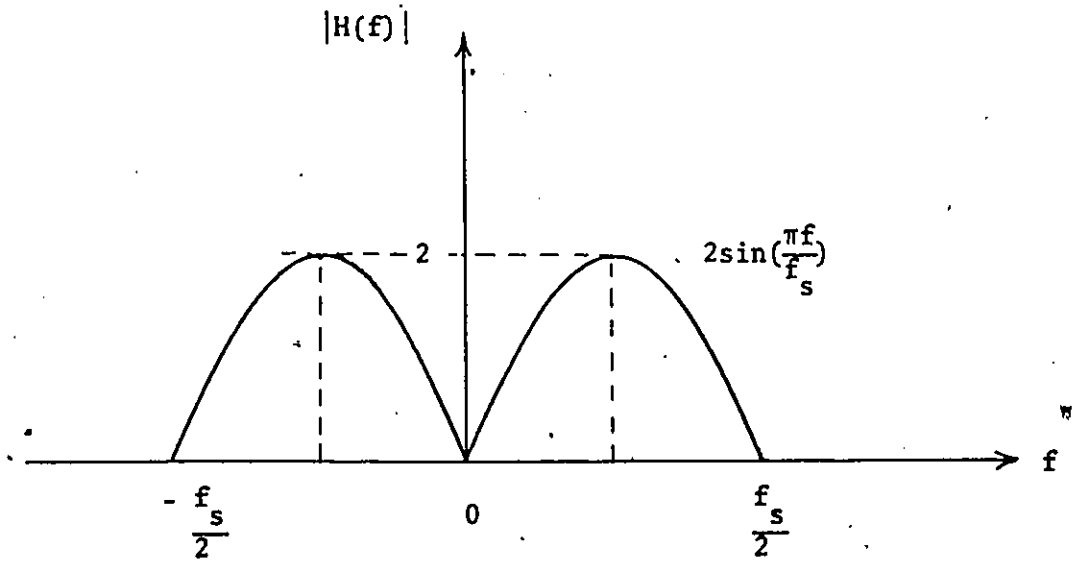

Figure 2-6. Transfer function of a Class IV PRS Scheme transmitting f_s symbols for second.

In addition to the spectral null at $f_s/2$, this class has a null at dc and has only a small amount of energy at low frequencies. This is advantageous because it can be easily adapted to single-sideband modulation since very sharp cut-off filters would not be needed — there would be very little power near the carrier frequency.

This kind of characteristic could allow vacation of a small band of the spectrum for service channel use. For instance, in the GTE Lenkurt 6.3 Mb/s 7-level FM system which uses the modified duobinary scheme, an 8kHz baseband bandwidth is reserved for a VF order wire and supervisory channel at the low end of the spectrum [20].

The corresponding impulse response is

$$h(t) = \int_{-\infty}^{\infty} A(f) e^{j2\pi ft} df = \int_{\frac{-f_s}{2}}^{\frac{f_s}{2}} j2\sin\left(\frac{2\pi f}{f_s}\right) e^{j2\pi ft} df$$

$$= \int_{\frac{-f_s}{2}}^{\frac{f_s}{2}} \left(e^{j2\pi \frac{f}{f_s}} - e^{-j2\pi \frac{f}{f_s}}\right) e^{j2\pi ft} df = \int_{\frac{-f_s}{2}}^{\frac{f_s}{2}} \left[e^{j2\pi f(t + \frac{1}{f_s})} - e^{j2\pi f(t - \frac{1}{f_s})}\right] df$$

$$= \left[\frac{e^{j2\pi f(t + \frac{1}{f_s})}}{j2\pi(t + \frac{1}{f_s})} - \frac{e^{j2\pi f(t - \frac{1}{f_s})}}{j2\pi(t - \frac{1}{f_s})}\right]_{\frac{-f_s}{2}}^{\frac{f_s}{2}}$$

$$= f_s\left[\frac{\sin\pi f_s(t + \frac{1}{f_s})}{\pi f_s(t + \frac{1}{f_s})} - \frac{\sin\pi f_s(t - \frac{1}{f_s})}{\pi f_s(t - \frac{1}{f_s})}\right]$$

Setting $f_s = 1/T$,

$$h(t) = f_s \text{sinc } f_s(t+T) - f_s \text{sinc } f_s(t-T) \qquad (2\text{-}18)$$

or

$$h(t) = \frac{2f_s}{\pi} \frac{\sin \pi f_s t}{(f_s^2 t^2 - 1)} \qquad (2\text{-}19)$$

From (2-19) it is evident that the response h(t) is a superposition of two sinc(f_st) responses of opposite polarity; one delayed by 2T secs from the other. In Fig. 2-7 the impulse response and its two components are shown.

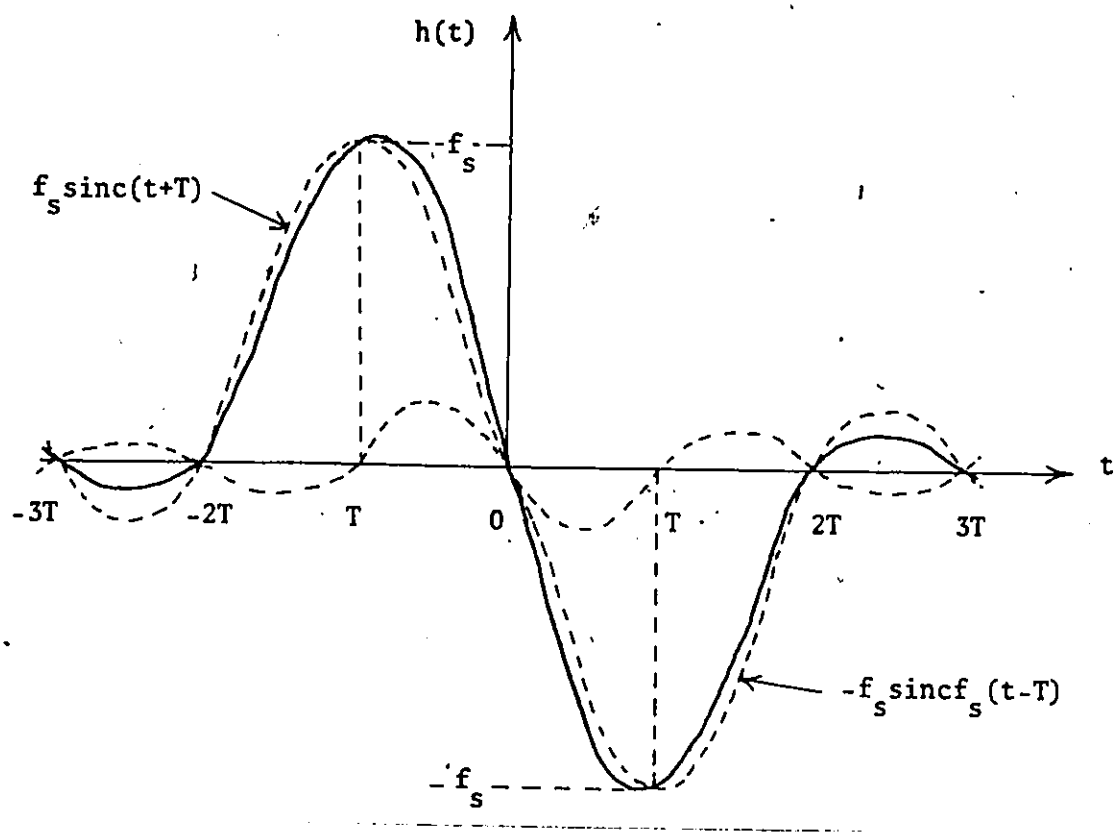

Figure 2-7. The impulse response and its components, for modified duobinary.

As can be seen from Fig. 2-7, the response has zeros at $t = nT$ $n = 0, \pm 2, \pm 3, \ldots$, and $h(\pm T) = \mp f_s$. If signalling is done with this impulse response, $h(t)$, at a rate of $f_s(=1/T)$, and the received waveform sampled at the time instants $=nT$, intersymbol interference will come only from the second previous symbol, as shown in Fig. 2-8.

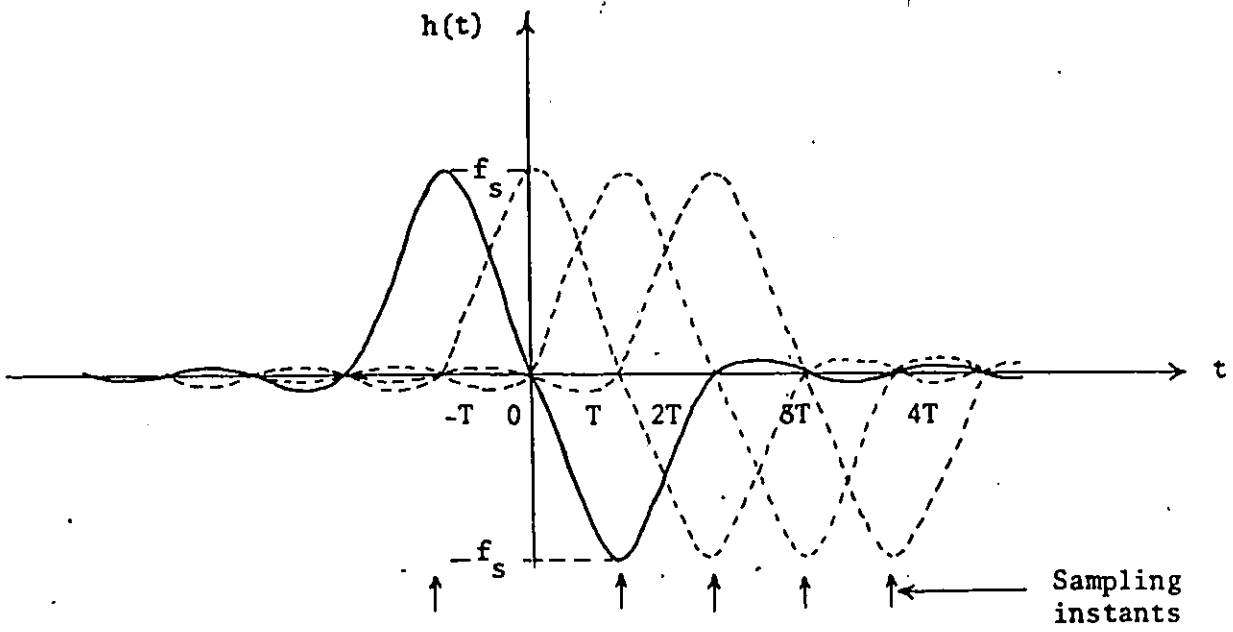

Figure 2-8. Signalling with modified duobinary pulses.

If pulse/no pulse transmission is assumed, the sampled waveform will have three distinct levels as shown in Table 1.

Table 1. Levels of Class IV PRS corresponding to pairs of bits (pairs refer to present bit and the second previous bit)

Binary Pair	Class IV PRS Output Level
00	0
01	$-f_s$
10	f_s
11	0

Using the same symbols as in (2-11), the sample value of the received waveform is

$$p_n = f_s a_n - f_s a_{n-2} + q_n \tag{2-20}$$

If at the sampling time, a_{n-2} has already been correctly detected, the detector then subtracts the term $-f_s a_{n-2}$ from p_n giving

$$g_n = p_n + f_s a_{n-2} = f_s a_n + q_n \tag{2-21}$$

From g_n, a_n can be detected.

Clearly, an error in detecting a symbol will most likely cause an error in the next but one symbol and error propagation as described earlier will occur. Again, for a binary input the penalty in signal-to-noise ratio caused by this error propagation is about 0.2 to 0.5 dB. To eliminate this error-extension effect, Lender also used a simple precoder for the modified duobinary [18, 21]. This is done by transforming the binary sequence $\{a_n\}$ into a new binary sequence $\{b_n\}$ such that

$$b_n = a_n \oplus b_{n-2} \tag{2-22}$$

or

$$a_n = b_n \oplus b_{n-2}$$

and b_n is used instead of a_n in (2.20).

Now, suppose that a new sequence $\{x_n\}$ is introduced such that

$$x_n = a_n \oplus x_{n-1} \tag{2-23}$$

and $\{c_n\}$ formed such that

$$c_n = x_n \oplus c_{n-1} \tag{2-24}$$

or

$$\therefore c_{n-1} = x_n \oplus c_n$$

$$c_{n-2} = x_{n-1} \oplus c_{n-1} \tag{2-24a}$$

Using (2.23) in (2.24),

$$c_n = (a_n \oplus x_{n-1}) \oplus c_{n-1} = a_n \oplus (x_{n-1} \oplus c_{n-1}) \tag{2-25}$$

Inserting (2.24a) into (2.25) gives

$$c_n = a_n \oplus c_{n-2} \tag{2-26}$$

Comparing (2-22) and (2-26), sequences $\{b_n\}$ and $\{c_n\}$ are seen to be identical. Hence the precoding represented by (2-22) can equally well

be achieved by a cascade of the two elementary coders of (2-23) and (2-24).

For the noiseless case, the precoded PRS sampled waveform becomes

$$p_n = f_s(b_n - b_{n-2}) \qquad (2\text{-}27)$$

Suppose $a_n = 0$, then from (2-22) $b_n = b_{n-2}$ and from (2-27) p_n is always 0. When $a_n = 1$, b_n is the reverse of b_{n-2}, and p_n is either $+f_s$ or $-f_s$. The decoding rule hence is

$$a_n = 0 \text{ if } p_n = 0$$

$$a_n = 1 \text{ if } p_n = \pm f_s$$

In contrast to Class I, a '0' is represented by the middle level while a '1' is represented by the extreme levels. Again a rectifier followed by a simple binary slicer may be used for detection in the presence of noise; alternatively two slicers with thresholds at $f_s/2$ and $-f_s/2$ will accomplish the same thing.

2.2.5 Generalisation of Partial-Response Signalling

Kretzmer extended the concept of duobinary and modified duobinary to other schemes by superimposing the impulse responses in various combinations [7, 8] to derive a generalised partial-response scheme. In more general terms, partial response can be defined as a method of

signalling where the signal is formed as a linear weighted superposition of input symbols a_n, the superposition memory extending over m bit periods.

$$p_n = \sum_{i=1}^{m} k_i a_{n-i+1} \tag{2-28}$$

where the k's are integer weighting coefficients.

For signalling with impulses, the generalised impulse response is

$$h(t) = \sum_{i=0}^{m-1} k_{i+1} \frac{\sin \pi f_s(t-iT)}{\pi f_s(t-iT)} \tag{2-29}$$

The generalised PRS system is shown in Fig. 2-9.

The corresponding transfer function is given by

$$H(f) = \int_{-\infty}^{\infty} h(t) e^{-j2\pi ft} dt \tag{2-30}$$

By choosing different values of k_i, different useful shapes of H(f), having a prescribed amount of interference over a span of a few digits can be obtained.

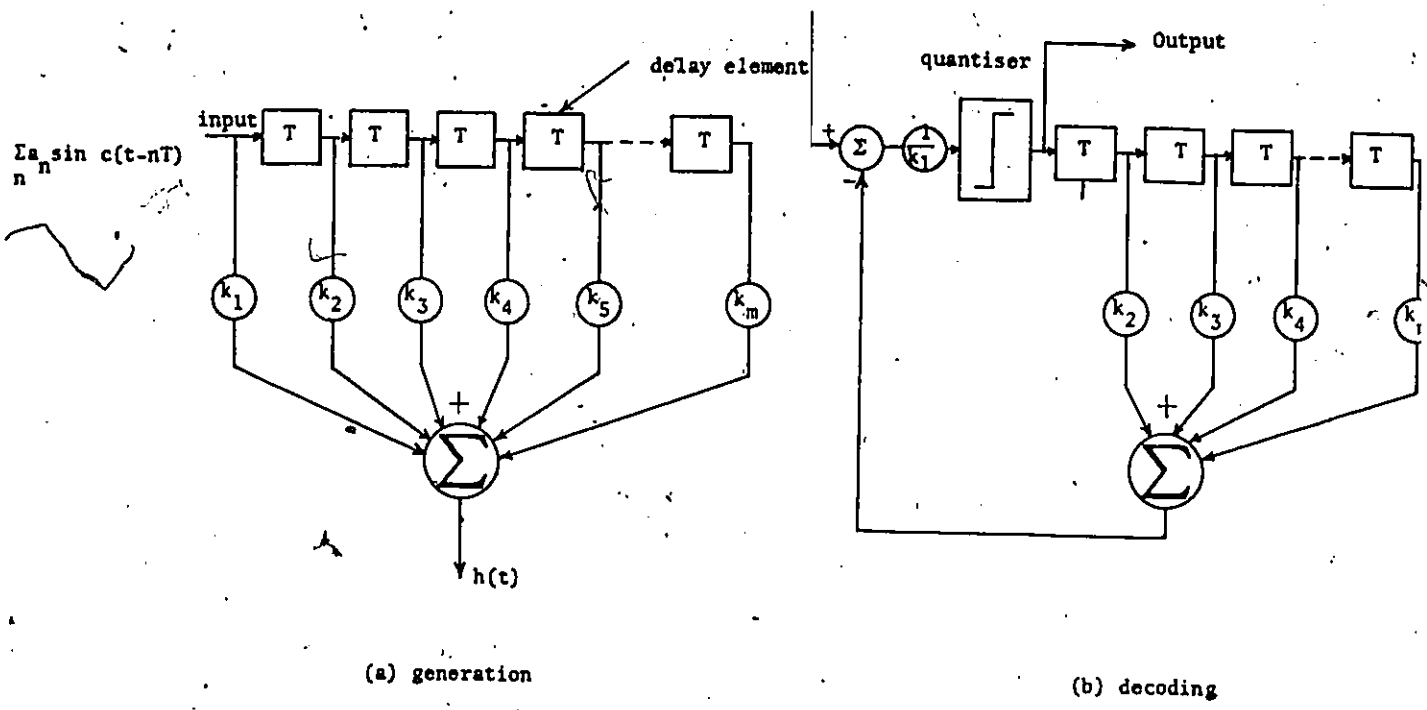

Figure 2-9. Generalised PRS signal generation and decoding.

In selecting H(f), two major considerations play an important part. The first is the number of output levels, since the greater the number of levels the more the degradation in error performance is likely to be. Furthermore, complexity of the equipment (especially the decoder) will increase with an increased number of output levels. With the present state-of-the-art more than five output levels are rarely used. The total number of levels is given by

$$L = \sum_{i=1}^{m} |k_i| + 1 \qquad (2\text{-}31)$$

The second consideration is the spectral nulls. A spectral null at $f = f_s/2$ is desirable since a pilot tone inserted at this point may be used for symbol timing recovery (STR). A spectral null at dc is also

very useful in systems such as dc powered cables, transformer coupled circuits, carrier systems with carrier pilot tones, and SSB modems. Further, the reduced low frequency components allow service channel transmission at the low frequency band in baseband for microwave radio transmission [20, 22]. For a spectral null at dc (or dc-free signalling), the sum of the weight coefficients must be zero, i.e.

$$\sum_{i=1}^{m} k_i = 0. \qquad (2\text{-}32)$$

Precoding can also be extended to the generalised partial response. The precoding algorithm is

$$a_n = k_1 b_n \oplus k_2 b_{n-1} \oplus k_3 b_{n-2} \oplus \cdots \oplus k_m b_{n-m+1} \qquad (2\text{-}33)$$

It should be noted that the terms with even coefficient, k, drop out from (2-33). Rewriting (2-28) with a_n replaced by b_n, one gets

$$p_n = k_1 b_n + k_2 b_{n-1} + k_3 b_{n-2} + \cdots + k_m b_{n-m+1} \qquad (2\text{-}34)$$

Comparing (2-33) and (2-34) it becomes immediately apparent that when $a_n = 0$, p_n is an even integer, while if $a_n = 1$, p_n is odd. That is to say, in any precoded PRS alternate levels represent '0' and '1' respectively. Hence in decoding at the receiver, preceding bits need not be referred to and error propagation is avoided.

Several classes of PRS have been proposed and studied [7, 15], the coefficients, k, in each class having certain relationships among themselves. As m increases within each class the output has a higher number of levels and the transfer function H(f) becomes more "concentrated", resulting in a more drastic spectral tapering. The full band $f_s/2$, however, is still needed to transmit f_s symbols/s. The performance margins are greatly reduced [8, 23]. Most of the PRS systems have therefore been kept to three or five output levels.

For Class I (also known as polybinary) [6, 23] all k_i's are unity i.e.

$$k_1 = k_2 = \ldots = k_m = 1.$$

The transfer function is given by

$$H(f) = \frac{\sin(m\pi\frac{f}{f_s})}{\sin(\pi\frac{f}{f_s})}, \qquad |f| \leq \frac{f_s}{2} \tag{2-35}$$

To avoid discontinuity in H(f) at $f_s/2$, odd values of m are not used. m = 2 corresponds to the three-level Class I PRS (or duobinary) discussed earlier.

For the case of Class IV (modified duobinary) $k_1 = 1$, $k_2 = 0$, $k_3 = -1$; and for Class V $k_1 = 1$, $k_2 = 0$, $k_3 = 2$, $k_4 = 0$, $k_5 = -1$, $m = 5$.

Only binary input symbols have been discussed so far. It is possible to have non-binary input symbols for a_n in (2-28). For example a bipolar input to a Class I PRS system was suggested and the resulting signal was termed "polybipolar" [6]. A combination of multilevel PAM and PRS (mainly the duobinary or modified duobinary) has been considered by many authors [9, 20, 24-26]. In particular, quarternary PAM as input to a duobinary system will yield a seven-level correlative system (duoquarternary) which has a bandwidth efficiency of 4 b/s/Hz in baseband. This would otherwise require a 16-level PAM system with $\alpha = 1$ or an 8-level PAM system with $\alpha = \frac{1}{2}$. These systems would be inferior to the 7-level correlative system in terms of required signal-to-noise ratio for a given probability of error. An 8-level PAM input yields a 15-level PRS system, with 6 b/s/Hz efficiency in baseband. A 64-level PAM system with $\alpha = 1$ (or a 32-level PAM system with $\alpha = \frac{1}{2}$) would otherwise be needed. In general, for an M-level input to a three-level Class I or Class IV PRS system, the output has $2M-1$ levels and a spectrum utilisation of $2 \log_2 M$ b/s/Hz.

Precoding has also been used for such systems to enable detection without having to compensate for past decisions (which would risk error propagation) [9, 14, 24, 27]. This precoding scheme is virtually the same as for a binary input except that addition is now modulo-M. For instance, for Class I PRS with M-ary input

$$b_n = a_n \oplus b_{n-1} \text{(modulo-M)} \qquad (2\text{-}36)$$

and for Class IV,

$$b_n = a_n \oplus b_{n-2} \text{(modulo-M)} \qquad (2\text{-}37)$$

The receiver decodes the received levels modulo-M to recover the original symbols a_n.

2.3 Digital Implementation

PRS can be obtained by passing binary data through an analogue filter having the transfer function H(f) given as described in the last section ($\cos(\pi f/f_s)$ for duobinary and $\sin(2\pi f/f_s)$ for modified duobinary). The various levels of a correlative coding system may also be generated in a digital manner which will be described next. Such digital conversion techniques have a higher degree of precision in forming the PRS level and are hence better than analogue techniques. Classes I and IV are now considered.

2.3.1 Class I (Polybinary)

Starting with a binary waveform with two signalling levels (MARK and SPACE) a partial-response waveform is formed in two steps. The first step is precoding as described earlier. Recall that for a general Class I PRS with M levels (M = m + 1) precoding is done by

converting the original binary waveform a_n into another waveform b_n [binary] such that the present digit of b_n is the modulo-2 sum of the present digit a_n and (M-2) immediately preceding digits of b_n.

$$b_n = a_n \oplus \underbrace{b_{n-1} \oplus b_{n-2} \oplus \cdots \oplus b_{n-M+2}}_{(M-2)\text{ digits}} \qquad \text{(modulo-2)}$$

In b_n, 0's and 1's do not represent SPACE and MARK.

The precoder is shown in Fig. 2-10.

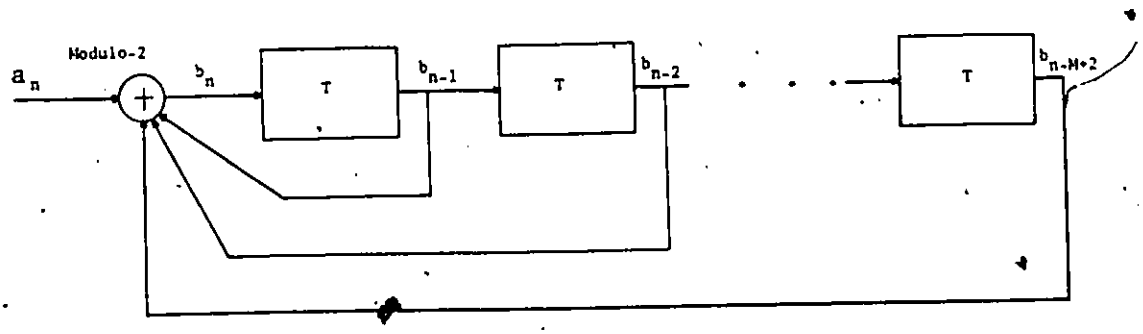

Figure 2-10. A Class I PRS precoder.

The delay T corresponds to one symbol period and is usually implemented using a clocked flip-flop having a clock rate of 1/T Hz. The second step entails adding algebraically the present digit of b_n to the (M-2) preceding digits of the waveform b_n.

$$p_n = \underbrace{b_n + b_{n-1} + b_{n-2} + \ldots + b_{n-M+2}}_{(M-1)\text{ digits}} \quad \text{(algebraic sum)}$$

In actual implementation, a scaling factor, c, may be involved, i.e.

$$p_n = c\sum_{i=0}^{M-2} b_{n-i} \tag{2-38}$$

This is shown in Fig. 2-11 below.

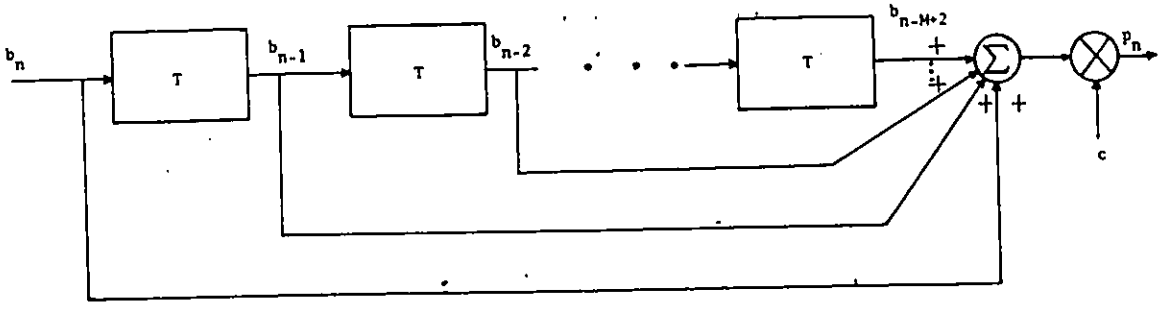

Figure 2-11. A General Class I Correlative Encoder.

In p_n, MARK and SPACE are mapped onto alternate levels. If the levels are numbered consecutively from zero to (M-1) starting from the bottom it is clear that SPACE is represented by an even-numbered level and MARK by an odd-numbered level. Detection of each digit in p_n can be done independently in spite of the strong correlation. The spectral energy of a_n is now compressed near low frequencies for p_n.

If a_n is equiprobable the spectral density of b_n is the same

as that of a_n and is given by [6]

$$W_b(f) = \frac{1}{4T}|G(f)|^2 \qquad (2\text{-}39)$$

where G(f) is the Fourier transform of the pulse shape. Considering the discrete-time filter of Fig. 2-11 above, and using z-transforms,

$$p(z) = \sum_{i=0}^{M-2} b(z)z^{-i} \qquad (2\text{-}40)$$

where p(z) and b(z) are the z-transforms of sequence p_n and b_n respectiely.

Hence the transfer function is*

$$H_p(z) = \sum_{i=0}^{M-2} z^{-i} \qquad (2\text{-}41)$$

In the frequency (ω) domain the transfer function becomes

* For a general PRS system the transfer function would be

$$H(z) = \sum_{i=0}^{M-2} k_i z^{-i}$$

$$H_p(e^{j\omega T}) = \sum_{i=0}^{M-2} e^{-ji\omega T} \qquad (2\text{-}42)$$

The sum in (2-42) is a sum of a geometric series with common ratio $e^{-j\omega T}$. Therefore the sum is given by

$$H_p(e^{j\omega T}) = \frac{1-e^{-j(M-1)\omega T}}{1-e^{-j\omega T}} = e^{-j(M-2)\frac{\omega T}{2}} \frac{\sin\frac{(M-1)}{2}\omega T}{\sin\frac{\omega T}{2}}$$

or (2-43)

$$|H_p(f)| = \frac{\sin(M-1)\pi fT}{\sin\pi fT}$$

The power spectral density of p_n is hence given by

$$W_p(f) = W_b(f)|H_p(f)|^2 = \frac{1}{4T}|G(f)|^2\left(\frac{\sin(M-1)\pi fT}{\sin\pi fT}\right)^2 \qquad (2\text{-}44)$$

For a rectangular pulse, $G(f) = T\frac{\sin\pi fT}{\pi fT}$

$$\therefore W_p(f) = \frac{(M-1)^2}{4} T\left(\frac{\sin(M-1)\pi fT}{(M-1)\pi fT}\right)^2 \qquad (2\text{-}45)$$

or

$$W_p(f) = \frac{(M-1)}{4}^2 T\, S_a[(M-1)\pi fT]$$

Two things seem to be worthy of note here. First, since the levels are formed by adding successive adjacent (M-1) bits, the only possible transitions between two successive digit-time slots is between two adjacent signalling levels. Hence, the intersymbol interference in terms of horizontal eye opening is small. Also, this correlation property of level transitions may be used for error detection, without introducing extra bits. Second, since odd-numbered levels represent a MARK and even-numbered levels a SPACE, a change of level from an odd-(even-)numbered one to another odd-(even-)numbered one does not actually result in an error. This alleviates somewhat the noise penalty.

Three-Level Class I (Duobinary) PRS

This is the simplest and most commonly used for Class I. In Fig. 2-12, the implementation of a three-level Class I PRS is shown.

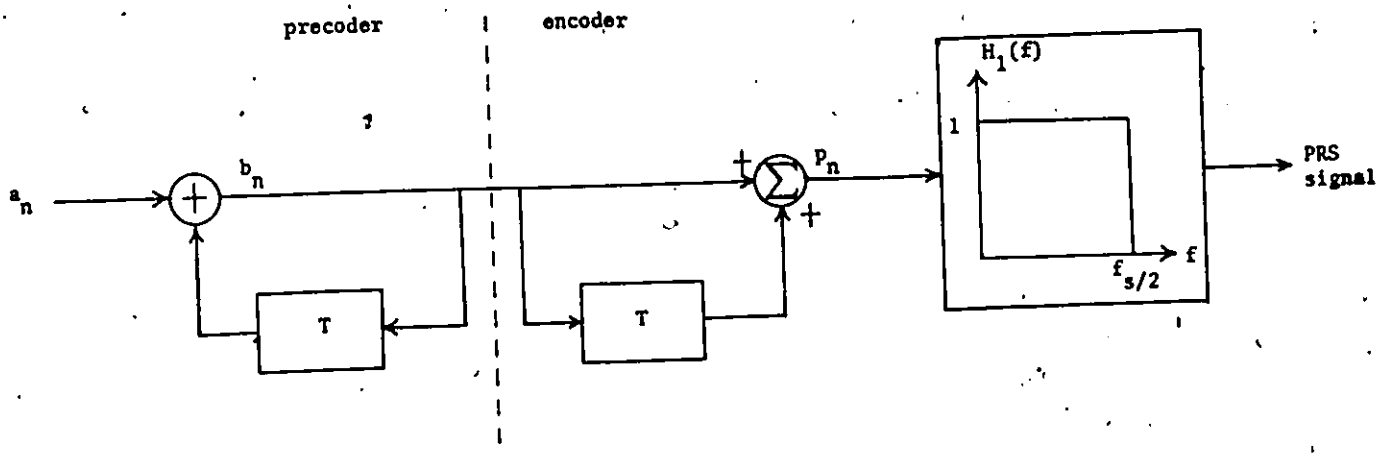

Figure 2-12. Duobinary encoder (with a precoder).

The transfer function of the encoder is obtained from (2-43) by putting M = 3. i.e.

$$H_p(f) = \frac{\sin 2\pi fT}{\sin \pi fT} = 2\cos \pi fT \qquad (2\text{-}46)$$

However f here extends to infinity i.e.

$$H_p(f) = 2\cos \pi fT, \qquad |f| < \infty \qquad (2\text{-}46a)$$

To limit the bandwidth of this discrete-time filter, an analogue low-pass filter is used in cascade with an idealised transfer function

$$H_1(f) = \begin{cases} 1, & |f| \leq 1/2T \\ 0, & \text{elsewhere} \end{cases} \qquad (2\text{-}46b)$$

Since $H_p(f)$ has very small values near $\frac{1}{2T}(= \frac{f_s}{2})$, a brickwall filter is not really necessary and a sharp low-pass filter, such as a Chebyshev equal ripple filter, is used in practice. In this case the filter does not have to be phase equalised near the edge of the band. The overall transfer function is a combination of (2-46a) and (2-46b) and is given by

$$H(f) = H_p(f)H_1(f) = \begin{cases} 2\cos \pi f/f_s, & |f| \leq f_s/2 \\ 0, & \text{elsewhere} \end{cases} \qquad (2\text{-}46c)$$

which is the same as (2-8).

The resulting power spectral density as obtained from (2-45) is as follows

$$W_p(f) = \begin{cases} T\left(\frac{\sin 2\pi fT}{2\pi fT}\right)^2, & |f| \leq \frac{1}{2T} \\ 0, & \text{elsewhere} \end{cases} \qquad (2\text{-}47)$$

Note that the position of the first spectral null is reduced by a factor of 2:1 with respect to that of binary.

Fig. 2-13 shows the conversion of a binary waveform to a duobinary

waveform. The first bit in b_n is arbitrary and it has been assumed to be zero. If a '1' were assumed, the only effect would be to

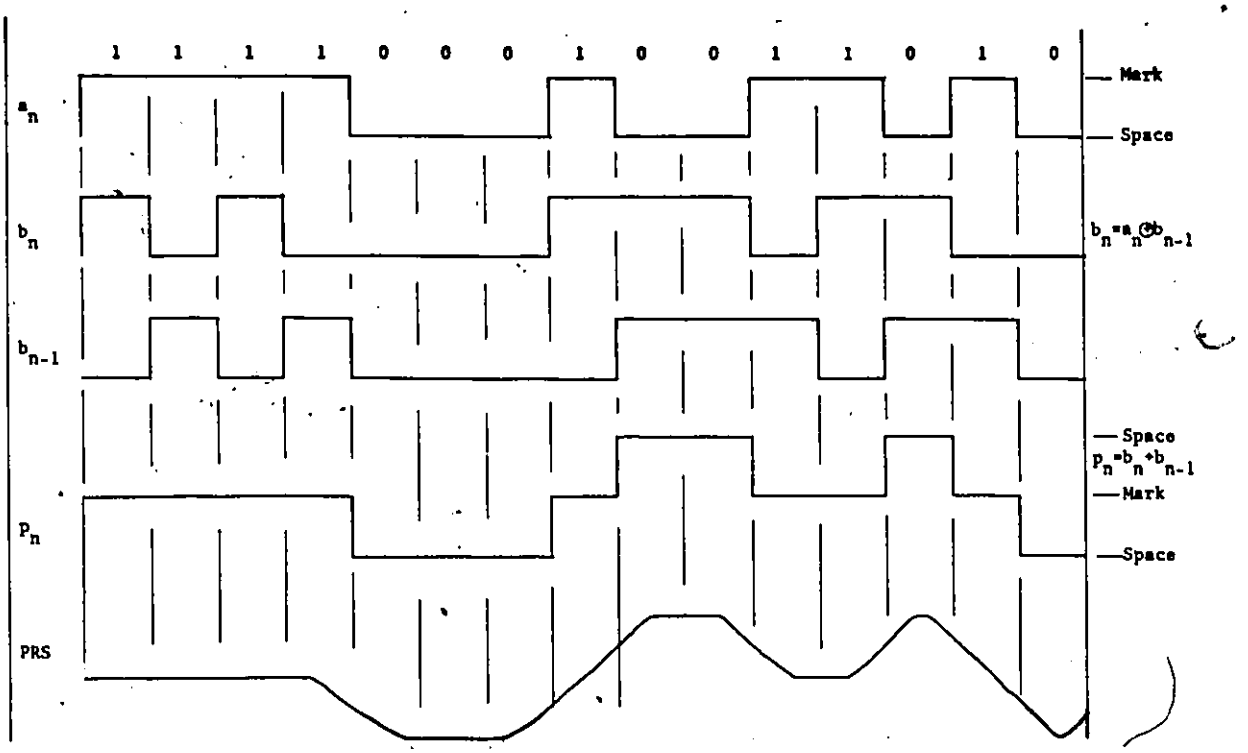

Figure 2-13. **The duobinary conversion.**

interchange the outermost levels in p_n. The following rules can be observed for p_n.

1. A MARK always appears at the centre level and a SPACE at the extreme levels.
2. Two successive SPACES have the same polarity if they are separated by an even number of MARKS.
3. Two successive SPACES have opposite polarity if they are separated by an odd number of MARKS. This means that a change from one extreme level to another is prohibited.

Fig. 2-14 shows a three-level eye diagram of a duobinary signal

generated in the laboratory.[1]

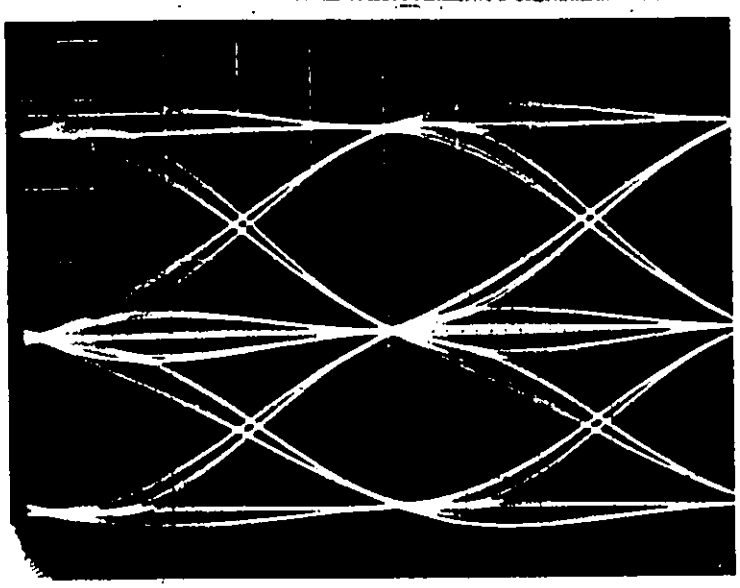

Data rate 100 kb/s

Filter cut off 60 kHz

2μsec/division

Figure 2-14. Experimental eye diagram for duobinary.

2.3.2 Class IV (modified duobinary)

The implementation of Class IV PRS is very similar to that of duobinary except that the correlation span now extends over three bits. The Class IV PRS encoder is shown in Fig. 2-15.

1. 'Laboratory', in this thesis, shall be taken to mean the Communications Laboratory of the University of Ottawa Electrical Engineering Department.

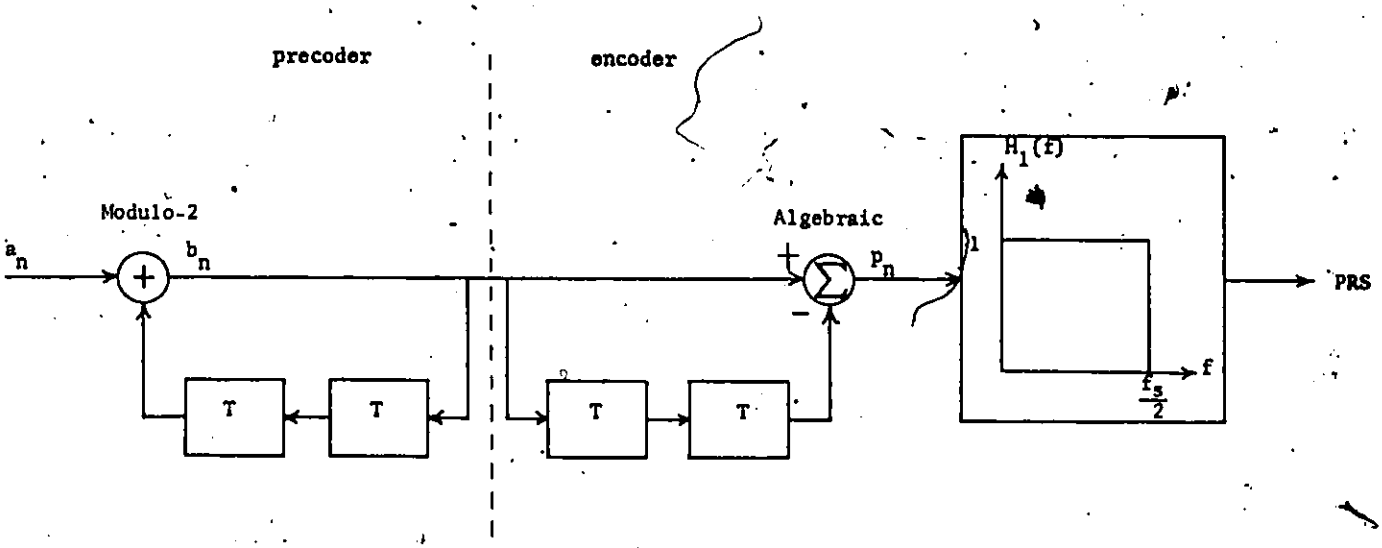

Figure 2-15. Modified duobinary encoder (with a precoder).

The various waveforms in Fig. 2-15 are related as follows:

$$b_n = a_n \oplus b_{n-2}$$

$$p_n = b_n - b_{n-2}$$

Again, if a_n is equiprobable, b_n is also equiprobable and has the same spectral density as a_n.

Regarding Fig. 2-15 as a discrete-time filter and using z-transforms, the transfer function becomes

$$H_p(z) = 1 - z^{-2} \tag{2-48}$$

and in the frequency domain,

$$H_p(e^{j\omega T}) = 1 - e^{-2j\omega T} = e^{-j\omega T}(e^{+j\omega T} - e^{-j\omega T})$$

$$= j2e^{-j\omega T}\sin\omega T$$

or

$$|H_p(f)| = 2|\sin 2\pi fT| \qquad |f| < \infty \tag{2-49}$$

Like for the duobinary the transfer function extends to infinity and a low-pass filter with the same characteristic as (2-46b) has been added in Fig. 2-15. The overall transfer function is hence given by (2-49) and (2-46b)

$$|H(f)| = |H_p(f)||H_1(f)| = \begin{cases} 2\left|\sin 2\pi\dfrac{f}{f_s}\right| & , |f| < \dfrac{f_s}{2} \\ 0 & , \text{elsewhere} \end{cases} \tag{2-50}$$

The power spectral density for a rectangular (NRZ) input is

$$W_p(f) = \frac{1}{4T}\left(\frac{T\sin\pi fT}{\pi fT}\right)^2(\sin 2\pi fT)^2 = T\left(\frac{\sin\pi fT}{\pi fT}\right)^2(\sin 2\pi fT)^2 \tag{2-51}$$

$$\text{i.e. } W_p(f) = \begin{cases} T\left(\frac{\sin\pi fT}{\pi fT}\right)^2(\sin 2\pi fT)^2 & , |f| < \frac{1}{2T} \\ 0 & , \text{ elsewhere} \end{cases}$$

It is clear that this power spectral density will have a spectral null at dc and $f_s/2$.

Note that in the modified duobinary, bits are correlated not with the previous bit as in duobinary but with the second bit back. This will permit all possible transitions between levels as can be seen in Fig. 2-16. This means that the intersymbol interference in terms of horizontal eye opening is larger than in the duobinary.

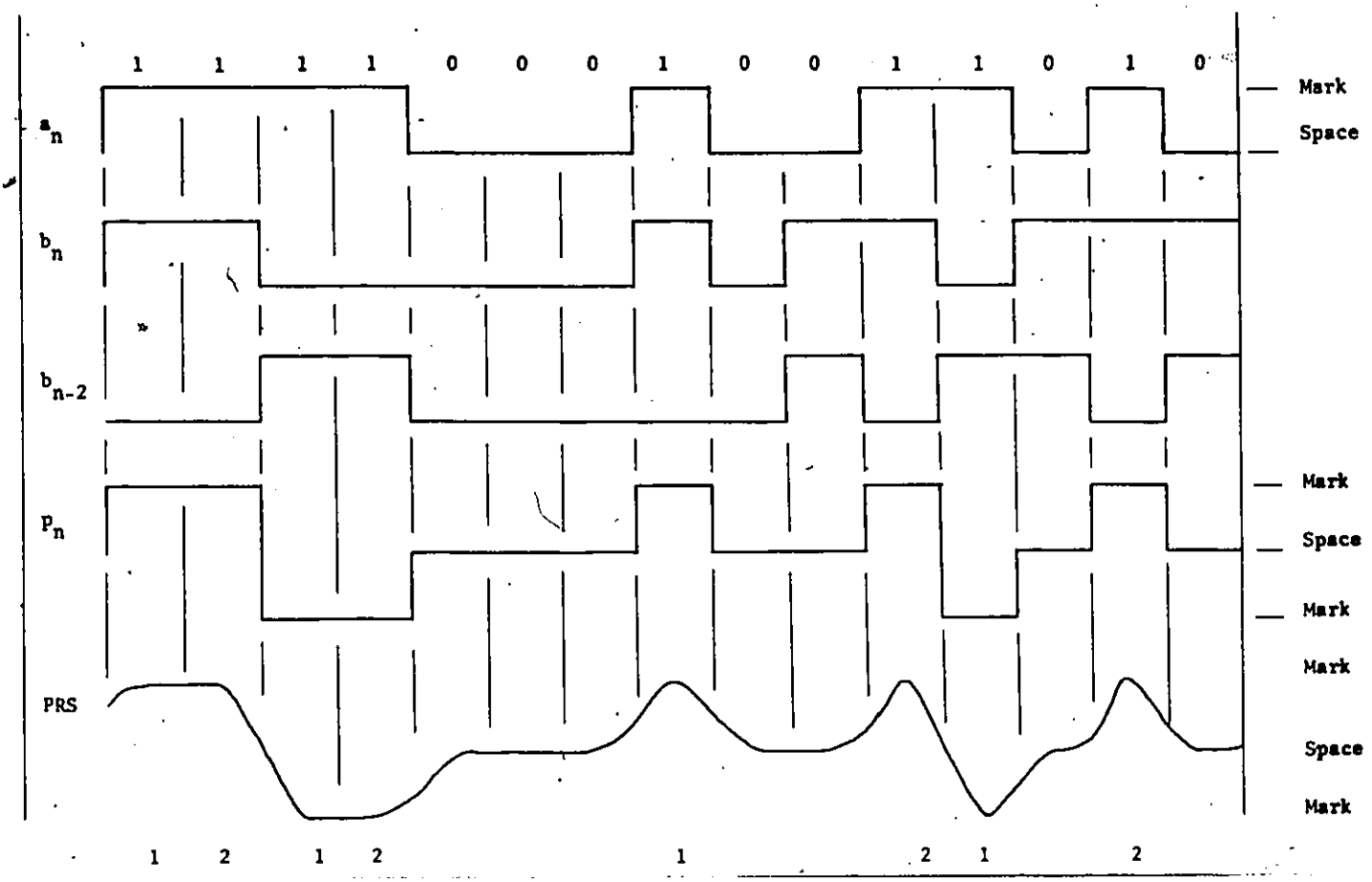

Figure 2-16. Conversion of a binary waveform into a modified duobinary waveform. (The first two bits in b_n are arbitrary and have been assumed to be 0.)

Some of the characteristics of the resulting waveform are:

1. A MARK always appears at the extreme levels and a SPACE at the center level.

2. If successive MARKS are grouped in pairs and numbered 1 and 2 as shown in Fig. 2-16, each MARK numbered 1 always has a polarity opposite to that of the MARK before it (numbered 2) [18].

3. The polarity of a MARK numbered 2 has the same polarity as the previous MARK (numbered 1) if separated from it by an even number of SPACES; and it has the opposite polarity if separated by an odd number of SPACES.

The three-level eye pattern of a modified duobinary signal, obtained from hardware designed in the laboratory, is shown in Fig. 2-17. The hardware will be described later.

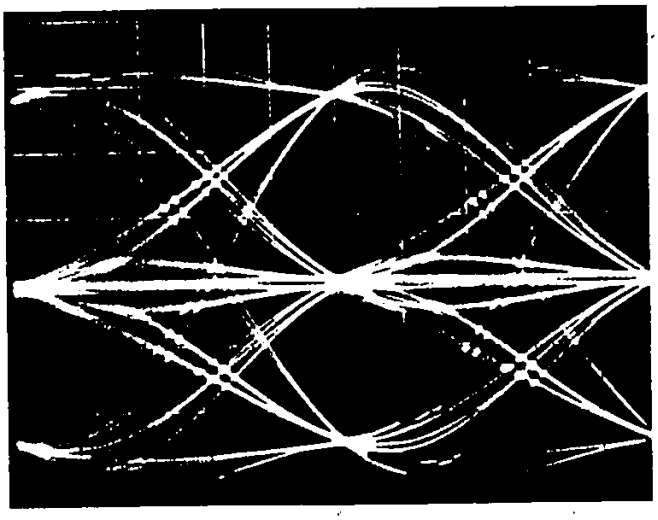

Data rate 100 kb/s

Filter cut off 60 kHz

2 μsec/division

Figure 2-17. Experimental eye diagram for a modified duobinary signal.

2.4 PRS Systems with a Pseudo-Random Binary Sequence (PRBS) Input

2.4.1 PRBS Sequences

Most often the data to be transmitted are random. Randomness refers to the *a priori* conditions of sequence generation, rather than the *a posteriori* consideration of what the sequence looks like. In th laboratory or industry, however, for test purposes, a truly random sequence is usually not available. However, generators exist that produce sequences which satisfy a set of statistical tests of the appearance of randomness [1]. These sequences, although strictly speaking deterministic, behave (a posteriori) as random sequences for the purposes of testing and are referred to as *pseudo-random binary sequences* (PRBS). Also known as *maximal-length shift register sequences* they can be generated by using a shift register, the input o which is a modulo-2 sum of certain stages of the register. Such a sequence has a period, N given by

$$N = 2^n - 1$$

where n is the number of shift register stages. An example of such a register is given in Fig. 2-18 for n = 15. The output is taken from the 15th delay element. The sequence generated by this register repeats itself after $2^{15} - 1 = 32,767$ bits.

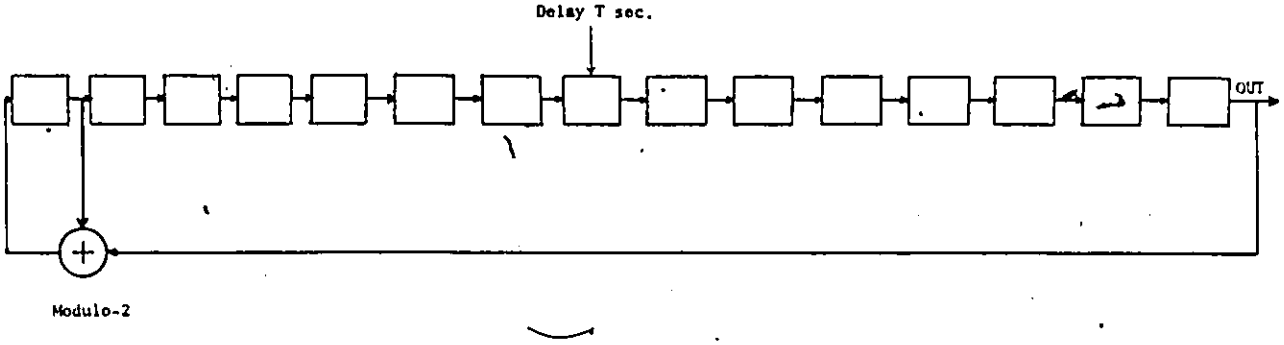

Figure 2-18. A 15-stage maximal-length shift register.

In the laboratory, such a sequence will be an input to a PRS system. The (discrete) power spectrum of a PRBS with period N is well known [1].

$$\Phi(\omega) = \frac{N+1}{N^2}\left(\frac{\sin(\frac{\omega T}{2})}{\frac{\omega T}{2}}\right)^2 \sum_{\substack{k=-\infty \\ k\neq 0}}^{\infty} \delta(\omega - \frac{2\pi k}{NT}) + \frac{1}{N^2}\,\delta(\omega) \qquad (2\text{-}52)$$

It is desired now to find the power spectral density of a PRS resulting from a PRBS input. To find this, one may use the well-known Wiener-Khintchine relations which state that the power spectral density G(f) and the autocorrelation function R(τ) constitute a Fourier transform pair.

$$G(f) = \int_{-\infty}^{\infty} R(\tau)e^{-j2\pi f\tau}d\tau$$

and

$$R(\tau) = \int_{-\infty}^{\infty} G(f)e^{j2\pi f\tau}df \qquad (2\text{-}53)$$

Although the power spectral density may be found by other means, this method is chosen because the autocorrelation function of a PRS sequence is not well covered in the available literature.

2.4.2 The Autocorrelation and Power Spectral Density of a PRS Sequence Formed From a PRBS Sequence

The autocorrelation of a (periodic) pseudo-random waveform is given by

$$R(\tau) = \left(\frac{1}{NT}\right) \int_{0}^{NT} x(t)x(t+\tau)dt \qquad (2\text{-}54)$$

For an NRZ, PRBS

$$R(\tau) = \begin{cases} 1 - \frac{N+1}{N}\frac{|\tau|}{T} & |\tau| < T \\ \frac{-1}{N} & \text{elsewhere.} \end{cases} \qquad (2\text{-}55a)$$

and $R(\tau)$ is periodic with period NT.

It can be easily verified that $\{R(\tau)\}$ gives $\Phi(\omega)$ in (2-52). As $N \to \infty$ a truly random sequence results and (2-55a) becomes

$$R(\tau) = \begin{cases} 1 - \dfrac{|\tau|}{T}, & |\tau| < T \\ 0, & \text{elsewhere} \end{cases} \qquad (2\text{-}55b)$$

and

$$\Phi(\omega) = \left(\frac{\sin \frac{\omega T}{2}}{\frac{\omega T}{2}} \right)^2$$

Consider now a precoded Class I PRS system, and let the input NRZ sequence $\{a_n\}$ be 1 1 1 1 0 0 0 1 0 0 1 1 0 1 0, which is a PRBS sequence with length 15. The resulting PRS sequence may be written $\{p_n\}$ = 0 0 0 0 -1 -1 -1 0 1 1 0 0 1 0 -1. To find the autocorrelation function, compare $\{p_n\}$ bit by bit with a cyclic shift of itself. Notice agreements and disagreements; designate A_0 an agreement of 0 and 0, and A any other agreement i.e. 1 and 1 or -1 and -1. Let D_0 denote a disagreement where one bit is 0, and D a disagreement not involving 0. Then the autocorrelation is given by

$$R(iT) = \begin{matrix} A-D \\ A+A_0+D+D_0 \end{matrix} \; 0 \qquad i = 0,1,2,\ldots, 15.$$

or (2-56)

$$R(iT) = \frac{A-D}{15} \qquad i = 0,1,2,\ldots, 15$$

Obviously $R(0) = \frac{T}{15}$. Applying (2-56) one finds

$$R(1) = \frac{3}{15}$$

$$R(2) = \frac{-1}{15}$$

$$R(3) = \frac{-1}{15}$$

.

.

.

$$R(13) = \frac{-1}{15}$$

$$R(14) = \frac{3}{15}$$

$$R(15) = \frac{7}{15}$$

Note that since $P_{n-i} = p_{n+15-i}$, $R(-i) = R(15-i)$.

From these values, one expects that (for N = 15),

$$R(\tau) = \begin{cases} \frac{7}{15} \frac{4}{15} \frac{|\tau|}{T} , & |\tau| < 2T \\ \frac{-1}{15} , & \text{elsewhere} \end{cases} \qquad (2\text{-}57)$$

and the period is NT. This will agree with the points $\tau = 0$, $\tau = T$, $\tau = 2T$ etc.

$R(\tau)$ is now graphically evaluated for $\tau \varepsilon [0,T]$, $\tau \varepsilon [T,2T]$ and $\tau \varepsilon [(n-1)T, nT]$ where n is an integer greater than 2, but less than 13.

i) The PRS waveform is displaced by an amount $\tau = \varepsilon$, $0 < \varepsilon < T$, as

shown in Fig. 2-19. The waveform $p(t-\varepsilon)$ is shown slightly displaced

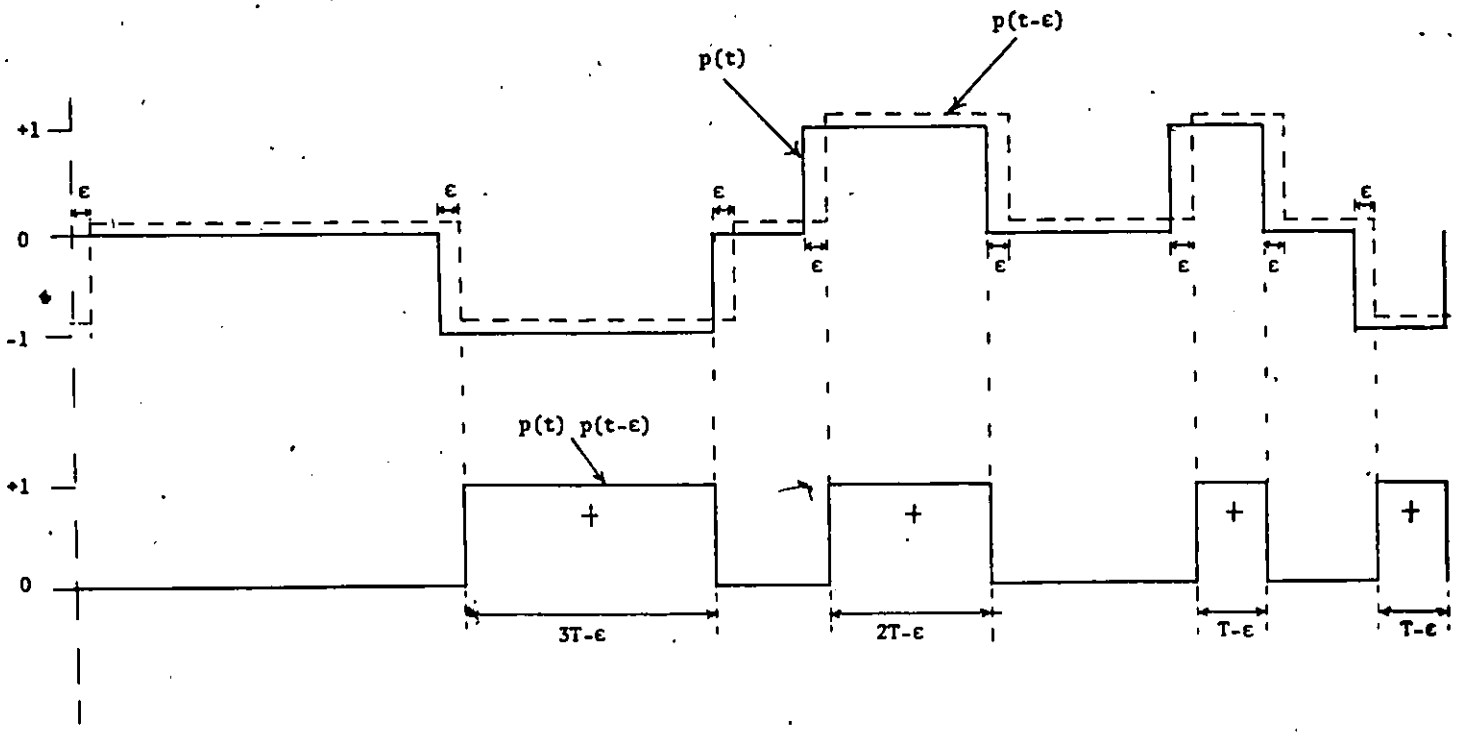

Figure 2-19. Graphical evaluation of $R_{\tau\varepsilon}(\tau)$ for $\tau\varepsilon(0,T)$.

upwards for clarity. The autocorrelation is now the area under the $p(t)p(t-\varepsilon)$ curve for one period, divided by 15T.

i.e. $R(\varepsilon) = R(-\varepsilon) = \frac{7T-4\varepsilon}{15T} = \frac{7}{15} - \frac{4\varepsilon}{15T}$, $|\varepsilon| < T$.

ii) Let the displacement be $\tau = \varepsilon$, $T < \varepsilon < 2T$. Let $\varepsilon = T + \Delta$. This is depicted in Fig. 2-20.

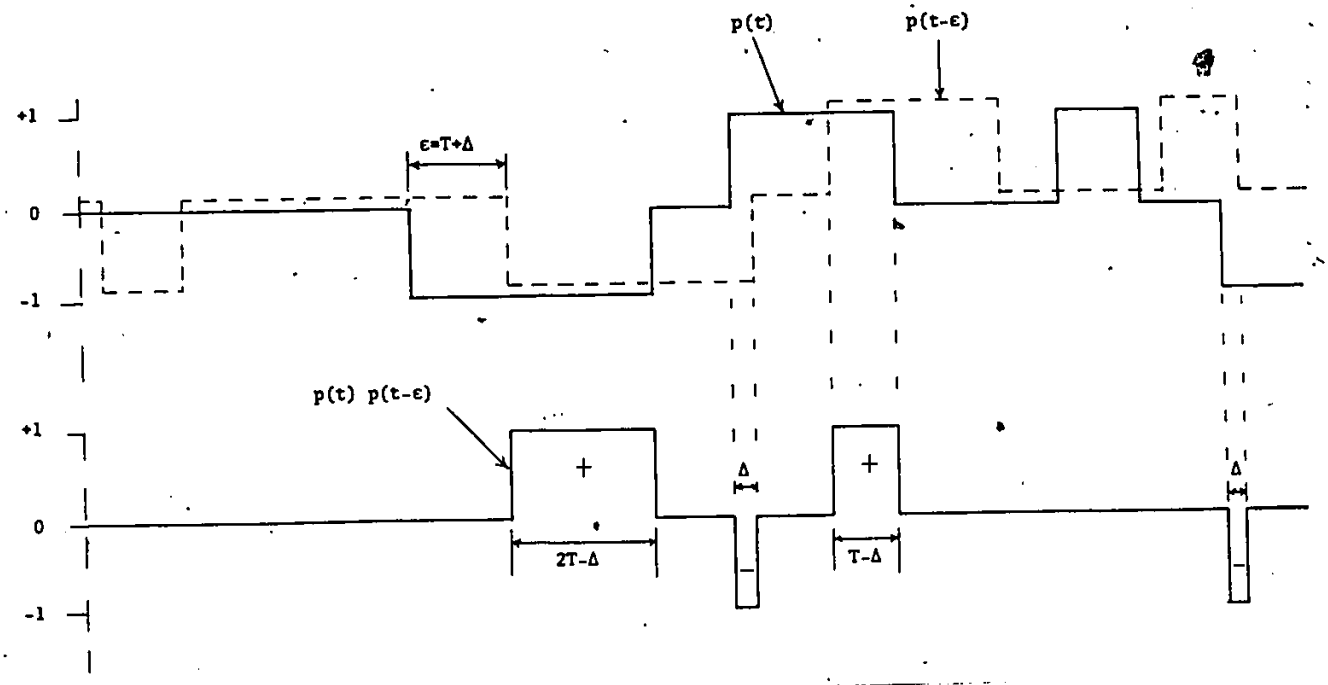

Figure 2-20. Evaluation of $R(\tau)$ for $\tau\varepsilon(T,2T)$.

From Fig. 2-20, it can be seen that

$$R(\varepsilon) = R(-\varepsilon) = \frac{(2T-\Delta) + (T-\Delta) - 2\Delta}{15T} = \frac{3}{15} - \frac{4\Delta}{15T}$$

But since $\Delta = \varepsilon - T$,

$$R(\varepsilon) = \frac{3}{15} - \frac{4(\varepsilon-T)}{15T} = \frac{7}{15} - \frac{4\varepsilon}{15T}, \quad T < |\varepsilon| < 2T.$$

iii) The displacement is how taken to be $\tau = \varepsilon$, $(n-1)T < \varepsilon < nT$, and $3 \leq n \leq 13$. Take for example $n = 5$. Let $\varepsilon = 4T + \Delta$ such that $\Delta = \varepsilon - 4T$. The displacement is shown in Fig. 2-21 below.

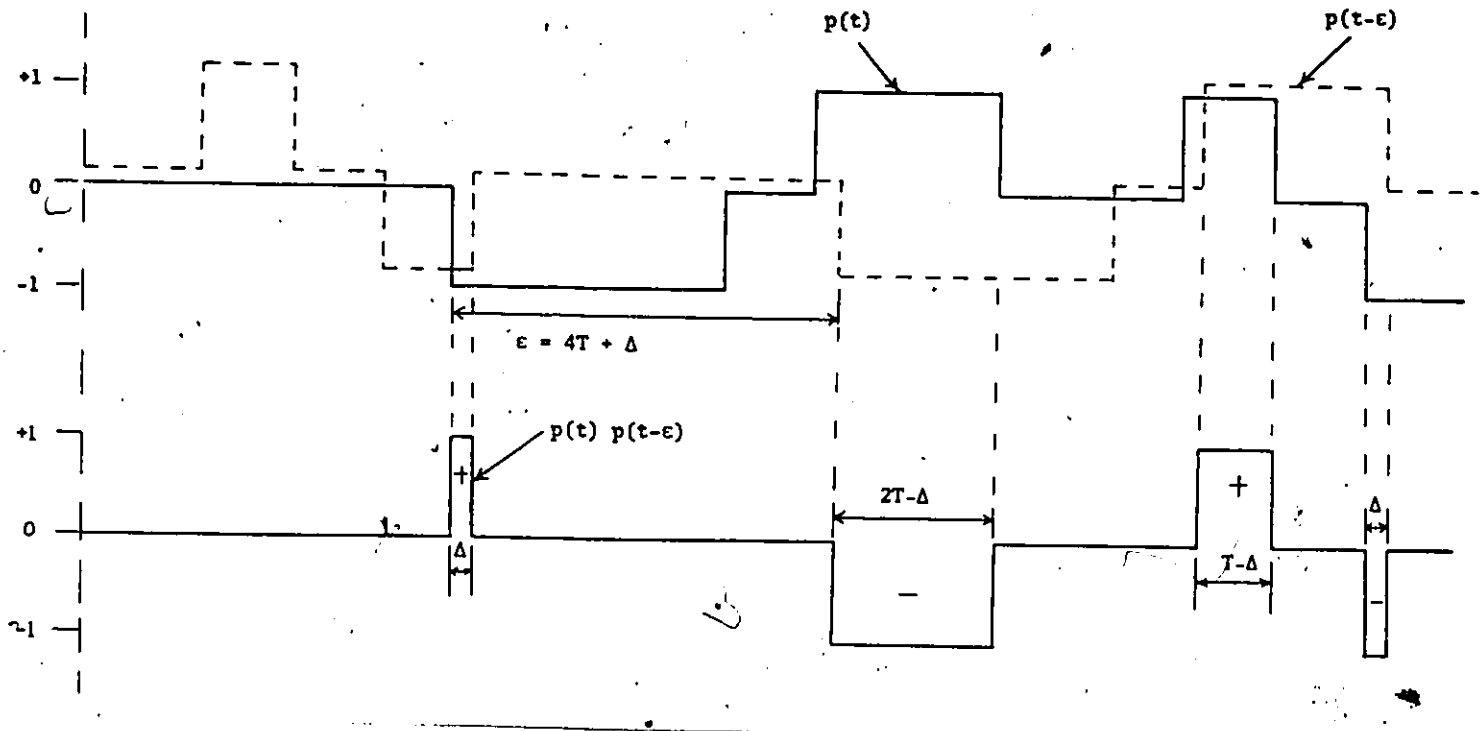

Figure 2-21. Graphic evaluation of $R(\tau)$ for $\tau \in [(N-1)T, nT]$, $3 \le n \le 13$. n is chosen as 5 here.

$$R(\varepsilon) = R(-\varepsilon) = \frac{\Delta + (T-\Delta) - (2T-\Delta) - \Delta}{15T} = -\frac{1}{15}.$$

i.e. $R(\varepsilon) = -\frac{1}{15}$, $3 \le |\varepsilon| \le 13$.

Combining the results of cases (i), (ii), and (iii),

$$R(\tau) = \begin{cases} \frac{7}{15} - \frac{4}{15}\frac{|\tau|}{T}, & |\tau| < 2T \\ \frac{-1}{15}, & \text{elsewhere} \end{cases}$$

with a period of 15T. Hence (2-57) is verified.

Generalising to any PRBS with a period N, the autocorrelation of the PRS sequence may be written as

$$R(\tau) = \begin{cases} \frac{(N-1)}{2N} - \frac{(N+1)|\tau|}{4NT}, & |\tau| < 2T \\ -1/N, & \text{elsewhere} \end{cases} \qquad (2\text{-}58a)$$

and the period is NT.

If N tends to infinity, i.e. the sequence is truly random, the autocorrelation reduces to only one peak, and the flat portion is zero.

$$R(\tau) = \begin{cases} \frac{1}{2} - \frac{|\tau|}{4T}, & |\tau| < 2T \\ 0, & \text{elsewhere} \end{cases} \qquad (2\text{-}58b)$$

The normalised autocorrelation function for a 3-level Class I PRS waveform formed from a PRBS sequence is shown in Fig. 2-22 for a PRBS of length N, and for a random sequence.

If (2-58b) is compared with (2-55a), it appears that the autocorrelation of a 3-level Class I PRS sequence has the same shape as that of a binary sequence except for an expanded scaling factor of two. Recall that the power spectral density had the same shape as that of binary but compressed by a factor of two. One would therefore expect that for a general Class I sequence with M output levels (since the power spectral density is compressed by a factor of (M-1) with respect to that of binary) the autocorrelation function would be expanded by a factor of M-1.

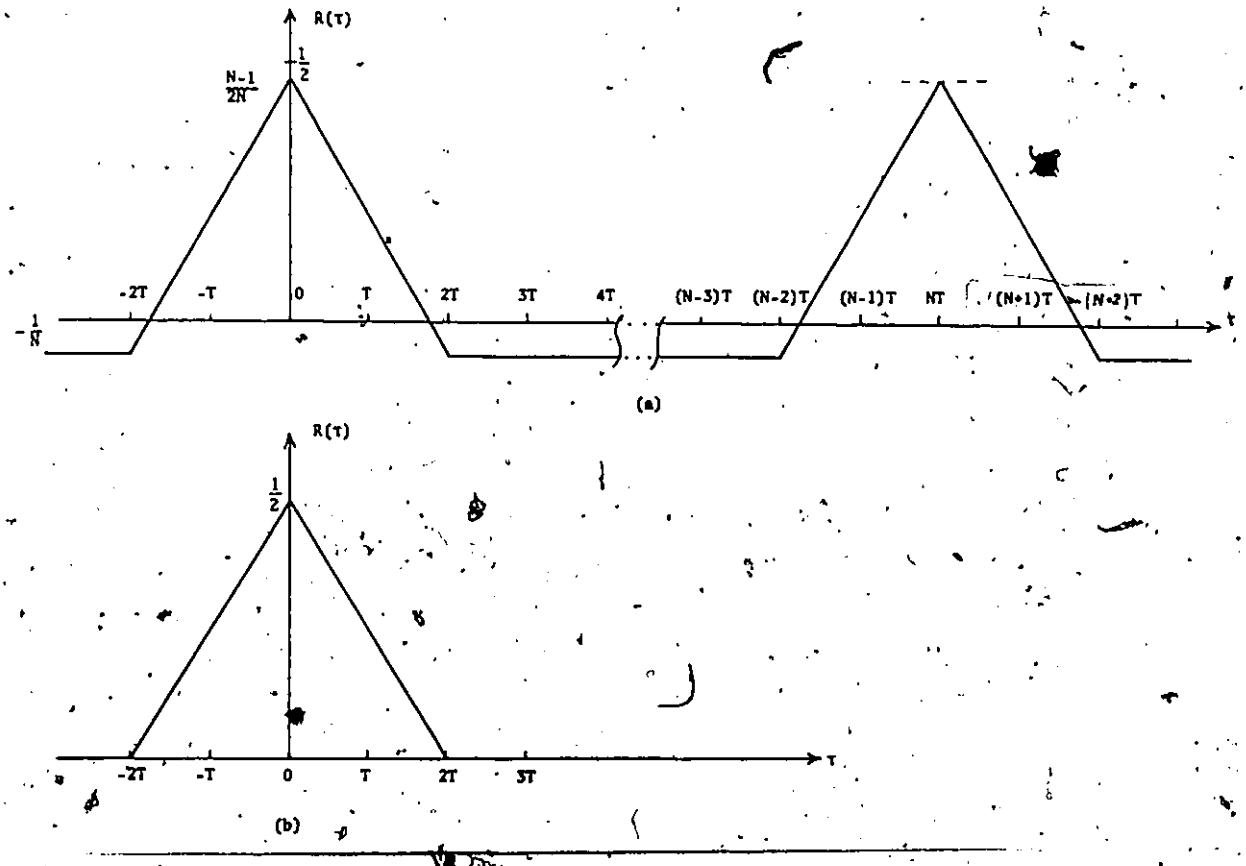

Figure 2-22. Autocorrelation function of a duobinary sequence. (a) With a PRBS input (b) with a random binary input.

From the shape of the autocorrelation function, it is apparent that it can be used to help establish synchronisation. If two identical PRS sequences are out of synchronisation by more than two bit periods, their crosscorrelation is zero. For time differences less than 2 bit periods, the cross correlation is nonzero and its magnitude gives an indication of how large the synchronisation error is.

The calculation of the power spectral density from the autocorrelation function, using (2-53), will now be attempted. Since $R(\tau)$ is periodic, the Fourier transform $G(\omega)$ is given by

$$G(\omega) = \frac{G_0(\omega)}{NT} \sum_{k=-\infty}^{+\infty} \delta(\omega - \frac{2k}{NT}) \qquad (2\text{-}59)$$

where $G_0(\omega)$ is the Fourier transform of one period of $R(\tau)$

$$\text{i.e. } G_0(\omega) = \int_{-NT/2}^{NT/2} R(\tau) e^{-j\omega t} dt$$

Because of the shape of $R(\tau)$, it lends itself to the use of the method of impulses in finding $G_0(\omega)$. This is based on the following properties of the Fourier transform:

If $\mathcal{F}\{f(t)\} = F(\omega)$, then

$$\mathcal{F}\{\frac{d^n f}{dt^n}\} = (j\omega)^n F(\omega)$$

$$\mathcal{F}\{f(t-t_0)\} = e^{-j\omega t_0} F(\omega) \qquad (2\text{-}60)$$

$$\mathcal{F}\{\delta(t)\} = 1$$

$R(\tau)$ is now differentiated (for one period only) until impulses only remain as shown in Fig. 2-23.

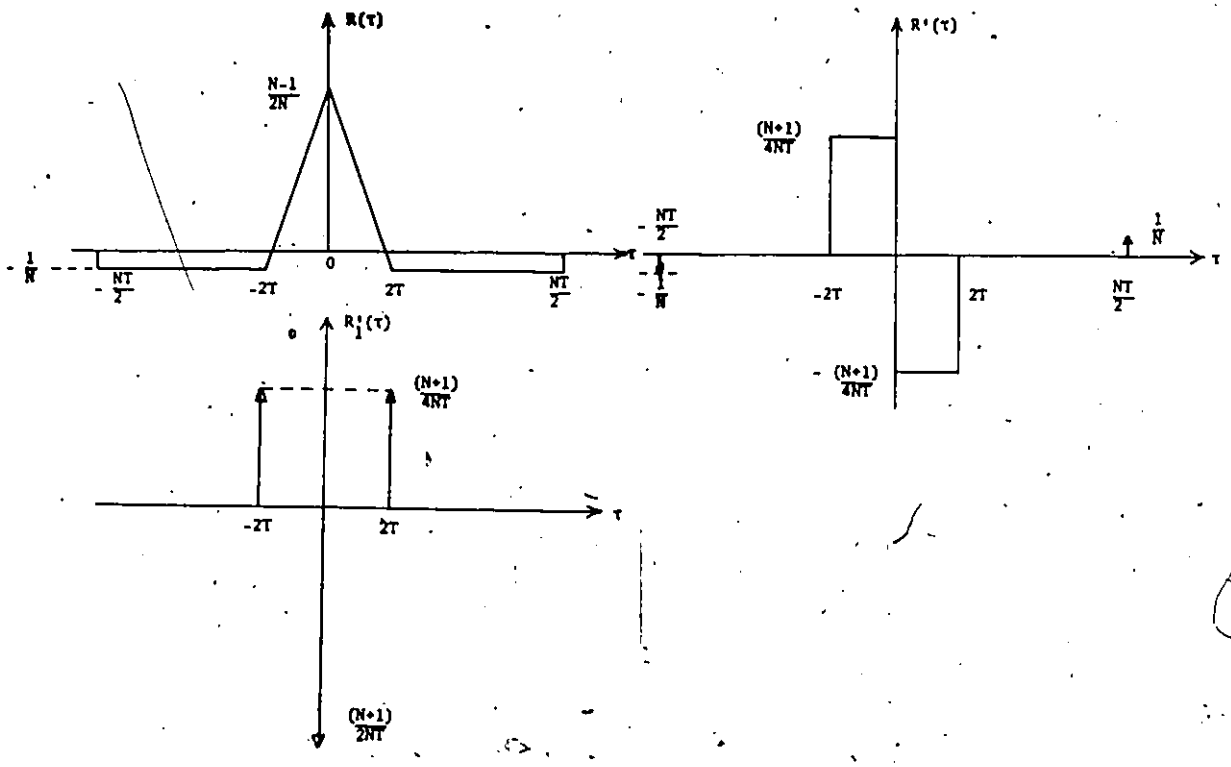

Figure 2-23. Differentiation of $R(\tau)$ to get impulses. $R_1(\tau)$ is $R'(\tau)$ without the impulses.

Using (2-60),

$$\mathcal{F}\{R(\tau)\} = \frac{1}{j\omega}\mathcal{F}\{-\frac{1}{N}\delta(\tau+\frac{NT}{2}) + \frac{1}{N}\delta(\tau-\frac{NT}{2})\} + \frac{1}{(j\omega)^2}\mathcal{F}\{\frac{N+1}{4NT}\delta(\tau+2T) - \frac{(N+1)}{2NT}\delta(\tau) + \frac{(N+1)}{4NT}\delta(\tau-2T)\}$$

$$\mathcal{F}\{R(\tau)\} = \frac{1}{N}\left[\frac{e^{-j\omega\frac{NT}{2}} - e^{j\omega\frac{NT}{2}}}{j\omega}\right] + \frac{N+1}{4NT}\left[\frac{e^{j2\omega T} - 2 + e^{-j2\omega T}}{-\omega^2}\right]$$

or $$G_0(\omega) = \frac{(N+1)}{N}\,T\left(\frac{\sin\omega T}{\omega T}\right)^2 - T\left(\frac{\sin\frac{\omega NT}{2}}{\frac{\omega NT}{2}}\right)$$

$$\therefore\ G(\omega) = \left[\frac{N+1}{N^2}\left(\frac{\sin\omega T}{\omega T}\right)^2 - \frac{1}{N}\left(\frac{\sin\frac{\omega NT}{2}}{\frac{\omega NT}{2}}\right)\right]\sum_{k=-\infty}^{\infty}\delta(\omega - \frac{2k}{NT}) \qquad (2\text{-}61)$$

Now if $\omega = 0$,

$$G(0) = \frac{N+1}{N^2} - \frac{1}{N} = \frac{1}{N^2} \qquad (2\text{-}62)$$

(2-61) and (2-62) may be combined to give

$$G(\omega) = \frac{N+1}{N^2}\left(\frac{\sin\omega T}{\omega T}\right)^2 \sum_{\substack{k=-\infty \\ k\neq 0}}^{\infty} \delta\left(\omega - \frac{2\pi k}{NT}\right) + \frac{1}{N^2}\,\delta(\omega) \qquad (2\text{-}63)$$

It might be worthy of note to point out that (2-63) can be expressed as

$$G(\omega) = \frac{1}{4}\,\Phi(\omega)\left|\, 2\cos(\omega T/2)\right|^2 \qquad (2\text{-}64)$$

$2\cos(\omega T/2)$ is the transfer function for the duobinary encoder. The factor of 4 comes in because for $\Phi(\omega)$, a polar binary sequence (+1 and -1) was assumed, whereas in forming the duobinary sequence here, a unipolar binary sequence (0's and 1's) was assumed.

The measured autocorrelation functions and power spectra for a PRBS of length N = 15 and random data inputs to a duobinary system are shown in Fig. 2-24. The data rate used in the laboratory for these measurements was 64 kb/s.

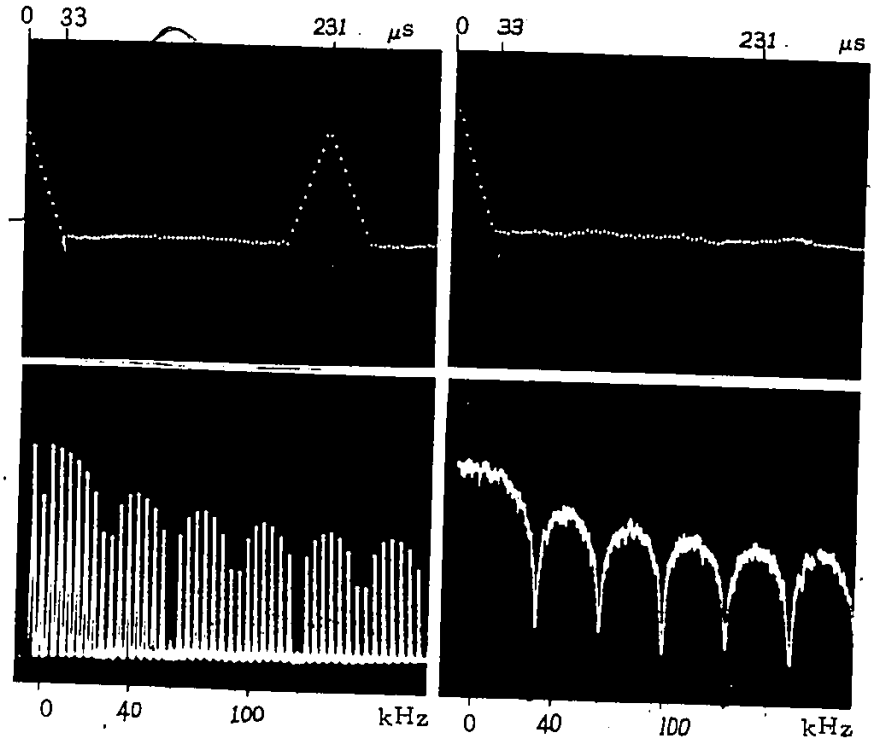

Figure 2-24. Autocorrelation functions and power spectra for duobinary system with
(a) PRBS input of length 15
(b) random input
for a data rate of 64 kb/s.

The transfer function and the spectrum given in (2-64) were obtained elsewhere by alternative methods. The spectrum derivation in this section, however, gave an alternate means to obtain the spectrum and the autocorrelation of a PRS sequence. A knowledge of the autocorrelation function is in turn useful for synchronisation purposes.

CHAPTER THREE

QUADRATURE PARTIAL-RESPONSE SIGNALLING

3.1 Modulation Systems Using PRS

In Chapter Two, partial-response signalling was seen to be an efficient baseband method of transmitting data. It is also suitable for any type of carrier modulation. Since its inception in the early nineteen-sixties, PRS has aroused considerable interest as a possible means of high-speed data transmission. Many authors report application of PRS techniques to various modulation schemes as well as to baseband systems. For example, GTE Lenkurt of the U.S.A.[1] reported a doubling of the capacity of existing baseband systems from 24 to 48 audio channels by retrofitting the existing T1 facilities with 9148A (modified) duobinary repeaters [28-30]. Lender described application of correlative coding techniques to FM [5, 18, 20], AM-PSK [6, 18], and quadrature amplitude modulation (QAM) [31]. Bell Telephone Laboratories used Class IV PRS in single-sideband (SSB) modulation to transmit 2400 b/s through a 1.2 kHz bandwidth on the switched telephone network [32]. GTE Lenkurt has recently completed experiments on a SSB system using seven-level correlative filtering to transmit 12.63 Mb/s in a 3.1 MHz RF bandwidth i.e. an RF bandwidth efficiency of 4 b/s/Hz [33]. Bell Telephone Laboratories also developed a hybrid transmission system whereby seven-level PRS was used to transmit 1.544 Mb/s in the usually vacant 500 kHz band below voice in the radio baseband spectrum

---

1 Companies mentioned hereafter will be of the U.S.A. unless otherwise stated.

[27]. The composite signal (data and voice) is transmitted over the radio as usual in FDM systems. Melvin and Middlestead proposed application of PRS to minimum shift keying (MSK) [34].

Although any of the above modulation methods may be used with PRS in operational systems, QAM enjoys more popularity and in this context it is referred to as Quadrature Partial-Response Signalling (QPRS). For example Avantek has a 2 GHz QPRS digital radio with a spectral efficiency of 1.8 b/s/Hz [35]. Fujitsu of Japan also has a 2 GHz QPRS digital radio which attains 2 b/s/Hz [36]. Microwave Associates has an 11 GHz QPRS digital radio with a spectral efficiency of 2 b/s/H [37]. And Bell-Northern Research (BNR) of Canada has developed an 8 GHz digital radio with 2.25 b/s/Hz of spectral efficiency [38]. The QPRS method is briefly described next.

3.2 The QPRS Method

A simplified block diagram of a QPRS modulator is shown in Fig. 3-1. The incoming (serial) data is scrambled, split into two parallel bit streams, and differentially encoded. Scrambling randomises the data to ensure that any repetitive sequences in the incoming data do not result in sharp spectral spikes in the output spectrum, and provides enough transitions in the demodulated data stream, for clock recovery. Differential encoding and decoding are used to resolve the phase ambiguities generated in recovering the coherent carrier at the receiver. Each of the two bit streams is now converted from the binary

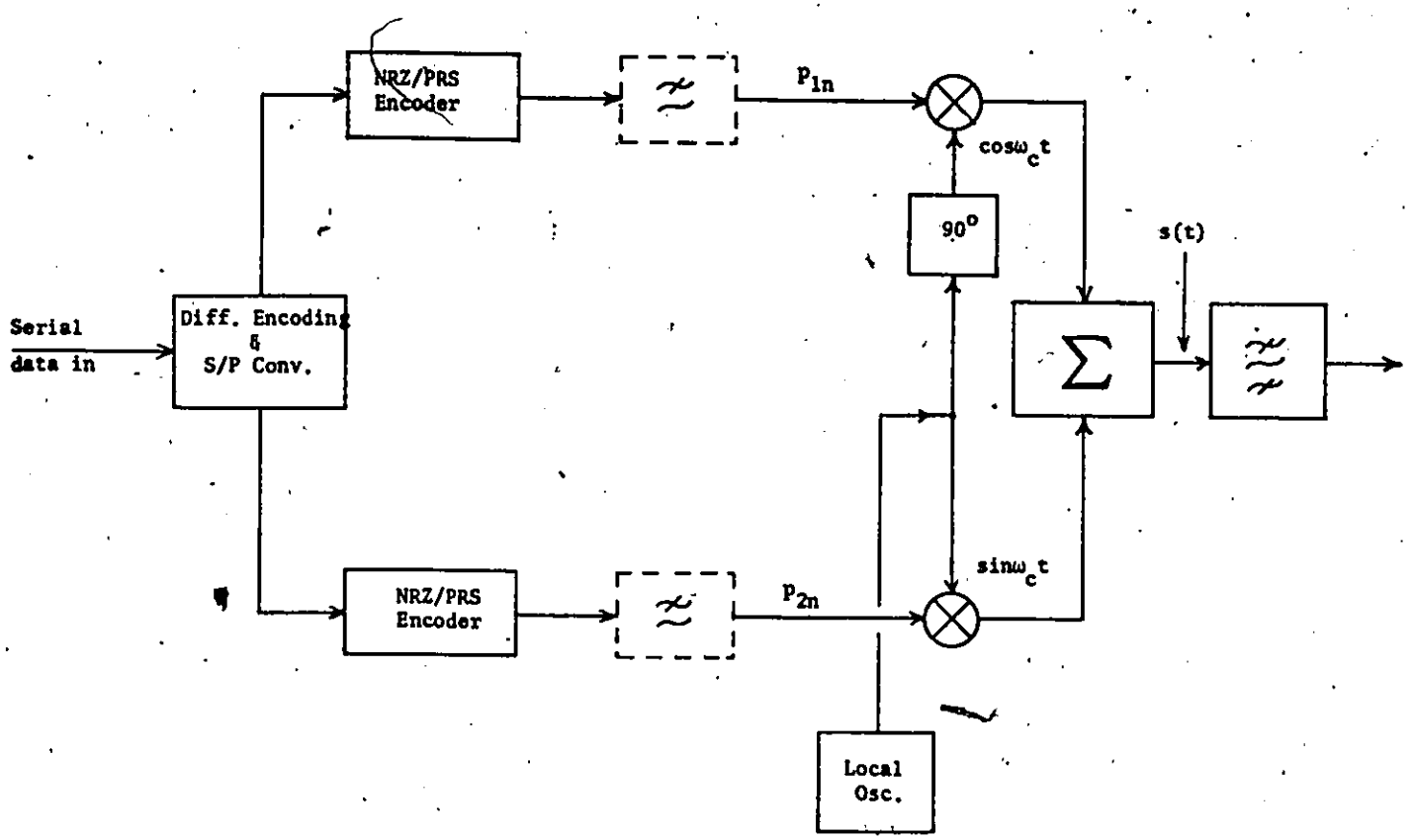

Figure 3-1. A simplified block diagram of a QPRS modulator.

NRZ form to PRS by a simple digital filter followed by a sharp low-pass filter as described in Section 2.3. The PRS data streams are then double-sideband suppressed-carrier amplitude modulated on two orthogonal carriers and the two signals combined. The RF signal is given by

$$s(t) = p_{1n}\cos\omega_c t + p_{2n}\sin\omega_c t \qquad (3\text{-}1)$$

where p_{1n} and p_{2n} are two PRS sequences and $s(t)$ is the resulting RF signal.

The RF signal may be amplified and band-pass filtered before

transmission. Using either Class I or Class IV, this RF signal has nine states as shown in Fig. 3-2. For a precoded Class I PRS signal, in the signal space diagram of Fig. 3-2, all even-numbered signal vectors are assigned to input binary data (0,0), signal vector 9 corresponds to input data (1,1), while all other odd-numbered vectors are assigned to (1,0) or (0,1) in such a way that two signal vectors differing in phase by 180° correspond to the same data input. If the data is equiprobable, signal vector 9 has a probability of 0.25, all even-numbered vectors together have a probability of 0.25, and odd-numbered vectors (excluding 9) have a combined probability of 0.5. These features are used to simplify the demodulator.

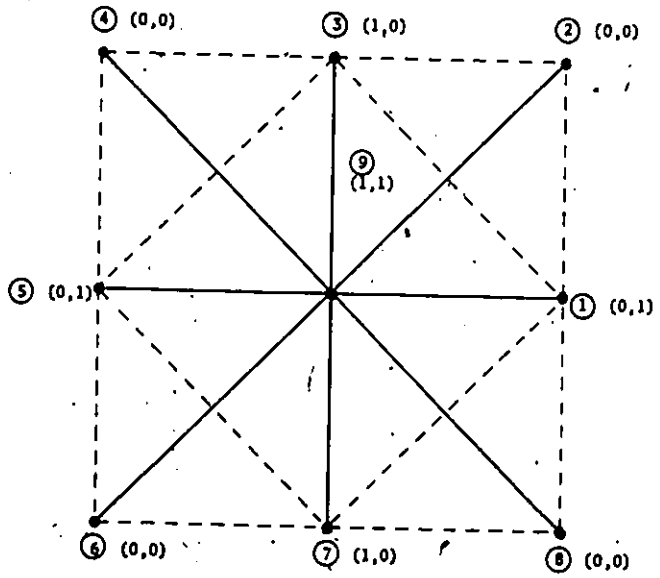

Figure 3-2. RF signal state diagram for QPRS. Data in brackets are for Class I.

Detection of the QPRS signal is most often coherent and very similar to QPSK detection. A simplified block diagram of a QPRS

demodulator is shown in Fig. 3-3. After band-pass filtering to limit noise, the incoming RF signal is split into two identical signals which are multiplied with recovered quadrature carriers. The resulting

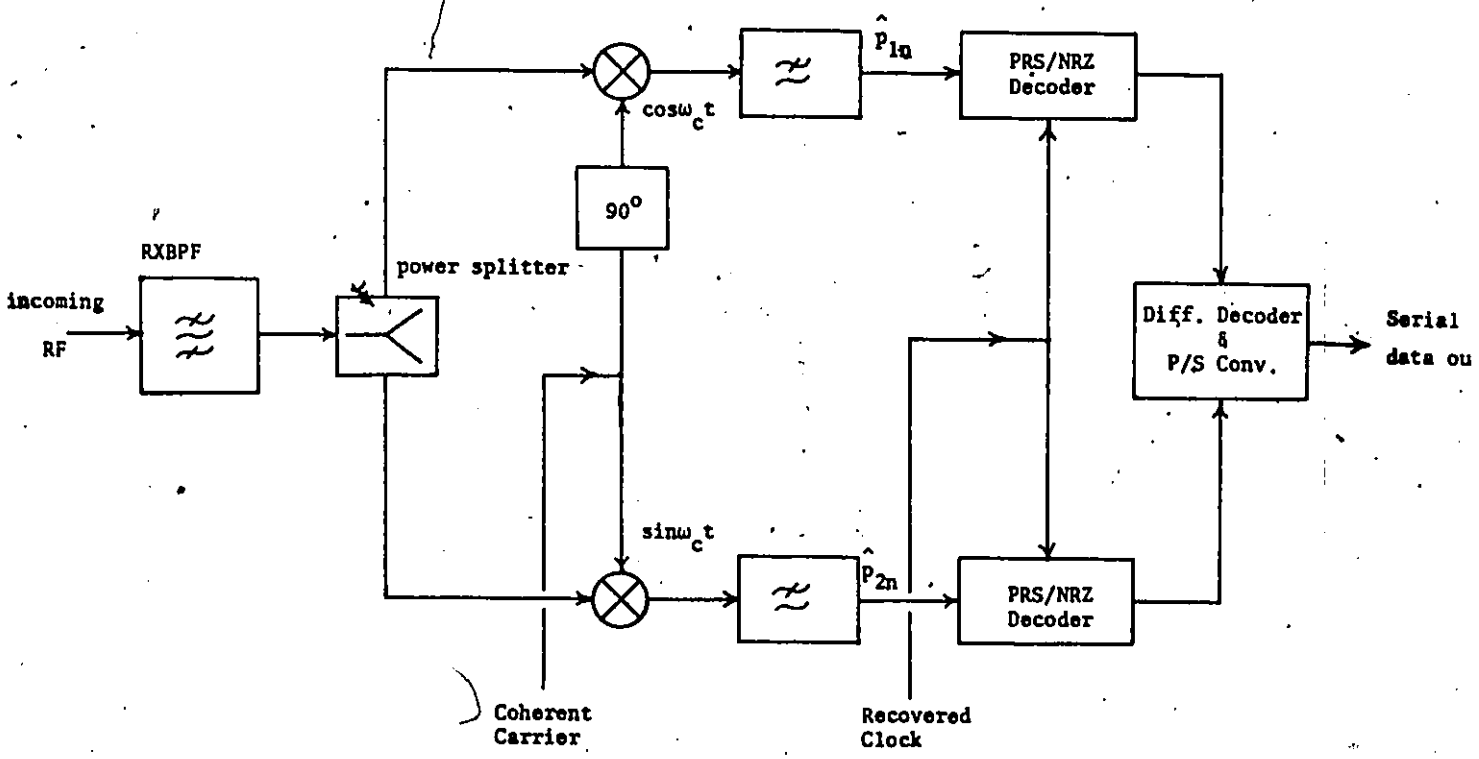

Figure 3-3. A simplified block diagram of a QPRS demodulator.

signals are then low-pass filtered to recover the three-level PRS signals ($\hat{p}_{1n}$ and $\hat{p}_{2n}$). The PRS to binary NRZ decoder may consist of either a full-wave rectifier followed by a threshold comparator or two slicers followed by simple combinatorial logic. The reverse operations to those of the transmitter then follow i.e. differential decoding, parallel-to-serial conversion, and descrambling.

The few paragraphs above have described the basic QPRS modem.

Many variations of this are usually found. For example, some systems do the modulation in two steps by using an intermediate frequency (IF) stage followed by an upconvertor whereas others use direct modulation at RF. Whereas PRS conversion is shown in Fig. 3-1 as being accomplished fully in the transmitter, it may also be split between the transmitter and receiver filters. Some systems have used a quadraphase modulator and filtered the resulting QPSK signal after the final power amplification [39]. To explain the problem associated with power amplification, a further comment on the signal state diagram of Fig. 3-2 appears warranted. The signal state diagram is very similar to that of the 8-ary amplitude-phase shift keying (APK) except that the latter does not have the extra state with zero amplitude. Both modulation methods have variations in signal amplitude. Owing to these amplitude variations, QPRS will suffer a degradation caused by AM/AM and AM/PM conversions in a system with nonlinearities, which affect the overall system gain [40]. For this reason, several companies have avoided it for satellite or microwave use.

However, as Lender showed [18], partial response can be generated by the use of filters designed using frequency domain concepts. The combined effect of the transmit and receive filtering after power amplification have been used by some companies to yield the PRS signal, thus eliminating the degradation due to nonlinearities.

A QPRS modem is relatively simple, being slightly more complex than that of QPSK. Hence QPRS becomes competitive to 8-ϕPSK as indicated by the rising number of digital radios using it.

In a gaussian noise environment, QPRS has a probability of error performance given by [36]

$$P(e) = (3/4)\ \mathrm{erfc}[(1/2)\ \sqrt{C/N}] \qquad (3\text{-}2)$$

where C is the average carrier power, and N is the noise power at the output of the receiving filter. In Fig. 3-4 the bit error-rate (BER) or P(e) characteristics for QPRS and other modulation methods are shown. It is seen that for $P(e) = 10^{-6}$, QPRS needs 3dB more CNR than QPSK and about 2dB less CNR than 8-ϕPSK.

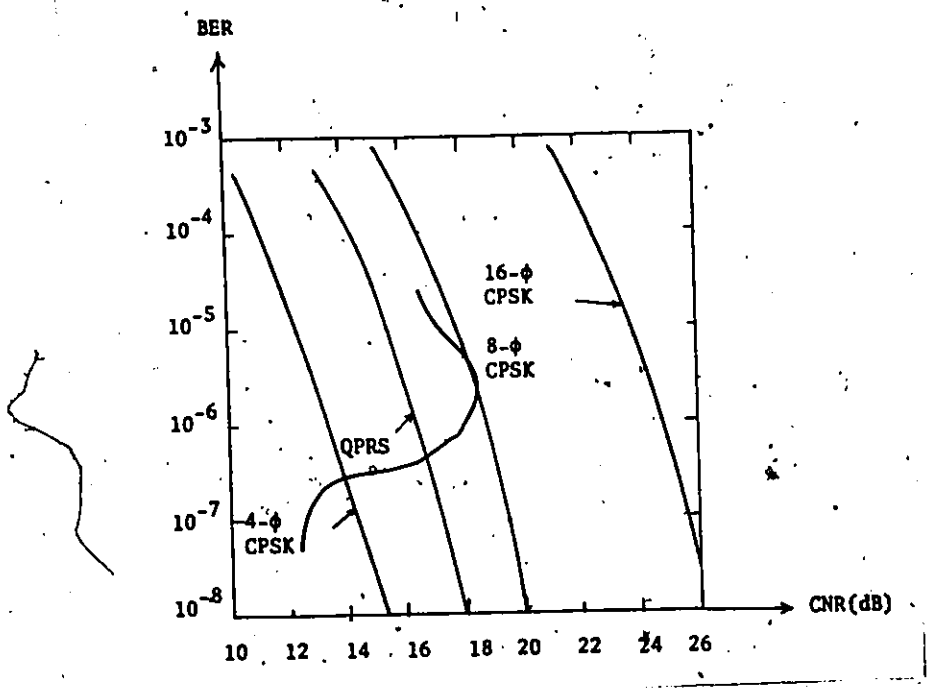

Figure 3-4. Bit error rate characteristics of various modulation techniques. Noise is measured in the Nyquist band.

For efficient data transmission by radio, QPRS competes with 8-ϕPSK [41]. The two methods will be compared. However, before the comparison, a brief review of the principles of 8-ϕPSK would not appear out of place and now follows.

3.3 Principles of Eight-Phase Modulation

Eight-phase PSK systems with eight phase states and a theoretical efficiency of 3 b/s/Hz are frequently used for high-speed data transmission. Based on the Nyquist minimum bandwidth theorem, it is possible to transmit one symbol per second in one hertz of radio frequency bandwidth. Practical systems nowadays exceed this minimum bandwidth by about 10% to 50%. Wideband filtering is desirable for achieving a faithful reproduction of the transmitted information (minimum intersymbol interference). However, in order to effectively utilise the spectrum and reduce both noise and interchannel inteference, narrow bandwidth is desirable. Therefore trade-offs must be made to obtain optimum performance [42].

A simple technique of producing an 8-ϕ PSK signal [4] is as indicated in the block diagram of Fig. 3-5. The incoming serial data stream (already scrambled) is split into three parallel data streams A, B, and C. The two-level to four-level coder provides one of the four possible levels of a polar baseband signal at "a" and "b". If the bit at A (or B) is a "1", then the output level at "a" ("b") has one of the two possible signal states (positive or negative). If it is a "0", then the output level at "a" (or "b") assumes the alternate state. The bit at C is used to determine whether the larger or smaller signal level should be present at "a" or at "b". When the bit at C is a "1", the amplitude of "a" is greater than that of "b"; if a "0", the opposite is true. The four-level polar baseband signals at "a" and "b" then double-sideband suppressed-carrier amplitude modulate two quadrature carriers. The two signals are combined, possibly amplified,

and band-pass filtered before being transmitted. The phase vector positions and their three bit designations are also shown in Fig. 3-5.

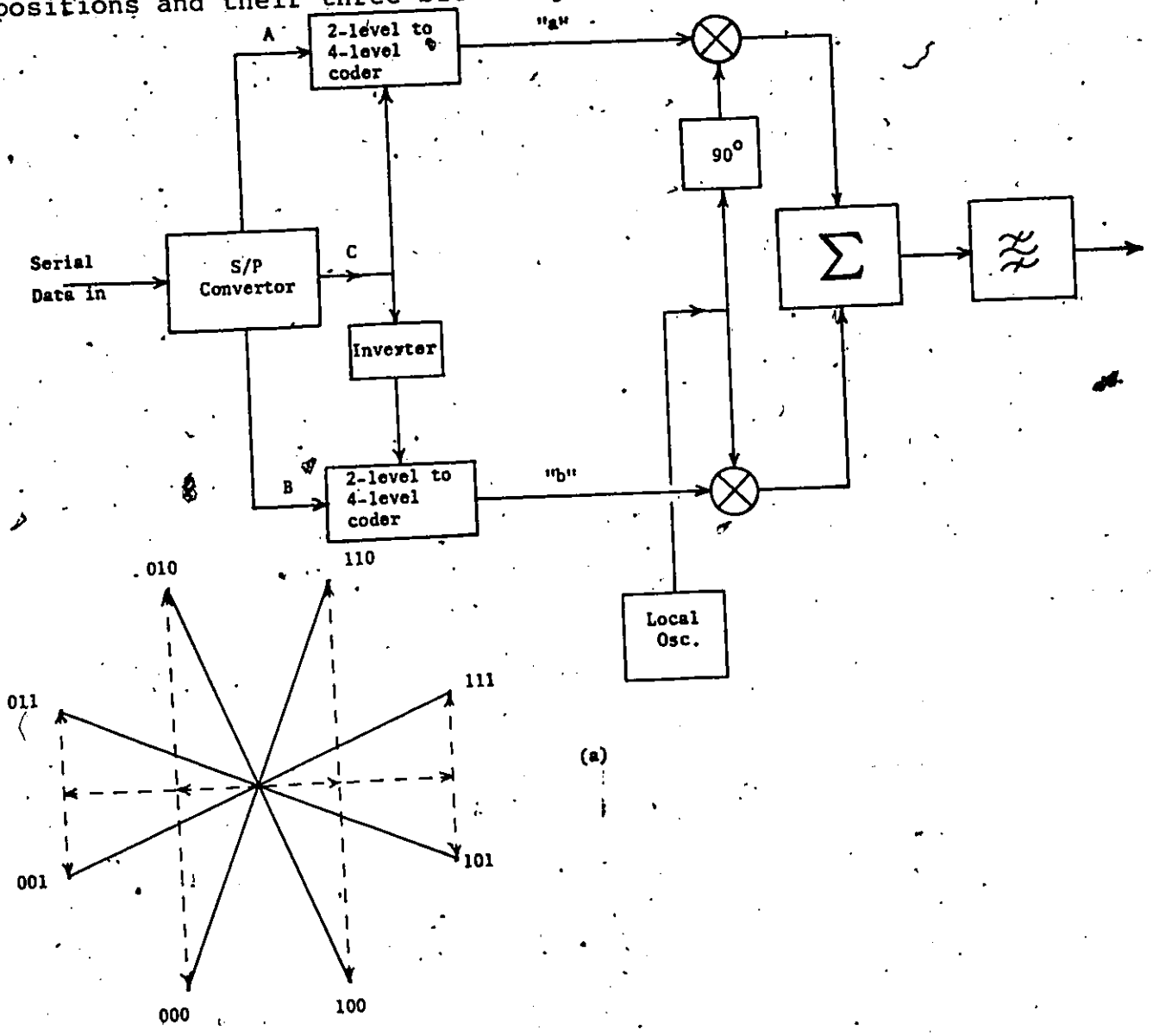

Figure 3-5. 8-phase PSK, (a) generation (b) phase positions and their bit designations.

Another method of generating an 8-ϕ PSK signal, using digital

phase-shifting network to generate each phase, has been reported by Wood [43].

Fig. 3-6 shows the block diagram of the coherent detection method for 8-ϕPSK. Each detector in the diagram consists of a double-balanced modulator followed by a low-pass filter and a zero-crossing detector. The four modulators are fed with a reference carrier at 0°, 90°, and 45° as shown. The 0° reference detector detects the digits of the A stream, the 90° reference detects the B stream digits, while

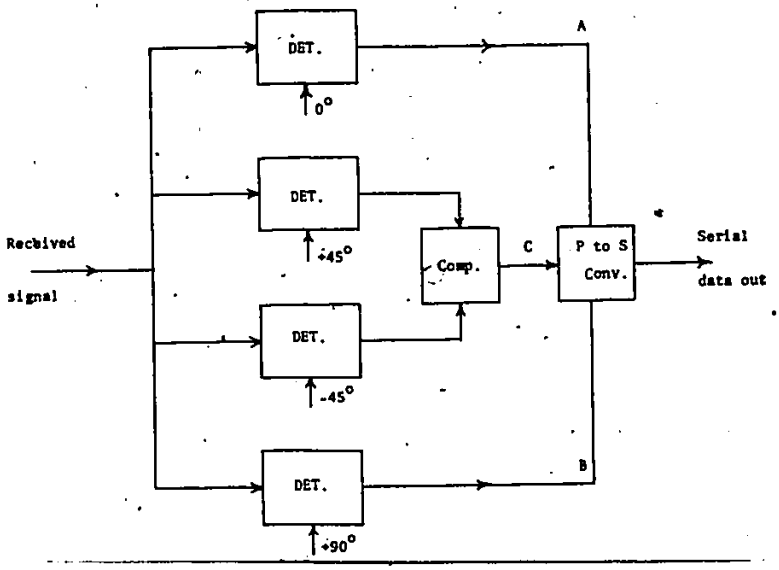

Figure 3-6. Coherent detection of an 8-ϕ signal.

digits of the C stream are determined by comparing the outputs of the ±45° reference detectors - like outputs indicate a "1" and unlike outputs a "0".

Sometimes the information may be encoded in terms of phase changes and detection done by comparing phases of adjacent symbols. This is called differential phase detection. Coherent phase detection

is theoretically optimum, but in certain cases of practical importance obtaining and maintaining a coherent phase reference in the receiver may not be feasible. Differential detection, on the other hand, requires only short-term phase stability in transmission.

It has been shown [17, 44], that for coherent detection of multiphase systems, the probability of error for high input S/N ratios can be expressed as

$$p(e) \approx \frac{e^{-\frac{S}{N}\sin^2\frac{\pi}{n}}}{\sqrt{\pi\frac{S}{N}}\sin\frac{\pi}{n}} \qquad (3\text{-}3)$$

where S = average signal power

N = mean noise power in the measured bandwidth and

n = number of phase positions,

and in the case of phase comparison detection:

$$p(e) = \frac{e^{-2\frac{S}{N}\sin^2\frac{\pi}{2n}}}{\sqrt{2\pi\frac{S}{N}}\sin\frac{\pi}{2n}} \qquad (3\text{-}4)$$

A comparison of equations (3-4) and (3-4) would indicate that for a high signal-to-noise ratio and a large n($n > 4$), phase comparison detection yields about a 3dB degradation over coherent detection. The relatively simpler hardware realisation of the phase comparison detector might, in some cases, justify this 3dB loss. However, most of

the recently developed modems have been implemented with coherent detection.

3.4 Comparison of 8-PSK and QPRS Systems

A comparison of digital microwave systems using 8-phase shift keying and quadrature partial-response signalling modulation methods is now made.

For about the same spectrum utilisation, same bit rate, and the same BER (say 10^{-6}), an excellent parameter for system comparison is the system gain. This is given, in dB, by the difference between the transmitter output power (dBm) and the receiver threshold or sensitivity (dBm) at a specified BER.

For a particular CNR ratio requirement, the receiver threshold can be obtained as the sum of that CNR and the noise power (dBm) in the bit-rate bandwidth. The noise power is given by

$$N_b = kTBF \qquad (3\text{-}5)$$

where N_b = noise power in watts

k = Boltzmann's constant (= 1.38×10^{-23} J/K)

T = absolute temperature in kelvins

B = bit rate bandwidth in hertz

F = receiver noise figure.

Taking T = 290 K (24.7 dB-K) and k = -228.6 dBW/K-Hz, one gets

$$C_{th} = CNR - 174 + 10 \log_{10} B + F \text{ (dBm)} \qquad (3\text{-}6)$$

where C_{th} is the receiver threshold and CNR is the required carrier-to-noise ratio (in the bit-rate bandwidth).

The theoretical energy per-bit-to-noise density ratio (E_b/N_o) requirements for a 10^{-6} BER are 12.7 dB and 14.2 dB for QPRS and 8-PSK respectively, giving QPRS a 1.5 dB advantage [40]. Nippon Electric Company of Japan gives measured results for single-hop system gain reduction (due to nonlinearities in the TWT amplifier) of 7 to 8 dB for QPRS and 2 to 3 dB for 8-phase PSK with a roll-off factor $\alpha = 0.5$. The difference is mainly due to amplitude variations in QPRS (Fig. 3-2) while 8-phase PSK has the same amplitude for all vectors (Fig. 3-5). Hence it was found that experimentally, QPRS required an E_b/N_o of 14.2 dB and a TWT output back-off of 5.5 dB, whereas 8-phase PSK with $\alpha = 0.5$ required an E_b/N_o of 16.2 dB and a back-off of 0 dB [40]. Based on this, it would appear that 8-phase PSK has a 3.5 dB of system gain advantage over QPRS for a BER of 10^{-6} when a TWT amplifier is used in a nonlinear mode. However, this assumes that partial-response filtering is done prior to the final power amplification. As noted earlier, PRS can be achieved by filtering after the final transmit amplifier thus reducing degradation due to nonlinearities.

Hardware complexity and cost can be a deciding factor in the choice of a modulation method. QPRS is relatively simple hardwarewise;

being a little more complex than QPSK. Eight-phase PSK has a higher complexity than QPRS, hence it might be more costly. In some cases, however, it is possible to reduce the system cost by using nonregenerative repeaters at the price of a small performance-reduction.

It is apparent therefore, that for E_b/N_o considerations, QPRS can give comparable performance (if filtering is done after the TWT) to 8-phase PSK while reducing the equipment complexity, hence cost. In linear applications, considering E_b/N_o, QPRS would seem a better modulation method. On the other hand, 8-phase PSK is more bandwidth efficient.

Several manufacturers have developed digital microwave radios which use either 8-ϕPSK or QPRS modulation techniques [45]. System performance of several digital microwave radio systems will be summarised in two tables. Only systems described in the readily available literature are considered [35-40, 42, 43, 46-50]. Table II lists some of the more significant parameters of the low- and medium-capacity systems, while Table III lists these parameters for the high-capacity systems. Low-capacity systems here are defined as systems with bit rates up to 10 Mb/s. Medium capacity refers to bit rates up to 45 Mb/s, while high-capacity systems are taken to mean those with bit rates more than 45 Mb/s. These tables provide an insight into the currently achieved performance of modern digital radio systems and in particular that of QPRS and 8-ϕPSK.

One should resist the temptation of classifying the systems listed in Tables II and III into any order of merit, because other

considerations should be taken into account for an absolute comparison. For example, some systems operate at 11 GHz while others operate at 8 GHz and 6 GHz, and it is more difficult to design a high power amplifier at higher frequencies than at lower frequencies. The insertion loss of the microwave filters (for those systems doing spectral shaping by filtering after the final transmit amplifier) has not been considered since no data were available on these. These would have an effect of decreasing the output power from the transmitter, thus reducing the system gain. Finally, the comparison would not be complete without the addition of an extra row labelled "cost".

From the tables, it is seen that low-capacity radio systems have bandwidth efficiencies ranging from 1.8 b/s/Hz to 2.2 b/s/Hz, while bandwidth efficiencies for high-capacity radio systems vary from 2 b/s/Hz to 3 b/s/Hz. Higher spectral efficiencies are achievable using more complex modulation techniques such as 16-ary APK [3] and single-sideband seven-level PRS [33], and in fact the race for 4 b/s/Hz and above is already under way.

Table II

SYSTEM PARAMETERS FOR LOW- AND MEDIUM-CAPACITY RADIOS

SYSTEM PARAMETER	NIPPON	FUJITSU	AVANTEK	NIPPON (Operated by SPC*
Frequency Band (GHz)	2	2	2	6(11)
Type of Modulation	8-PSK	QPRS	QPRS	8-PSK
Bit Rate (Mb/s)	6.3 (7.8)	6.302	6.313	43.315
Capacity	4T1 (5T1)	4T1	4T1	28T1
Transmitter Output Power (dBm)	+34.8	+27	+27	+35
Receiver Sensitivity for 10^{-6} BER (dBm)	-81.5 (-85)	-82.7	-82	-68 (-66) (for 10^{-8})
System Gain at 10^{-6} BER (dB)	116.3 (119.8)	109.7	109	103 (101)
Receiver Noise Figure (dB)	6 (2.5)	5	6	8 (10)
Noise Power (in bit rate B.W.)(dBm)	-100 (-103.5)	-101	-100	-89.7 (-87.6)
Required Practical C/N (in bit rate B.W.) for 10^{-6} B.E.R. (dB)	18.5	18.3	18	21.6 (21.6)
Theoretical Required C/N (in bit rate B.W.) for 10^{-6} B.E.R. (dB)	13.8	12.7	12.7	13.8
Occupied RF Bandwidth (MHz)	3.5	3.5	3.5	22.6
Spectral Efficiency (b/s/Hz)	1.8 (2.2)	2	1.8	2

Figures in this column are for a FET amplifier used at the receiver.

* SPC - Southern Pacific Communications (previously DATRAN)

Table III

SYSTEM PARAMETERS FOR HIGH-CAPACITY RADIOS

SYSTEM PARAMETER	NEC-6 GHz	NEC-11 GHz	GTE LENKURT	RAYTHEON	COLLINS	MICROWAVE ASSOCIATES	BNR	COLLINS 6 GHZ
Frequency Band (GHz)	6	11	11	6	11	11	8	6
Type of Modulation	8-PSK	8-PSK	8-PSK	8-PSK	8-PSK	QPRS	QPRS	8-PSK
Bit Rate (Mb/s)	78	90	90	90	90.258	79.2	91.040	90.258
Capacity	48T1	56T1	56T1	56T1	56T1	48T1	56T1	56T1
Transmitter Output Power (dBm)	+37	+37	+37	+40	+40	+26	+40	+40
Receiver Sensitivity for 10^{-6} B.E.R. (dBm)	-69 (-72)	-68	-66	-65.5	-68	-69	-68.3	-68.6
System Gain at 10^{-6} B.E.R. (dB)	106 (109)	105	103	105.5	108	95	108.3	108.6
Receiver Noise Figure (dB)	6.5 (3.5)	8	10	6.5	8	8*	8*	8
Noise Power (in bit rate B.W.)(dBm)	-88.6(-91.6)	-86.5	-84.5	-88.0	-86.4	-87.0	-86.4	-86.4
Practical Required C/N (in bit rate B.W.) for 10^{-6} B.E.R. (dB)	19.6	18.5	18.3	22.5	18.4	18	18.1	17.9
Theoretical Required C/N (in bit rate B.W.) for 10^{-6} B.E.R. (dB)	13.8	13.8	13.8	13.8	13.8	12.7	12.7	12.7
Occupied RF Bandwidth (MHz)	30	40	40	30	40	39.6	40.74	30
Spectral Efficiency (b/s/Hz)	2.6	2.3	2.25	3	2.25	2	2.25	3

Figures in this column are for a FET amplifier used at the receiver.

* Assumed

CHAPTER FOUR

PERFORMANCE OF PRS SYSTEMS

4.1 Introduction

Any transmission system is disturbed by the ubiquitous thermal (or gaussian) noise and various types of interferences. The performance of PRS systems, as reported in the literature, has been evaluated mainly in a random additive white gaussian noise (AWGN) environment. However, the effect of a spurious signal, or interference, falling in the band of the desired signal is important especially in a congested frequency plan where adjacent channels are closely spaced. The performance analysis of PRS systems in an interference environment has not been fully reported in the readily available literature [55].

In this chapter, as well as evaluating the performance of a PRS system in an AWGN environment, the effect of an interfering signal on the performance of a PRS system is considered. Performance is first evaluated where interference, sinusoidal or square-wave is the only perturbing factor, and then where both AWGN and interference additively corrupt the desired signal.

The performance of a system depends on how the required transfer function, H(f), is achieved. Any series combination of the transmit filter, channel, and receive filter may be used. Several apportionment of the transfer function between the transmitter and the receiver have been considered [15, 51]. For example Kretzmer [7] considered the filtering equally distributed between the transmitter and the receiver. This model is known to be optimum in the sense that for a given

probability of error, it has the smallest signal-to-noise ratio requirement compared to other models. In practice, however, it might be difficult to implement the transfer function $|H(f)|^{\frac{1}{2}}$, and it might not meet FCC or other regulations. A straightforward method of generation of a PRS signal is where the transmitter and the channel determine the spectral shaping while the receive filter is used to bandlimit the noise [52]. This model is usually easier to implement although it is not optimum in performance. Other models can be obtained by designing a suitable transmit filter which together with the corresponding receive filter give the desired characteristic. This may be combined with a decision feedback equaliser at the receiver [38].

4.2 Performance in an AWGN Environment

In this section the effect of random gaussian noise is considered. An M-level Class I (polybinary) signal with precoding is assumed. It may be recalled from Section 2.3, that for an M-level Class I signal, if the levels are numbered consecutively from zero to M-1 starting from the bottom, then a SPACE or "0" is represented by an even-numbered level and a MARK or "1" by an odd-numbered level. It then follows that an error occurs only when noise changes an odd-numbered level into an even-numbered level or vice-versa.

Let the peak-to-peak amplitude of the signal be 2V volts, as shown in Fig. 4-1. Then the distance between any two adjacent levels is $\frac{2V}{M-1}$. Decision threshold levels are set midway between any two adjacent levels. Hence, the distance between any signalling level and the adjacent threshold level is

$$d = \frac{V}{M-1} \tag{4-1}$$

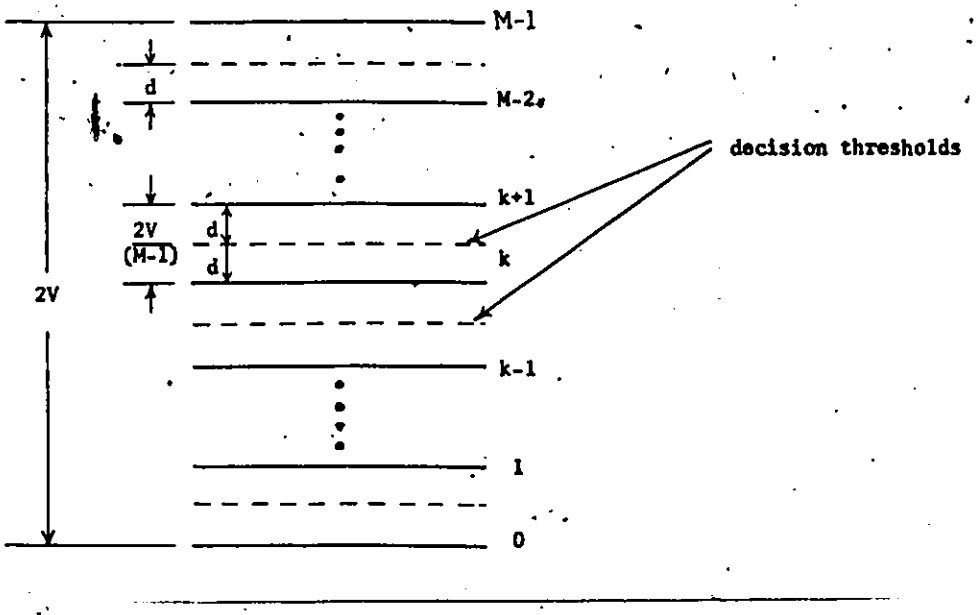

Figure 4-1. Polybinary signalling levels.

If the a priori probability that the k^{th} level is transmitted is P_k, and the conditional probability that an error is made in detection when the k^{th} level is transmitted is $P_{e|k}$, then the probability of error is given by

$$P(e) = \sum_{k=0}^{M-1} P_k P_{e|k} \tag{4-2}$$

The probability P_k is found as follows.

Each level of a polybinary signal is formed by adding (M-1) digits of the precoded sequence $\{b_n\}$. The level is k if there are exactly k 1's in that group of digits.

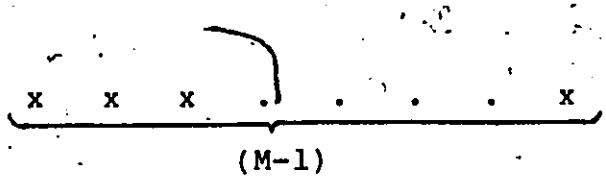

If MARK and SPACE are equally likely, i.e., $P(1) = P(0) = \frac{1}{2}$, then sequence $\{b_n\}$ is purely random, i.e. each bit can be a 1 or a 0 with probability $\frac{1}{2}$.

The probability that there are exactly k 1's in a group of (M-1) digits is

$$(\tfrac{1}{2})^{k}(\tfrac{1}{2})^{M-1-k} = (\tfrac{1}{2})^{M-1}$$

But there are $\binom{M-1}{k}$ such possible combinations.

$$\therefore P_K = (\tfrac{1}{2})^{M-1}\binom{M-1}{k} \qquad k = 0, 1, 2, \ldots, M-1 \qquad (4-3)$$

To find $P_{e|k}$ in (4-2) consider the case when the k^{th} level is transmitted. An error will occur if at the sampling instant, the sum of level k and noise, i.e. the sampled value, is in one of the regions $(2d(k\pm1)-d,\ 2d(k\pm1)+d)$, $(2d(k\pm3)-d,\ 2d(k\pm3)+d)$, etc. In other words an error occurs if noise is in the amplitude zones $(\pm d, \pm 3d)$, $(\pm 5d, \pm 7d)$ etc. These zones are shown in Fig. 4-2 below.

It should be borne in mind that the end levels (k = 0, M-1) have detection zones $(-\infty, d)$ and $((2M-3)d, \infty)$ respectively.

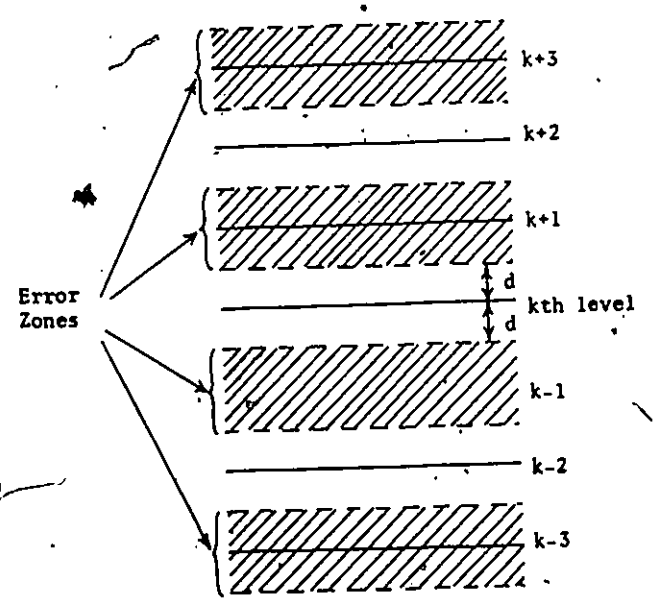

Figure 4-2. Error zones when k^{th} level is transmitted.

Several cases are distinguished.

1) M-1 is even

(a) k is even, $\therefore$ M-1-k even

In this case levels k, 0, and M-1 represent the same bit. This implies that noise pulling the kth level into the regions $((2M-3)d, \infty)$ and $(-\infty, d)$ causes no error. The error zones are shown in Fig. 4-3 (a).

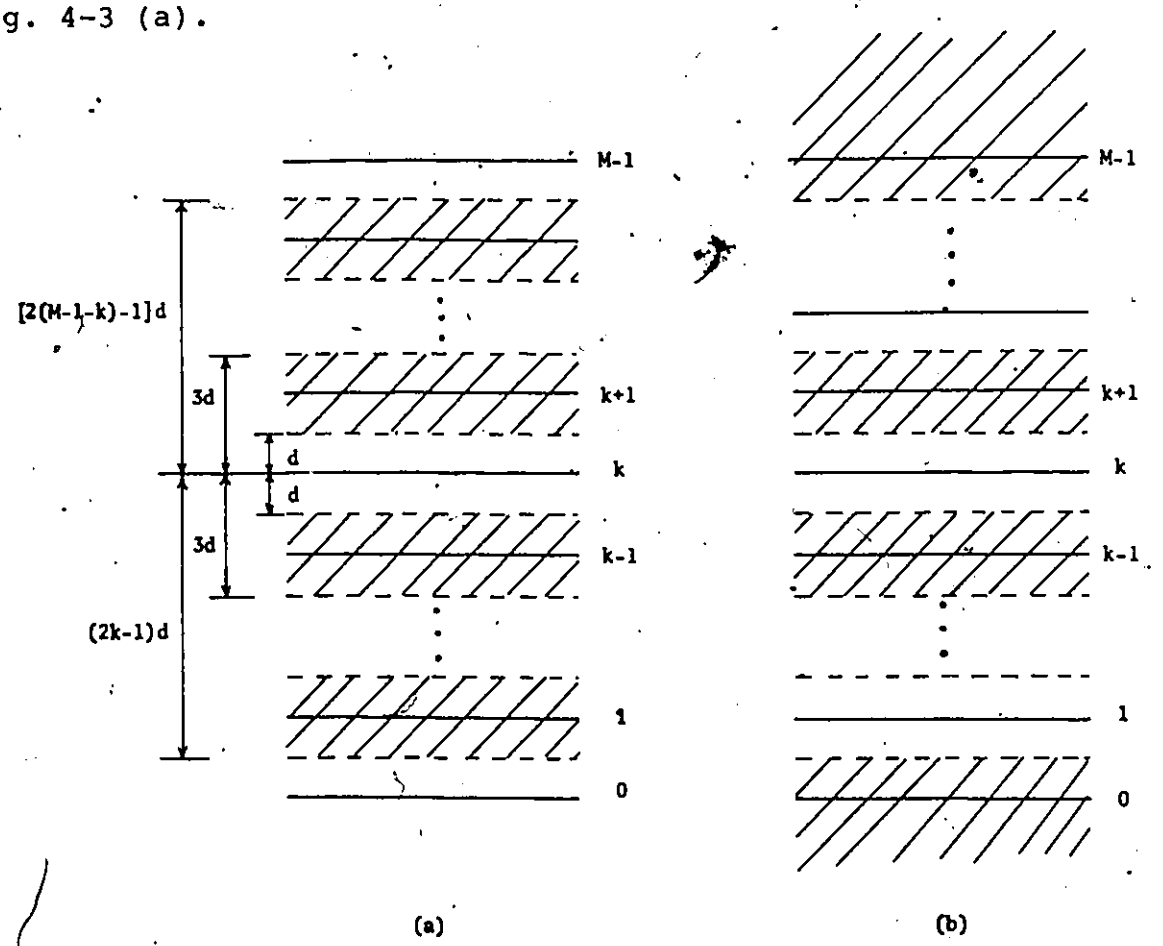

Figure 4-3. Error zones for when kth level is transmitted, for M-1 even, (a) k is even (b) k is odd.

Errors due to noise of positive amplitudes have a probability given by

$$P^{+}_{e|\ k\ \text{even}} = \sum_{i=1}^{M-1-k} (-1)^{i} Q[(2i-1)d]. \qquad (4\text{-}4)$$

where Q(nd) is the area under the gaussian curve, bounded by the ordinates 0 and nd.

Errors due to noise of negative amplitudes have a probability given by

$$P^{-}_{e|\ k\ \text{even}} = \sum_{i=1}^{k} (-1)^{i} Q[(2i-1)d] \qquad (4\text{-}5)$$

Therefore, the probability of error $P_{e|\ k\ \text{even}}$ is given by

$$P_{e|\ k\ \text{even}} = P^{+}_{e|\ k\ \text{even}} + P^{-}_{e|\ k\ \text{even}} = \sum_{i=1}^{M-1-k} (-1)^{i} Q[(2i-1)d] + \sum_{i=1}^{k} (-1)^{i} Q[(2i-1)d] \qquad (4\text{-}6)$$

(b) k is odd . M-1-k is odd.

In this case the level k represents a bit which is opposite to that represented by both levels 0 and M-1. The error zones are shown in Fig. 4-3(b). It is evident that

$$P^{+}_{e|\ k\ \text{odd}} = \tfrac{1}{2} + \sum_{i=1}^{M-1-k} (-1)^{i} Q[(2i-1)d] \qquad (4\text{-}7)$$

and

$$P^{-}_{e|\ k\ \text{odd}} = \tfrac{1}{2} + \sum_{i=1}^{k} (-1)^{i} Q[(2i-1)d]$$

Therefore, the probability of error $P_{e|\ k\ \text{odd}}$ is given by

$$P_{e|\ k\ \text{odd}} = P^{+}_{e|\ k\ \text{odd}} + P^{-}_{e|\ k\ \text{odd}} = 1 + \sum_{i=1}^{M-1-k} (-1)^{i} Q[(2i-1)d] + \sum_{i=1}^{k} (-1)^{i} Q[(2i-1)d] \tag{4-8}$$

Now the probability of error for M-1 even is given from (4-2) by

$$P(e) = \sum_{k=0}^{M-1} P_k P_{e|\ k} = \sum_{k=0}^{M-1} \left\{ P_{k\ \text{odd}} P_{e|\ k\ \text{odd}} + P_{k\ \text{even}} P_{e|\ k\ \text{even}} \right\} \tag{4-9}$$

Using (4-6), (4-8), and (4-9) one gets

$$P(e) = \sum_{k=0}^{M-1} P_{k\ \text{odd}} + \sum_{k=0}^{M-1} \left\{ (P_{k\ \text{odd}} + P_{k\ \text{even}}) \left[\sum_{i=1}^{M-1-k} (-1)^{i} Q[(2i-1)d] + \sum_{i=1}^{k} (-1)^{i} Q[(2i-1)d] \right] \right\} \tag{4-10}$$

Now $P_{k \text{ odd}} + P_{k \text{ even}} = P_k$. Since a SPACE is represented by all even levels and a MARK by all odd levels one may write

$$\sum_{k=0}^{M-1} P_{k \text{ odd}} = P(\text{MARK}) = \tfrac{1}{2}$$

because $P(\text{SPACE}) = P(\text{MARK}) = \tfrac{1}{2}$.

Hence (4-10) becomes

$$P(e) = \tfrac{1}{2} + \sum_{k=0}^{M-1} P_k \left\{ \sum_{i=1}^{M-1-k} (-1)^i Q[(2i-1)d] + \sum_{i=1}^{k} (-1)^i Q[(2i-1)d] \right\} \quad (4\text{-}11)$$

2) M-1 is odd

(a) k is even. $\therefore$ M-1-k is odd

Here levels 0 and k represent the same bit while level M-1 represents the opposite bit. Fig. 4-4(a) shows the error zones for the k^{th} level.

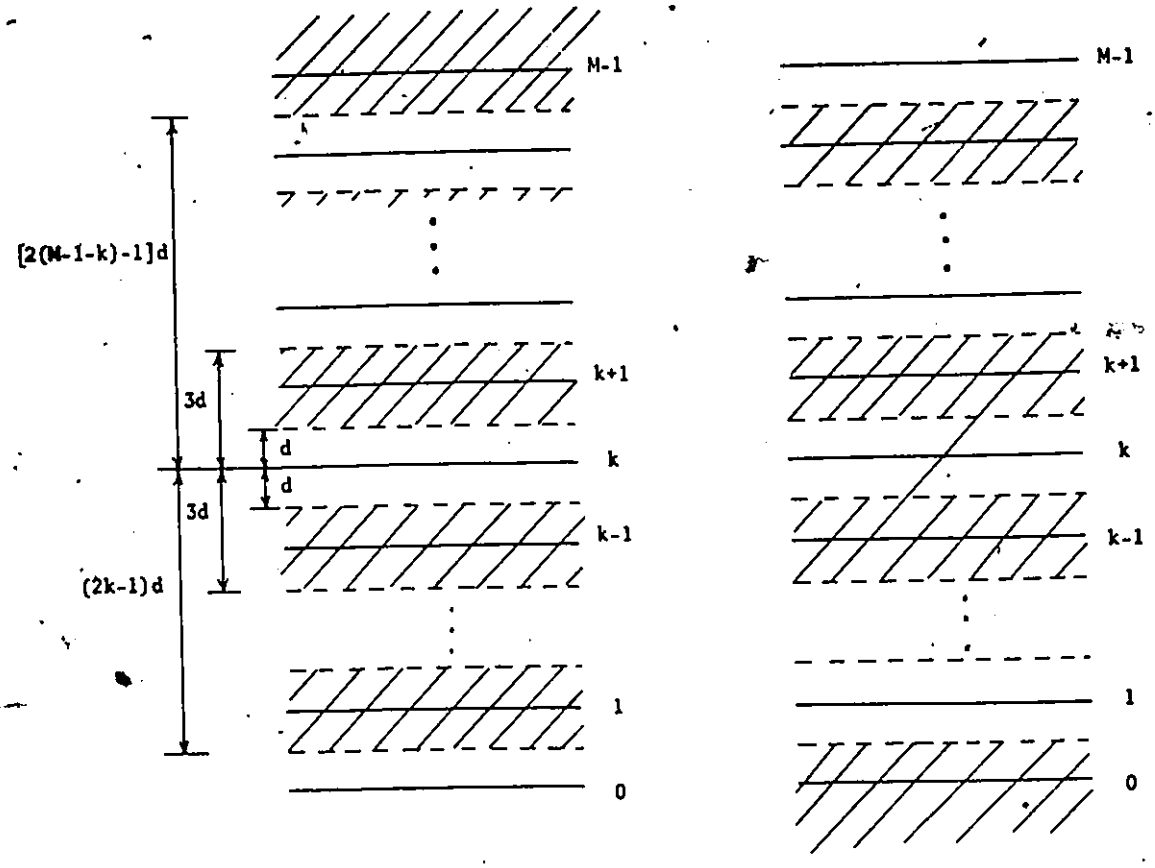

Figure 4-4. Error zones for when the k^{th} level is transmitted, for M-1 odd, (a) k is even (b) k is odd.

For this case, the probability, $P^{+}_{e|\ k\ \text{even}}$, of an error due to noise of positive amplitude is easily seen to be

$$P^{+}_{e|\ k\ \text{even}} = \sum_{i=1}^{M-1-k} (-1)^{i} Q[(2i-1)d], \tag{4-12}$$

and the probability, $P^{-}_{e|\ k\ \text{even}}$, of an error due to noise of negative amplitude is given by

$$P^{-}_{e|\ k\ \text{even}} = \sum_{i=1}^{k}(-1)^{i}Q[(2i-1)d]. \qquad (4\text{-}13)$$

Hence, the probability of error $P_{e|\ k\ \text{even}}$ is given by

$$P_{e|\ k\ \text{even}} = P^{+}_{e|\ k\ \text{even}} + P^{-}_{e|\ k\ \text{even}} = \tfrac{1}{2} + \sum_{i=1}^{M-1-k}(-1)^{i}Q[(2i-1)d] + \sum_{i=1}^{k}(-1)^{i}Q[(2i-1)d]. \qquad (4\text{-}14)$$

(b) <u>k is odd</u> $\therefore$ M-1-k is even.

Now levels k and M-1 represent the same bit which is opposite to that represented by level 0. The error zones for the k^{th} level are as indicated in Fig. 4-4(b) above. One immediately sees that

$$P^{+}_{e|\ k,\ \text{odd}} = \sum_{i=1}^{M-1-k}(-1)^{i}Q[(2i-1)d] \qquad (4\text{-}15)$$

and

$$P^{-}_{e|\ k\ \text{odd}} = \tfrac{1}{2} + \sum_{i=1}^{k}(-1)^{i}Q[(2i-1)d] \qquad (4\text{-}16)$$

Hence,

$$P_{e|\,k\ \text{odd}} = \tfrac{1}{2} + \sum_{i=1}^{M-1-k} (-1)^i Q[(2i-1)d] + \sum_{i=1}^{k} (-1)^i Q[(2i-1)d] \quad (4\text{-}17)$$

Therefore the probability of error for M-1 odd becomes

$$P(e) = \sum_{k=0}^{M-1} \Bigg\{ \tfrac{1}{2} P_{k\ \text{odd}} + P_{k\ \text{odd}} \Bigg[\sum_{i=1}^{M-1-k} (-1)^i Q[(2i-1)d] + \sum_{i=1}^{k} (-1)^i Q[(2i-1)d] \Bigg] + \tfrac{1}{2} P_{k\ \text{even}} + P_{k\ \text{even}} \Bigg[\sum_{i=1}^{M-1-k} (-1)^i Q[(2i-1)d] + \sum_{i=1}^{k} (-1)^i Q[(2i-1)d] \Bigg] \Bigg\}$$

which reduces to

$$P(e) = \tfrac{1}{2} + \sum_{k=0}^{M-1} P_k \Bigg\{ \sum_{i=1}^{M-1-k} (-1)^i Q[(2i-1)d] + \sum_{i=1}^{k} (-1)^i Q[(2i-1)d] \Bigg\} \quad (4\text{-}18)$$

It is therefore seen that whether M-1 is even or odd, the probability of error is given by the same expression, (4-11) or (4-18). Recalling the definition of Q(.), the expression for P_k (equation (4-3)), and for d (equation (4-1)), (4-18) can be written as

$$P(e) = \frac{1}{2} + \frac{1}{2^M}\sum_{k=0}^{M-1}\binom{M-1}{k}\left\{\sum_{i=1}^{M-1-k}(-1)^i \operatorname{erf}\left[(2i-1)\sqrt{\frac{V^2}{2(M-1)^2\sigma^2}}\right]\right.$$

(4-19)

$$\left. + \sum_{i=1}^{k}(-1)^i \operatorname{erf}\left[(2i-1)\sqrt{\frac{V^2}{2(M-1)^2\sigma^2}}\right]\right\}$$

where σ^2 is the variance of the gaussian noise and

$$\operatorname{erf}(x) = 2/\pi \int_0^x e^{-u^2}\, du.$$

It is shown in Appendix II, that

$$\sum_{k=0}^{M-1}\binom{M-1}{k}\left\{\sum_{i=1}^{M-1-k}\Lambda_i + \sum_{i=1}^{k}\Lambda_i\right\} = 2\sum_{k=1}^{M-1}\binom{M-1}{k}\sum_{i=1}^{k}\Lambda_i \qquad (4\text{-}20)$$

where

$$\Lambda_i = (-1)^i \operatorname{erf}\left[(2i-1)\sqrt{\frac{V^2}{2(M-1)^2\sigma^2}}\right]$$

Using (4-20) in (4-19) yields

$$P(e) = \tfrac{1}{2} + \frac{1}{2^{M-1}} \sum_{k=1}^{M-1} \binom{M-1}{k} \sum_{i=1}^{k} (-1)^i \operatorname{erf}\left[(2i-1)\sqrt{\frac{V^2}{2(M-1)^2\sigma^2}}\right] \quad (4-21)$$

Now, the average signal power of the polybinary signal will be obtained. Assume first that the levels take on values from 0 volts to 2V volts. The average normalised signal power is hence

$$S = \sum_{k=0}^{M-1} (\tfrac{1}{2})^{M-1} \binom{M-1}{k} \left(\frac{2Vk}{M-1}\right)^2 \quad (4-22)$$

This is shown in Appendix III, to be

$$S = \frac{V^2 M}{(M-1)} \quad (4-23)$$

Using this in (4-21) one gets

$$P(e) = \tfrac{1}{2} + 2^{1-M} \sum_{k=1}^{M-1} \binom{M-1}{k} \sum_{i=1}^{k} (-1)^i \operatorname{erf}\left[(2i-1)\sqrt{\frac{S/N}{2M(M-1)}}\right] \quad (4-24)$$

where $N = \sigma^2$ is the noise power.

It is more usual, however, to transmit a signal that is symmetrical about zero such that no (unnecessary) dc power is transmitted. If the polybinary signal is transmitted such that the levels assume values from -V to V, the power transmitted becomes

$$S = \sum_{k=0}^{M-1} \left(\tfrac{1}{2}\right)^{M-1} \binom{M-1}{k} \left(\frac{2Vk}{M-1} - V\right)^2 \qquad (4\text{-}25a)$$

It is an easy task to show that this reduces to

$$S = \frac{V^2 M}{(M-1)} - V^2 = \frac{V^2}{(M-1)} \qquad (4\text{-}25b)$$

Thus the peak-to-rms factor in dB for Class I PRS is

$$\rho = 10 \log_{10}(M-1) \qquad (4\text{-}25c)$$

One can obtain (4-25b) directly by observing that the power in this case is the power given by (4-22) minus the dc power, which is V^2.

Using (4-25b) in (4-21) yields

$$P(e) = \tfrac{1}{2} + 2^{1-M} \sum_{k=1}^{M-1} \binom{M-1}{k} \sum_{i=1}^{k} (-1)^i \operatorname{erf}\left[(2i-1)\sqrt{\frac{S/N}{2(M-1)}}\right] \qquad (4\text{-}26)$$

This is the final expression for the error rate in a general Class I PRS (with precoding) as a function of signal-to-noise ratio.

The probability of error expression was given by Lender [6] in the form expressed in (4-24) but details of the derivation were never presented. As noted earlier, this expression assumes a signal format that is rarely used in practice, hence (4-26) is preferable. Equation (4-26)

is plotted in Fig. 4-5 for several values of M.

To get an approximation to (4-26) one uses the relation

$$\text{erf}(x) \doteq 1 - \text{erfc}(x) \tag{4-27}$$

where $\text{erfc}(x) = \frac{2}{\sqrt{\pi}}\int_x^\infty e^{-u^2} du$.

Then (4-26) becomes

$$P(e) = \tfrac{1}{2} + 2^{1-M}\sum_{k=1}^{M-1}\binom{M-1}{k}\sum_{i=1}^{k}(-1)^i$$

$$- 2^{1-M}\sum_{k=1}^{M-1}\binom{M-1}{k}\sum_{i=1}^{k}(-1)^i \text{erfc}\left[(2i-1)\sqrt{\frac{S/N}{2(M-1)}}\right] \tag{4-28}$$

It is proved in Appendix IV that

$$\sum_{k=1}^{M-1}\binom{M-1}{k}\sum_{i=1}^{k}(-1)^i = -2^{M-2} \tag{4-29}$$

Hence (4-28) may be rewritten as

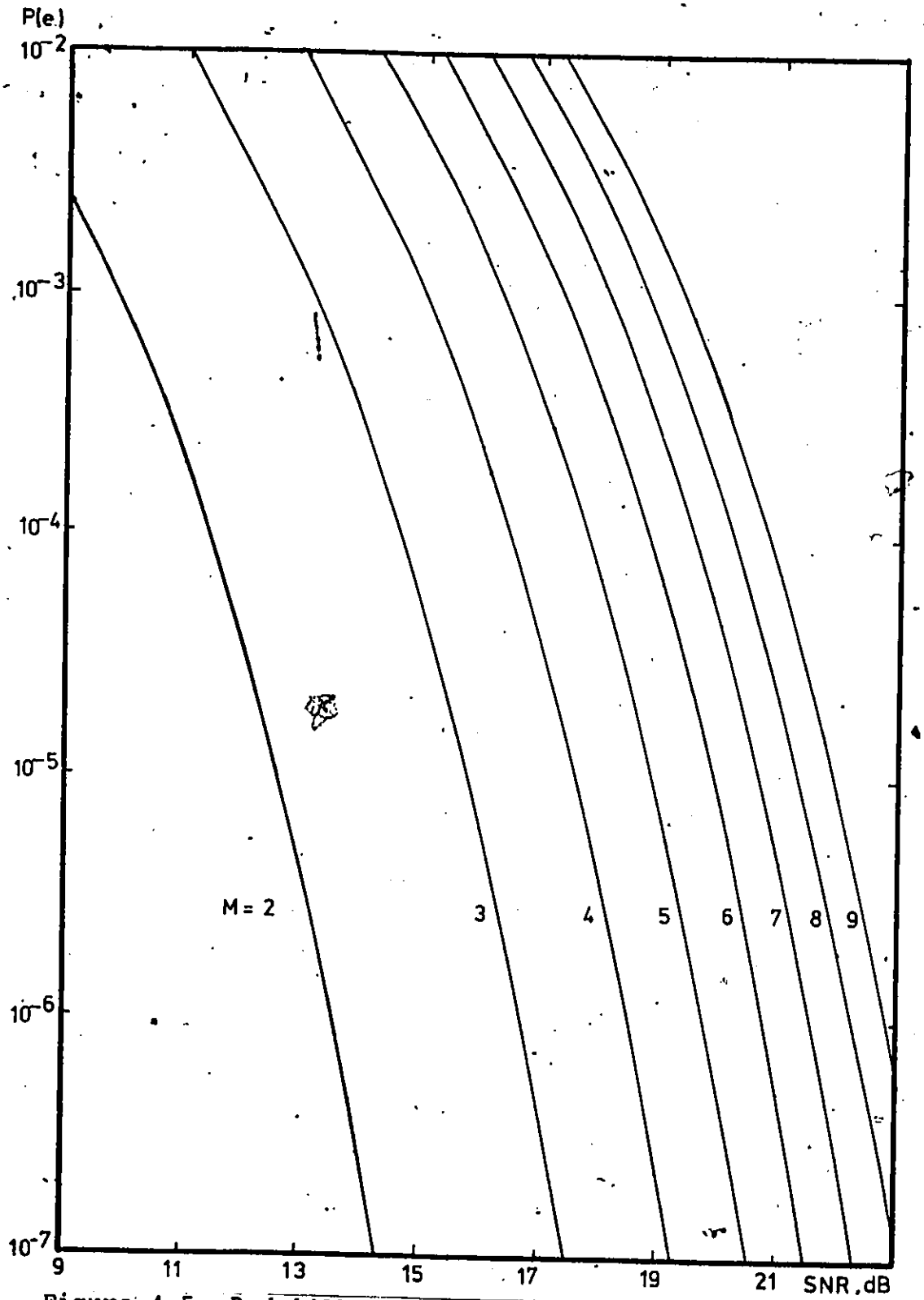

Figure 4.5. Probability of error versus signal-to-noise ratio in dB. Measured at input of decoder

$$P(e) = -\,2^{1-M}\sum_{k=1}^{M-1}\binom{M-1}{k}\sum_{i=1}^{k}(-1)^{i}\,\mathrm{erfc}\left[(2i-1)\sqrt{\frac{S/N}{2(M-1)}}\right] \qquad (4\text{-}30)$$

Now, knowing the behaviour of the erfc(x) function, terms in (4-30) arising from values of i greater than 1 may be neglected. The resulting approximation is

$$P(e) = \frac{2^{M-1}-1}{2^{M-1}}\,\mathrm{erfc}\left(\sqrt{\frac{S/N}{2(M-1)}}\right) \qquad (4\text{-}31)$$

This approximation is equivalent to assuming that only errors caused by transitions to adjacent levels need be considered. For a two-level binary NRZ signal, the probability of error in the presence of AWGN is obtained from (4-30) by setting M = 2, giving the well-known formula

$$P(e) = \tfrac{1}{2}\,\mathrm{erfc}\left(\sqrt{\frac{S}{2N}}\right) \qquad (4\text{-}32)$$

It is then seen that an M-level polybinary system is approximately

$$10\log_{10}(M-1)\,\mathrm{dB}$$

worse, in performance, than the binary system.

The performance of a three-level Class I PRS system (duobinary system) may be obtained from (4-30) by setting M = 3. Thus,

$$P(e) = \frac{3}{4}\,\mathrm{erfc}\left(\sqrt{\frac{S/N}{4}}\right) - \frac{1}{4}\,\mathrm{erfc}\left(3\sqrt{\frac{S/N}{4}}\right) \qquad (4\text{-}33)$$

For values of S/N of practical importance, the second term in (4-33) is usually negligible compared to the first one, hence (4-33) is approximated to

$$P(e) = \frac{3}{4}\,\mathrm{erfc}\left(\sqrt{\frac{S/N}{4}}\right) \qquad (4\text{-}34)$$

This is seen to be approximately 3 dB worse than the binary case in (4-32).

Class IV PRS (modified duobinary) is directly analogous to the three-level Class I PRS, and has the same probability of error given by (4-34).

4.3 Interference in PRS Systems

In certain cases interference is so much larger than thermal noise that the system can be considered to be perturbed by interference alone; for example, in radio systems an unmodulated carrier wave interference, a faulty oscillator or a misalignment in an upconvertor might cause this effect. It is thus of interest to consider the effect of interference alone on the performance of the system. Square-wave interference is considered because it gives the same performance as when the desired signal is disturbed by crosstalk from a binary NRZ signal nearby, say in wire paired cable transmission for example. A

random sequence or a periodic square-wave give the same result. Sinusoidal interference is important because very often the interfering signal is a carrier which may be angle modulated as in interchannel interference (adjacent or co-channel). Low-frequency hum of ac power lines, harmonics of ac-to-dc power converters, and pilot and control tones are also among the frequent sources of sinusoidal interference.

For the sake of simplicity only a three-level (Class I or Class IV) PRS signal is considered in the analysis hereafter. However, the principle of the analysis may be extended to PRS signals with more levels.

4.3.1 Square-wave Interference

Consider a square wave i(t) (or an equiprobable binary sequence) with peak values ±A volts. The probability density function of this signal is evidently given by

$$p(i) = \tfrac{1}{2}\,[\delta(i+A) + \delta(i-A)] \qquad (4\text{-}35)$$

This function is shown in Fig. 4-6 below.

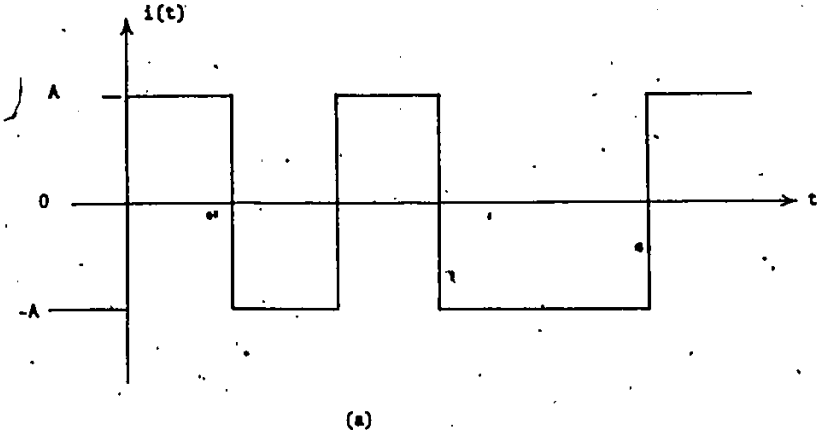

(a)

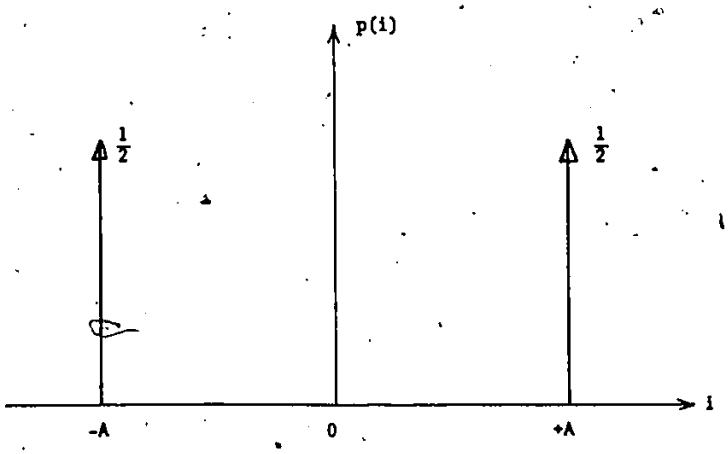

(b)

Figure 4-6. (a) Time-domain representation of a random binary pattern.
(b) p.d.f. of an interfering square wave or random binary pattern.

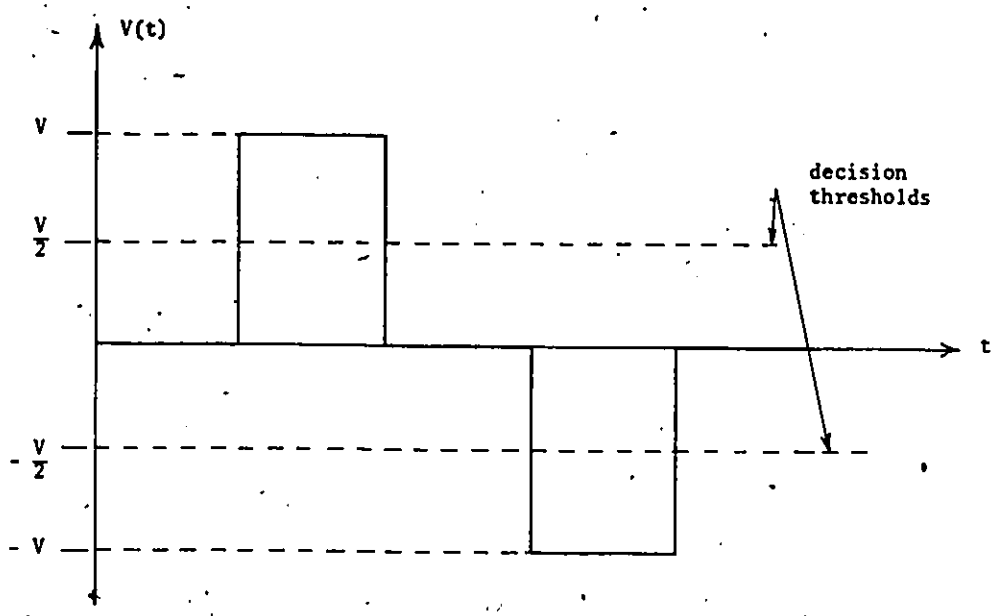

Figure 4-7. An example of a Class I PRS signal.

Consider now a non bandlimited three-level PRS signal, with precoding, having levels -V, 0, and +V as shown in Fig. 4-7. Decision thresholds are set at - V/2 and V/2. If either of the two outermost levels (-V or +V) is received, an error will occur if, at the sampling instant, the interference sample is of the opposite polarity and has a magnitude exceeding V/2. If level 0 is received, an error will be committed if the interference sample has a magnitude greater than V/2. The probability of error is hence given by

$$P(e) = P(-V)P\{i > V/2\} + P(0)P\{|i| > V/2\} + P(V)P\{i < -V/2\} \quad (4\text{-}36)$$

$$- P(-V)P\{i > 3/2\ V\} - P(V)P\{i < -3/2\ V\}.$$

The last two terms in (4-36) are added because the two outermost levels, -V and +V, represent the same bit and hence no error will be committed in detection if one is mistaken for the other. It should be noted that (4-36) applies independently of the probability density

function (pdf) of the random variable i, i.e. it is equally applicable whether i is sinusoidal interference or some other kind of interference. [For example if i is random gaussian noise with zero mean and variance σ, (4-36) reduces to (4-33).]

For square-wave interference, the probability of error is obtained by using (4-35) and (4-36). Two cases are distinguished:

(i) $A < V/2$. In this case, the interference level will never exceed the threshold V/2, hence no errors will occur i.e., P(e) = 0. Let S_{rms} and I_{rms} stand for the rms voltage values of the signal and the interference respectively, and S and I represent the mean signal and interference powers respectively. From (4-25b), $S = V^2/2$ hence $S_{rms} = V/\sqrt{2}$ and since the peak-to-rms ratio for a square wave is 0 dB, $I_{rms} = A$ or $I = A^2$. Hence one can say that if $S/I > 2$ or $S_{rms}/I_{rms} > 2$ (SIR exceeds 3 dB), no errors will occur.

(ii) $A > V/2$. This implies that $P\{i > V/2\} = P\{i < -V/2\} = \frac{1}{2}$ and $P\{|i| > V/2\} = 1$. Since $P(0) = \frac{1}{2}$ and $P(V) = P(-V) = \frac{1}{4}$, (4-36) then becomes

$$P(e) = \frac{3}{4} - \frac{1}{4}\left[P\{i > 3V/2\} + P\{i < -\frac{3V}{2}\}\right] \qquad (4\text{-}37)$$

If $V/2 < A < 3V/2$, $P(e) = 3/4$

If $A > 3V/2$ or (SIR < -6.5 dB), $P(e) = \frac{1}{2}$.

Thus

$$P(e) = \frac{3}{4}\, u(3-SIR) - \frac{1}{4}\, u(-6.5-SIR) \qquad (4-38)$$

where u(.) is the Heaviside unit step function and SIR is the signal-to-interference ratio in dB. This expression is shown in Fig. 4-8.

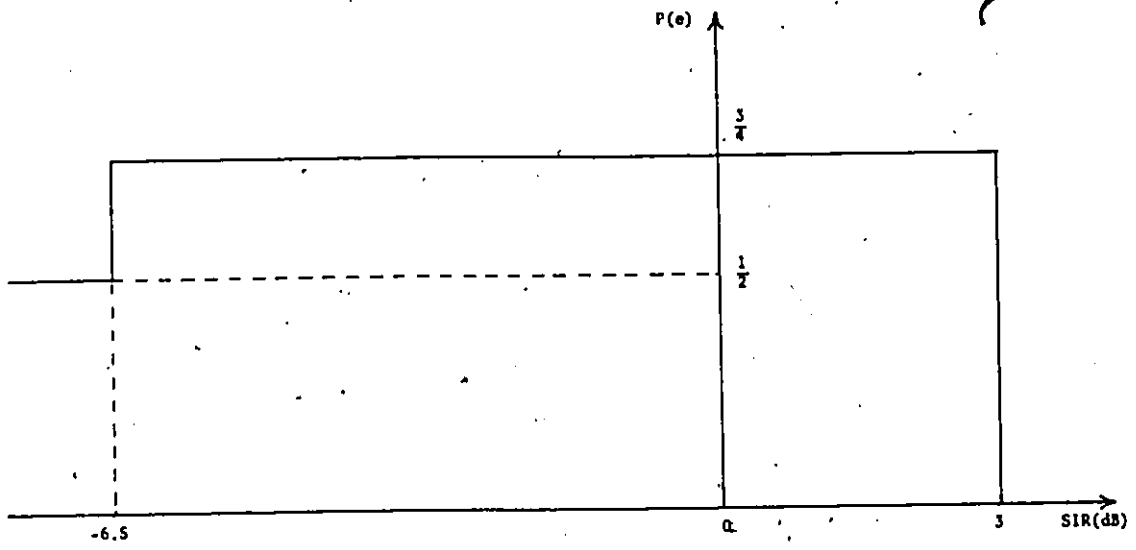

Figure 4-8. P(e) versus SIR for square-wave interference.

It should be pointed out, however, that for data transmission, the range of probability of error that occurs in (4-38) for SIR < 3 dB is of no practical interest; hence interference should of necessity be kept (theoretically) at least 3 dB below the signal level. In most practical systems it is more than 20 dB below. This analysis however is intended for the extreme threshold performance.

4.3.2 Sinusoidal Interference

For a sinusoidal interfering signal with peak value A, the

amplitude probability density function (pdf) shown in Fig. 4-9(b) is given by [54]

$$p(i) = \begin{cases} \dfrac{1}{\pi\sqrt{A^2-i^2}} & , |i| < A \\ 0 & , \text{elsewhere} \end{cases} \qquad (4\text{-}39)$$

One notes that this is independent of frequency of the sinusoid and hence the probability of error should be independent of the frequency of interference (as long as the interference falls within the receiver bandwidth).

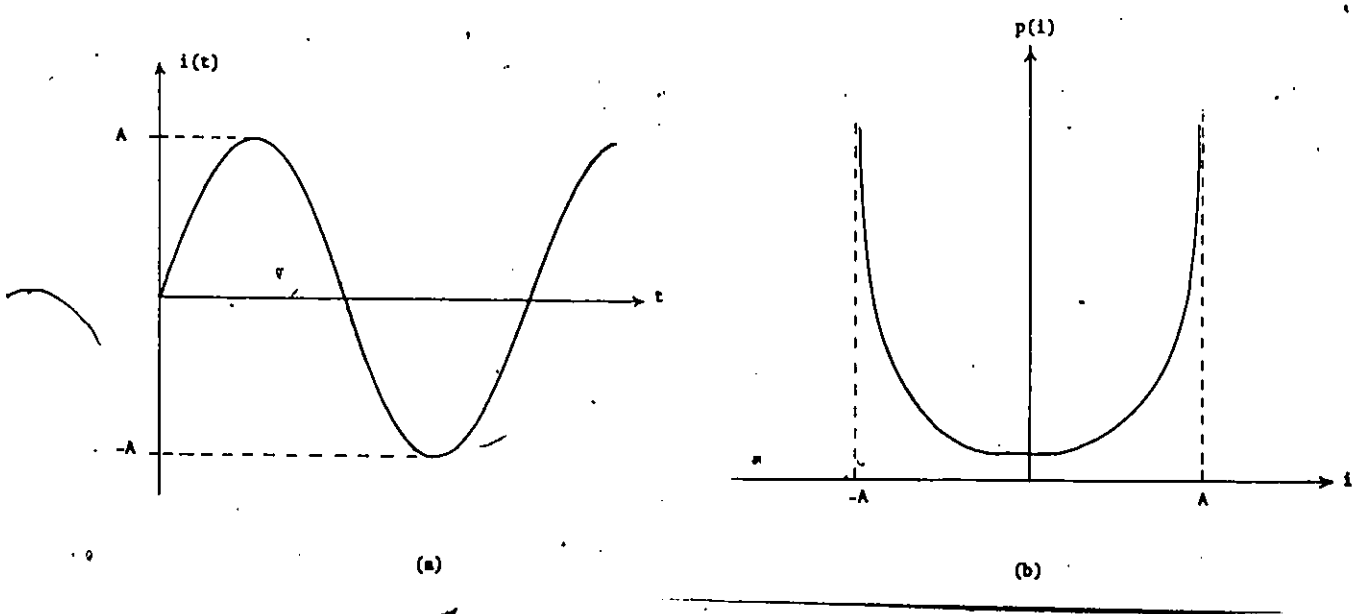

Figure 4-9. (a) Time-domain representation of a sinusoid
(b) P.d.f of a sinusoid.

The binary NRZ case is considered here for completeness.

Consider a random binary sequence with levels V and -V, and the threshold at 0. An error occurs if at the sampling instant, the

interference has an instantaneous value greater than V in magnitude but opposite in sign to the level being detected. Hence the probability of error is

$$P(e) = P(0)\ P\{i > V\} + P(1)\ P\{i < -V\} \qquad (4\text{-}40)$$

From symmetry of (4-39), $P\{i > V\} = P\{i < -V\}$. Therefore $P(e) = P\{i > V\}$.

a) If $A \leq V$, it is not difficult to see that no errors will occur, that is $P(e) = 0$ as long as $S/I > 2$ (or SIR > 3 dB), S and I being the average binary signal and the sinusoidal powers respectively.

b) If $A > V$ or SIR < 3 dB, then $P(e) = P\{i > V\}$. Using (4-39),

$$P(e) = \int_V^A \frac{di}{\pi\sqrt{A^2 - i^2}}$$

and letting $i = A\sin t$,

$$P(e) = \frac{1}{\pi} \int_{\sin^{-1}(\frac{V}{A})}^{\pi/2} dt$$

i.e. $P(e) = \frac{1}{2} - \frac{1}{\pi} \sin^{-1}(V/A)$

Since $S_{rms} = V$ and $I_{rms} = A/\sqrt{2}$,

$$P(e) = \tfrac{1}{2} - \frac{1}{\pi} \sin^{-1}\left(\sqrt{2}\,\frac{S_{rms}}{I_{rms}}\right) \text{ for } \frac{S_{rms}}{I_{rms}} < \sqrt{2}.$$

Hence, in the absence of other perturbations, the probability of error due to sinusoidal interference is given by

$$P(e) = \begin{cases} \tfrac{1}{2} - \frac{1}{\pi} \sin^{-1}\left(\sqrt{S/2I}\right), & \text{SIR} \leq 3 \text{ dB} \\ 0, & \text{SIR} \geq 3 \text{ dB} \end{cases} \qquad (4\text{-}41)$$

Consider now a PRS signal having levels -V, 0, and +V and let thresholds be set at ± V/2 as before. Equation (4-36) will again apply here except that here i is given by $i(t) = A\cos\omega t$ with a pdf p(i) given by (4-39). From symmetry (4-36) becomes

$$P(e) = 2\,P\{i > V/2\}[P(V) + P(0)] - 2\,P(V)P\{i > 3V/2\} \qquad (4\text{-}42)$$

(i) If $A \leq V/2$, the interference level will never exceed the threshold V/2, thus no errors will occur i.e. P(e) = 0.

Letting, as before, S_{rms} and I_{rms} be the rms values of the signal and the interference respectively, $S_{rms} = V/\sqrt{2}$ and $I_{rms} = A/\sqrt{2}$ and $S = V^2/2$, $I = A^2/2$, since the peak-to-rms ratio for a sine wave is 3 dB. Hence one can say that P(e) = 0 as long as S/I > 4 (or SIR > 6 dB).

(ii) For $V/2 \leq A \leq 3V/2$, since $P(V) = \tfrac{1}{4}$, $P(0) = \tfrac{1}{2}$, (4-42) becomes

$$P(e) = \frac{3}{2} P\{i > V/2\} - \frac{1}{2} P\{i > 3V/2\} \qquad (4\text{-}43)$$

Since max [i(t)] = A < 3V/2, the second term in (4-43) is nil, hence

$$P(e) = \frac{3}{2} P\{i > V/2\} = \frac{3}{2} \int_{V/2}^{A} \frac{di}{\pi\sqrt{A^2-i^2}}$$

Using the substitution i = Asint, one gets

$$P(e) = \frac{3}{2} \{\tfrac{1}{2} - \frac{1}{\pi} \sin^{-1}(\tfrac{1}{2}\sqrt{S/I})\} \qquad (4\text{-}44)$$

(iii) For A < 3/2 V or SIR < -3.5 dB, (4-43) applies but the second term is now non-zero, hence one gets

$$P(e) = \frac{3}{2} \int_{V/2}^{A} \frac{di}{\pi\sqrt{A^2-i^2}} - \frac{1}{2} \int_{3V/2}^{A} \frac{di}{\pi\sqrt{A^2-i^2}}$$ and letting i=Asint,

$$P(e) = \tfrac{1}{2} - \frac{1}{2\pi} \{3 \sin^{-1}(\tfrac{1}{2}\sqrt{S/I}) - \sin^{-1}(\tfrac{3}{2}\sqrt{S/I})\} \qquad (4\text{-}45)$$

Equations (4-41) and (4-45) are graphically plotted in Chapter 5 and compared with the measured results.

4.3.3 Combined Noise and Interference

The case most likely to be encountered in an actual system is where both a spurious signal, or interference, and random gaussian noise are added to the desired signal. Each of these (interference and noise) is a random variable with well-known pdfs say $p_i(i)$ and $p_n(n)$ respectively. It follows therefore that the sum disturbance will be another random variable, called herein z, with a pdf p(z). The pdf of the sum of two random variables is found from the convolution of the pdf's of the two random variables.

$p_i(i)$ is given in equation (4-39) and

$$p_n(n) = \frac{1}{\sqrt{2\pi}\sigma} e^{-n^2/2\sigma^2}.$$

It follows that

$$p(z) = p(i) * p(n) = \int p_i(z-u)p_n(u)du \qquad (4-46)$$

$$p(z) = \int_{z-A}^{z+A} \frac{1}{\pi A\sqrt{2\pi}\sigma} \frac{e^{u^2/2\sigma^2}}{\sqrt{1-\left(\frac{z-u}{A}\right)^2}} du \qquad (4-47)$$

By changing variables, $\frac{z-u}{A} = \sin x$, one gets

$$p(z) = \frac{1}{\pi\sqrt{2\pi}\sigma} \int_{-\pi/2}^{\pi/2} e^{-(z-A\cos x)^2/2\sigma^2} dx \qquad (4-48a)$$

or

$$p(z) = \frac{1}{\pi\sqrt{2\pi\sigma}} \int_0^{\pi} e^{-(z-A\cos x)^2/2\sigma^2}\, dx \qquad (4\text{-}48b)$$

This integral has no closed-form solution and has to be evaluated numerically.

Take now the PRS treated in the previous section. Equation (4-36) will apply with i replaced by z. Hence the probability of error expression can be written as

$$P(e) = \frac{3}{4} P\{z > +\frac{V}{2})\} + \frac{3}{4} P\{z < -\frac{V}{2}\} - \tfrac{1}{4} P\{z > 3V/2\} \qquad (4\text{-}49)$$

$$- \tfrac{1}{4} P\{z < -3V/2\}$$

Since p(z) is a convolution of two even functions, it is an even function and (4-49) may be written as

$$P(e) = \frac{3}{2} P\{z > V/2\} - \tfrac{1}{2} P\{z > 3V/2\} \qquad (4\text{-}50)$$

Combining (4-48b) and (4-50)

$$P(e) = \frac{3}{2\pi\sqrt{2\pi}\sigma}\int_{V/2}^{\pi}\int_{0}^{\pi} e^{-(z-A\cos x)^2/2\sigma^2}\,dx\,dz$$

$$- \frac{1}{2\pi\sqrt{2\pi}\sigma}\int_{3V/2}^{\infty}\int_{0}^{\pi} e^{-(z-A\cos x)^2/2\sigma^2}\,dx\,dz \qquad (4\text{-}51)$$

This expression can only be evaluated numerically to give the probability of error. Probability of error is usually plotted against the signal-to-noise ratio, SNR, with the signal-to-interference ratio, SIR, used as a parameter. Sometimes, SNR may be used as a parameter and P(e) plotted against SIR.

The performance of the PRS system in different environments considered here were evaluated for a simple sample and detect receiver, that is, no signal processing was assumed at the receiver. As mentioned in Chapter One however, it is possible to improve the performance of a PRS system by using ambiguity-zone detection (or soft decoding) methods or by applying the maximum-likelihood detection (MLD) algorithm. The details of the performance when such methods are used are too complex to include here.

In the next chapter, experimental verification of some of the expressions derived here are described.

CHAPTER FIVE

AN EXPERIMENTAL PRS SYSTEM

This chapter presents the design and evaluation of an experimental partial-response signalling system. As said earlier, a three-level Class I (or Class IV) is the simplest PRS system; hence it will be considered here. Following the circuit description of the experimental system, the measurement techniques used are briefly described. Based on the equivalence of performance of linearly modulated systems employing coherent demodulation with that of baseband systems [17, Chapter 7], the evaluation starts with the performance of the baseband system and one expects that these results will apply to QPRS. The probability of error performance, as a function of signal-to-noise ratio of the baseband partial-response system in an additive white gaussian noise environment is measured. Measured results for the performance in various interference environments are also reported. Performance is first evaluated where interference, sinusoidal or square-wave, is the only perturbing factor, and then where both AGWN and interference additively corrupt the desired signal. These measured results are compared to the theoretical values obtained in the last chapter.

Given a certain amount of interference, it is shown that the best performance is obtained when all the power is concentrated in one interferer, and deteriorates when the number of interferers increase.

5.1 The Encoder

The block diagram of the duobinary encoder was presented in Fig.

2-12. The precoding and correlative-level coding may be combined to save one delay unit as shown in Fig. 5-1.

The encoder was implemented using TTL logic devices in addition to resistors and capacitors. The delay units are realised using D-type flip-flops clocked at the bit-rate frequency. The modulo-2 summation is easily accomplished by using an EXCLUSIVE-OR gate while the

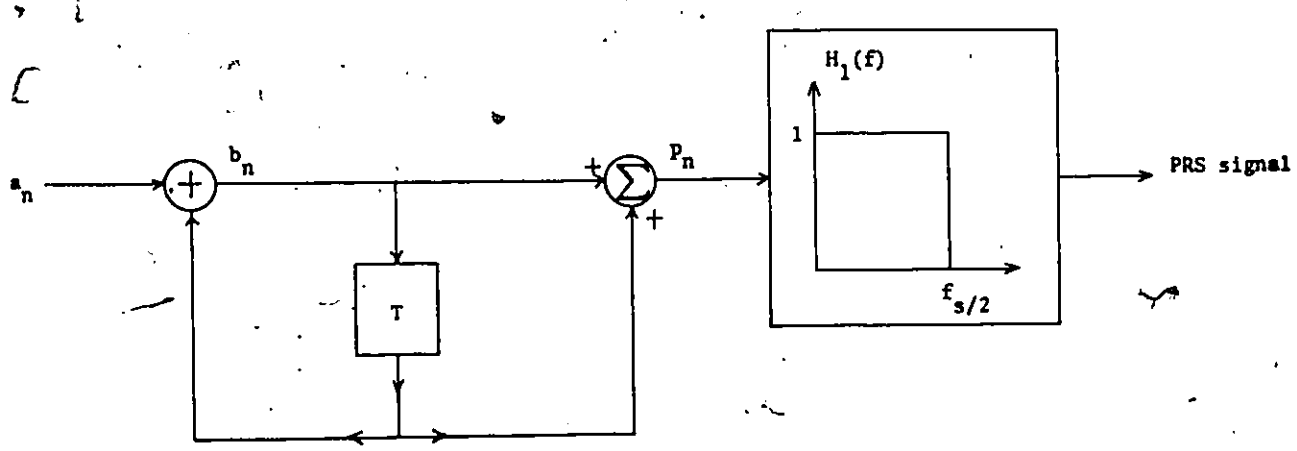

Figure 5-1. Combination of precoding and correlative level coding to save one delay unit.

analogue summation requires just a simple resistive adder. To make the PRS signal symmetric about zero volts, a level shifting circuit is needed. A capacitor may be used as in the first circuit realised. However an operational amplifier with a variable negative-voltage input was found to be more suitable because it is more manageable and acts as a buffer at the same time. The first circuit used only one flip-flop as in Fig. 5-1, however it was found that the signal at the output of

the EX-OR gate was full of glitches and these appeared on the output PRS signal. To avoid the glitches two flip-flops were used. A switch was inserted such that precoding can be included or excluded at will. The circuit diagram of the encoder appears in Fig. 5-2. Fig. 5-3 shows the input binary NRZ waveform and the corresponding PRS waveform (infinite bandwidth) for a bit-rate of 1.6 Mb/s.

The block diagram of the modified duobinary encoder was shown in Fig. 2-15. As mentioned earlier, the same delay units may be used for precoding as well as for level conversion, thus saving two flip-flops. However, as before, to avoid glitches, one more flip-flop is used as shown in Fig. 5-4. The level conversion into a modified duobinary waveform entails analogue subtraction of a delayed sequence from the undelayed one. This requires an analogue inverter. In the circuit of Fig. 5-4, instead of subtraction, addition is done but with the $\overline{Q}$ output instead of the Q output for the delayed sequence, thus no inverter is needed. Fig. 5-5 shows the time domain waveform for a Class IV PRS encoder.

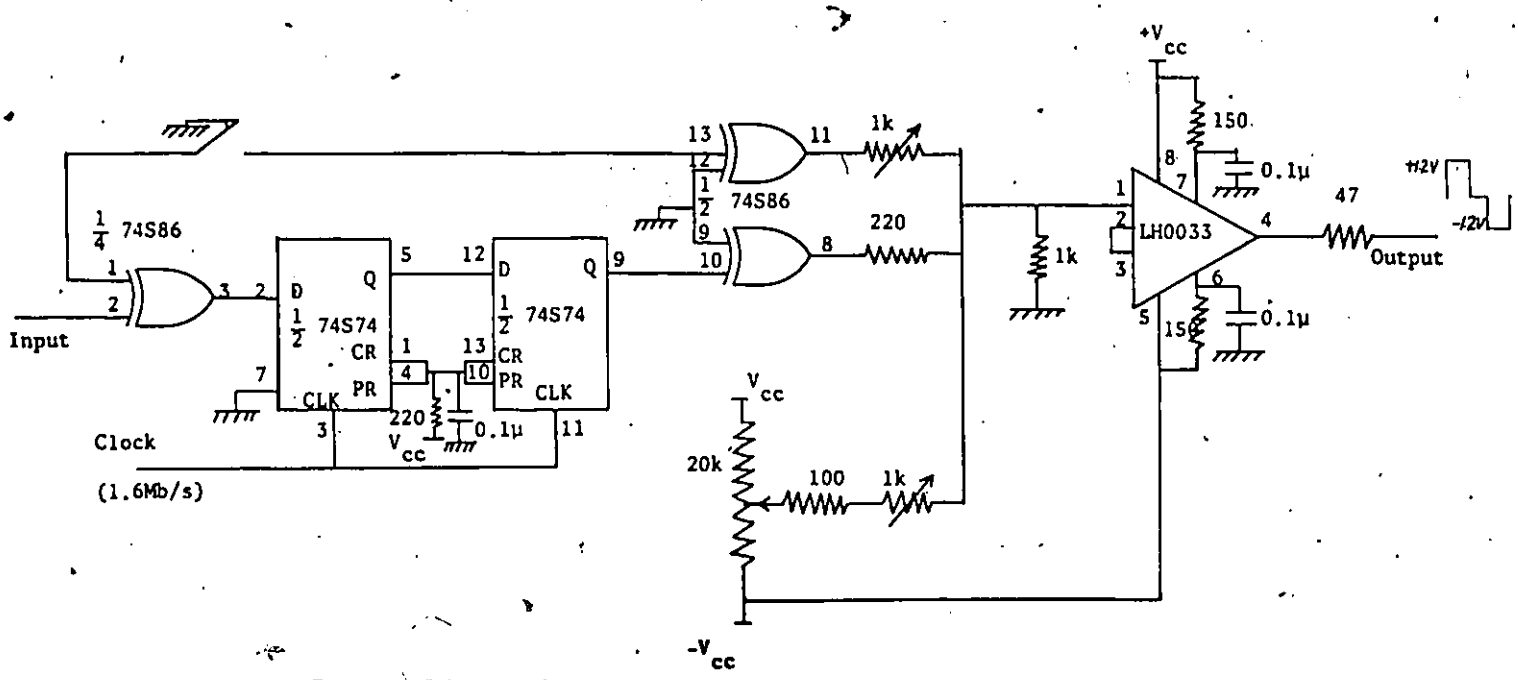

V_{CC}= 5V - All resistor values in ohms - All capacitor values in farads

Figure 5-2. Circuit diagram of a duobinary encoder.

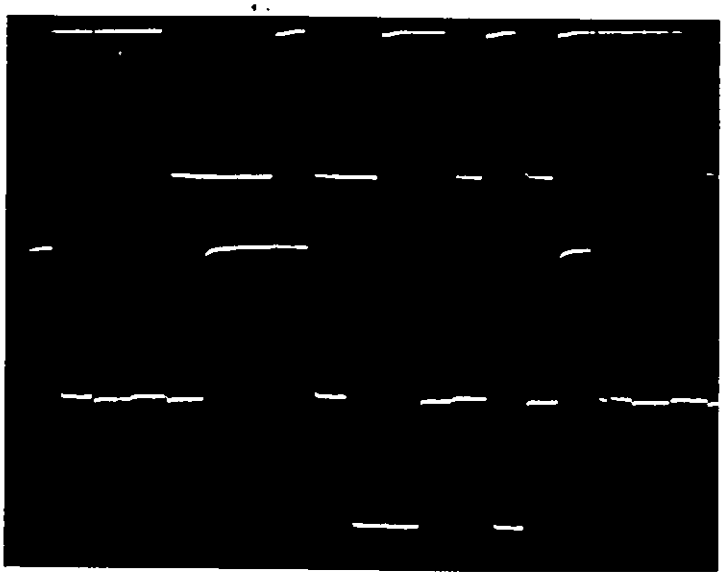

Data rate 1.6 Mb/s

Figure 5-3. The duobinary waveform (below) resulting from a binary NRZ input (above).

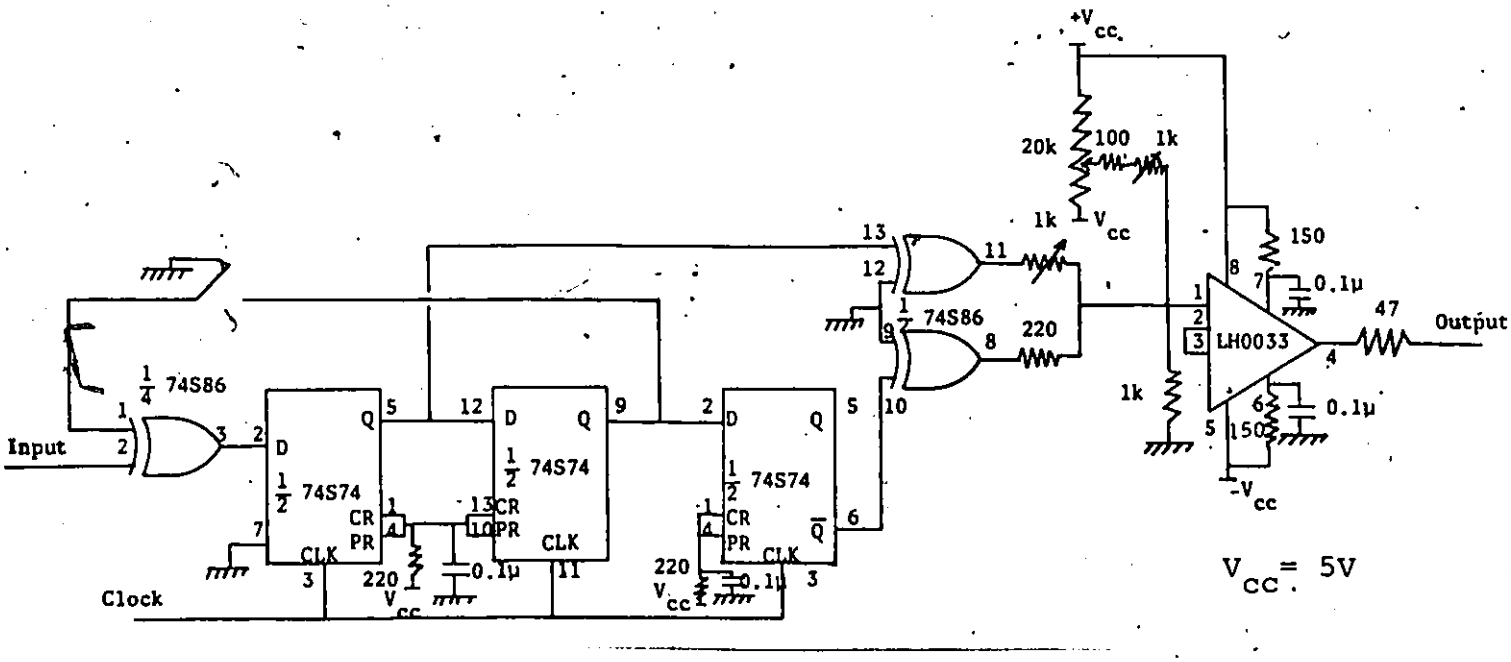

Figure 5-4. Circuit diagram of a modified duobinary encoder.

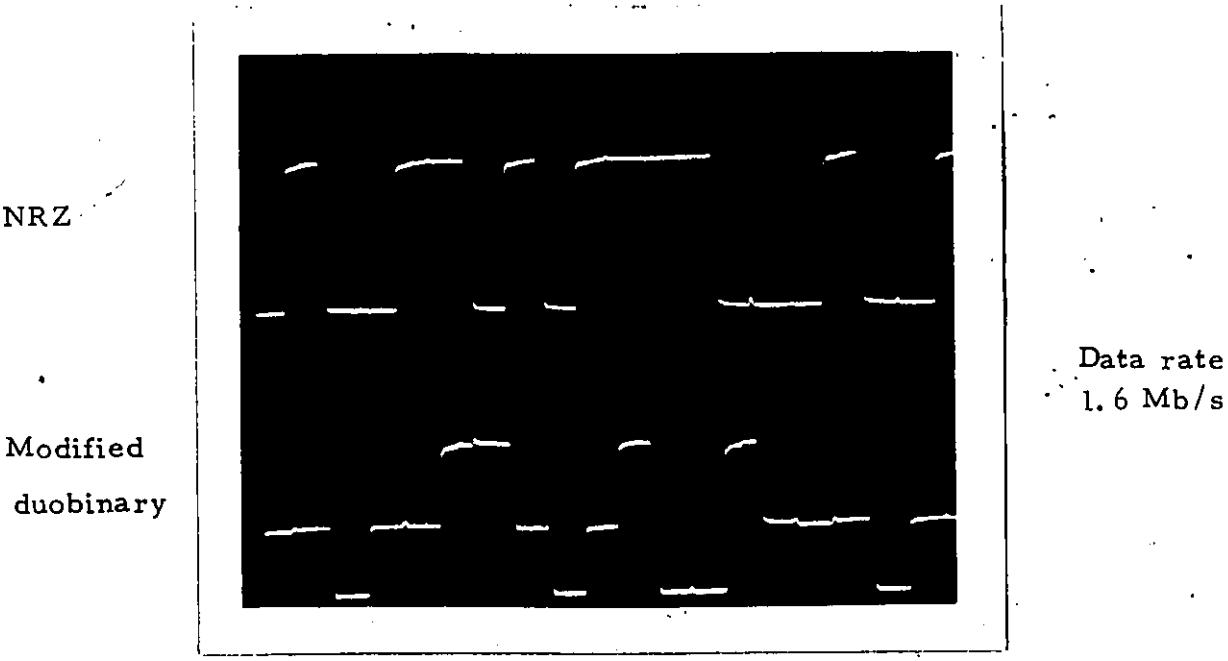

Figure 5-5. The modified duobinary waveform.

5.2 The Decoder

From the characteristics of the duobinary and modified duobinary waveforms (given in Sections 2.3.1 and 2.3.2 respectively) it is quickly seen that the outputs of the Class I and Class IV decoders are respectively given by the expressions:

$$V_0 = 3[u(V_i+\Delta V) - u(V_i-\Delta V)] \qquad (5\text{-}1)$$

and

$$V_0 = 3[1+u(V_i-\Delta V) - u(V_i+\Delta V)] \qquad (5\text{-}2)$$

where V_i is the voltage at the input of the decoder (assumed to vary from $-2\Delta V$ volts to $2\Delta V$ volts), and V_0 is the output voltage. The factor of 3 represents the TTL binary "1" voltage level. The input/output transfer characteristics represented by (5-1) and (5-2), are shown in Fig. 5-6.

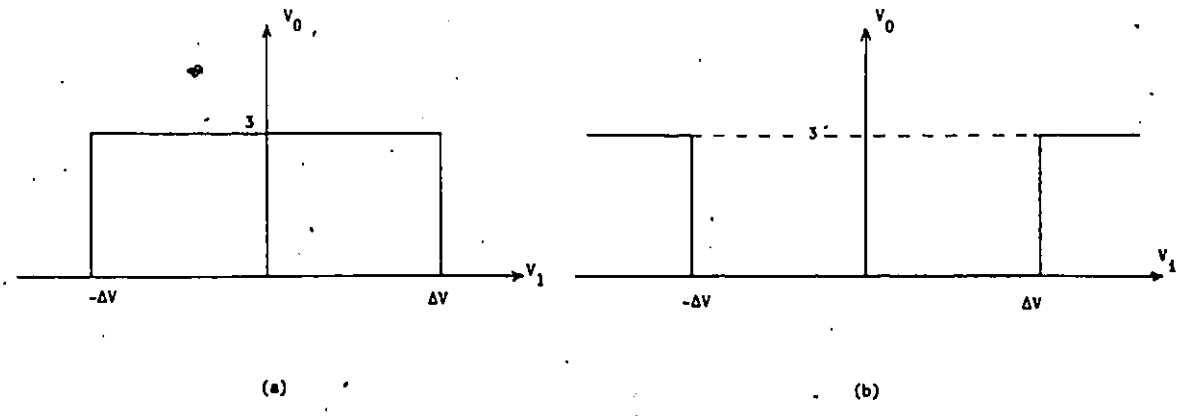

Figure 5-6. Input/output transfer characteristics for (a) duobinary decoder (b) modified duobinary decoder.

These transfer characteristics are easily achieved by means of two

threshold comparators followed by simple combinatorial logic. A block diagram of such a decoder is depicted in Fig. 5-7 below. The diagram applies to both Class I and Class IV with only a change in the combinatorial logic from one class to another.

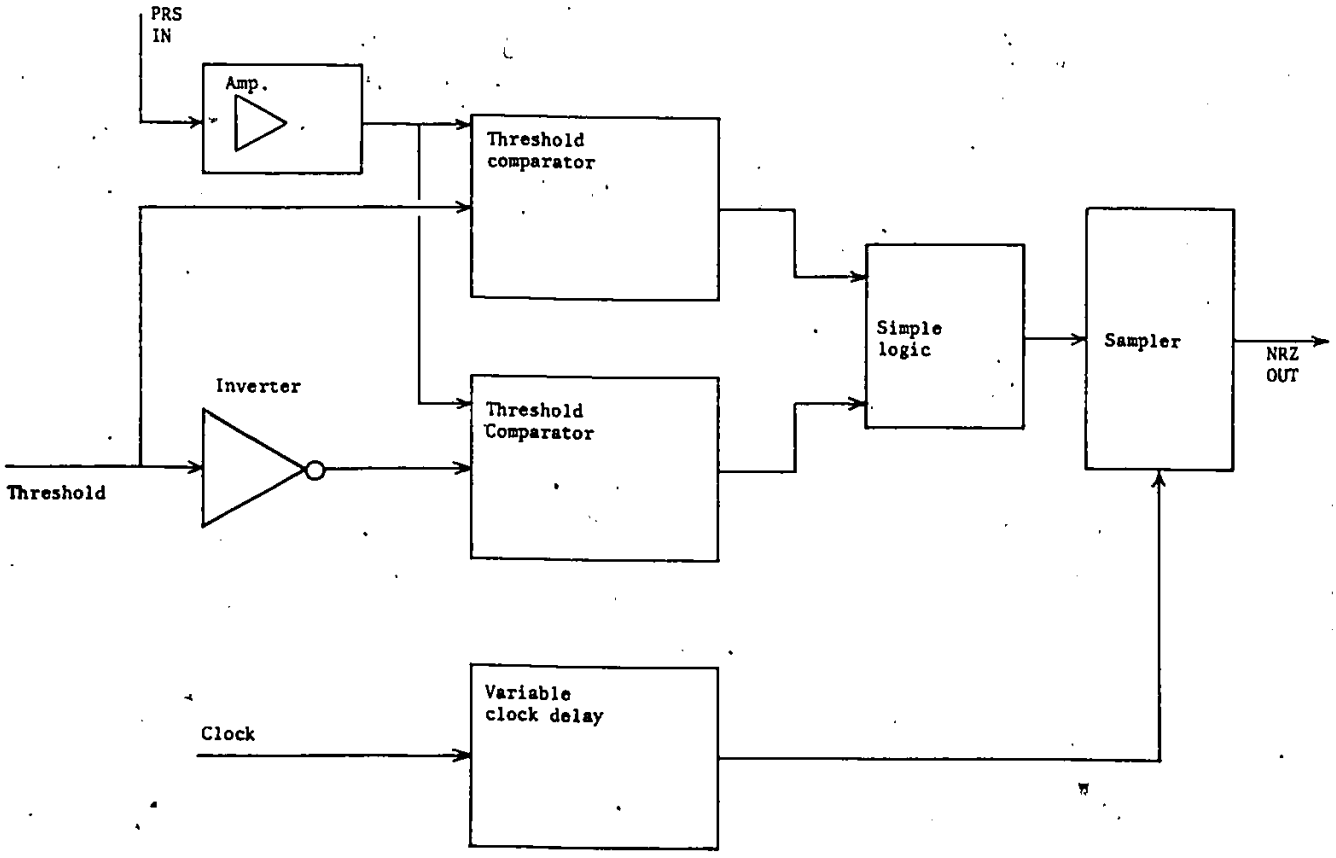

Figure 5-7. A three-level PRS decoder (Class I or Class IV).

If the threshold voltages are applied to the inverting inputs of the threshold comparators, the input/output transfer characteristics are as

indicated in Fig. 5-8(a). If they are applied to the noninverting inputs the transfer characteristics are as shown in Fig. 5-8(b). In either case, it is clear that to get the characteristic of Fig. 5-6(a) the combinatorial logic needed is simply an EX-OR gate.

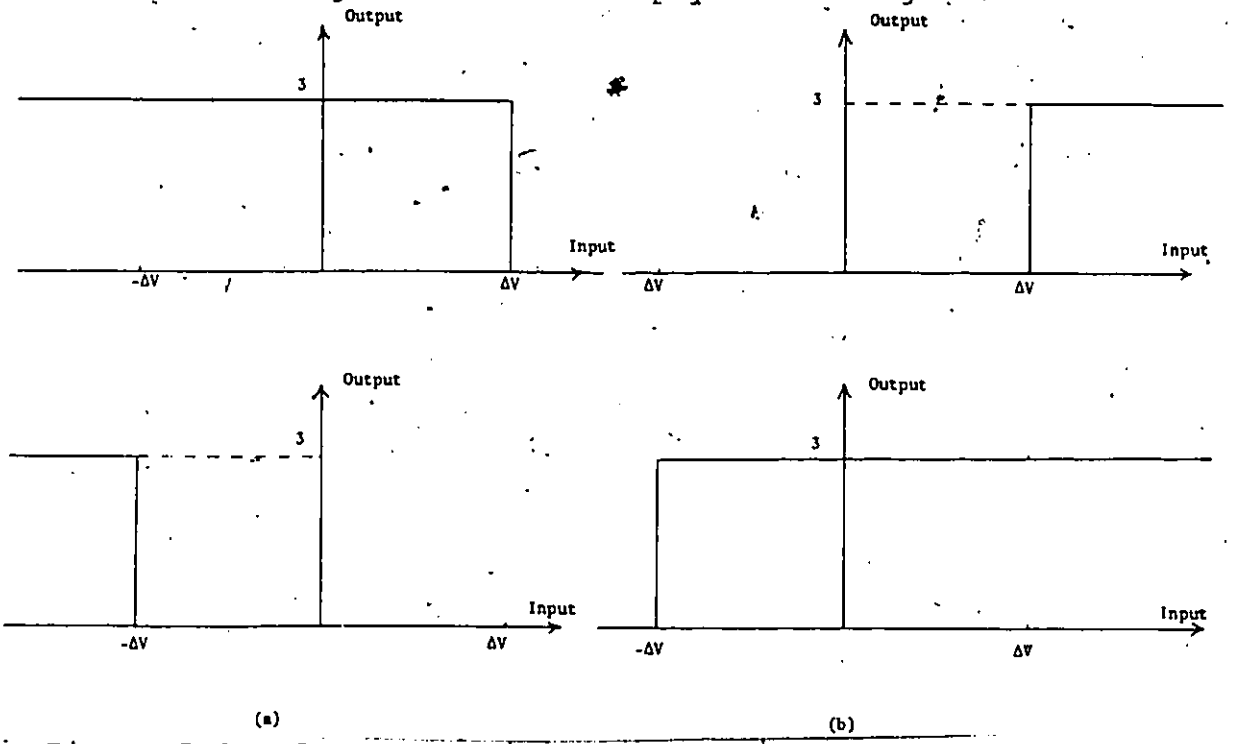

Figure 5-8. Comparator input/output transfer characteristics. The top characteristic is for the comparator with a positive threshold voltage; the bottom one is for the comparator with a negative threshold voltage. (a) Thresholds to inverting inputs of the comparators. (b) Thresholds to noninverting inputs of the comparators.

The output of the combinatorial logic (EX-OR gate) is not clean and may have glitches. To clean the output and make it sharp and glitch-free, this signal is sampled at the data rate. Since the delay of the input PRS signal depends on the filter, and may vary slightly, the sampling clock should have a variable delay. This ensures that

sampling is always at the middle of the eye. It was arranged that the delay could be varied by adjusting a potentiometer knob. Note that no clock recovery circuitry was used in this circuit; the clock was taken from the transmitter. The circuit diagram of the three-level Class I decoder is given in Fig. 5-9.

The three-level Class IV decoder is identical to the Class I decoder except that instead of an EX-OR gate, an EX-NOR gate is used just prior to the sampler. Alternatively, the Class I decoder can be used as it is and a logic inverter attached at the output.

5.3 The QPRS System

In this section, a paper design or a guideline to the design of a QPRS modem is presented. The actual testing of the modem was not completed. The block diagrams of a QPRS modulator and demodulator were presented in Fig. 3-1 and 3-3 respectively. The QPRS modem is designed to transmit 3.0 Mb/s of binary data. The NRZ/PRS encoder shown in Fig. 3-1 is the same as described in Section 5.1 above.

The first stage of the modulator is the differential encoder and serial-to-parallel (S/P) converter. Since no carrier recovery is being done for the demodulator (the carrier is "stolen" from the modulator), differential encoding is not necessary and hence it is not implemented. The S/P converter divides the 3.0 Mb/s NRZ data into two streams of NRZ data at the rate of 1.5 Mb/s each. The circuit diagram of the S/P converter used along with its timing diagram is shown in Fig. 5-10. The converter alternates between its two outputs, the first bit at the input being present at output B, the second bit at the input being present at output C, third bit at input going to B, fourth bit at

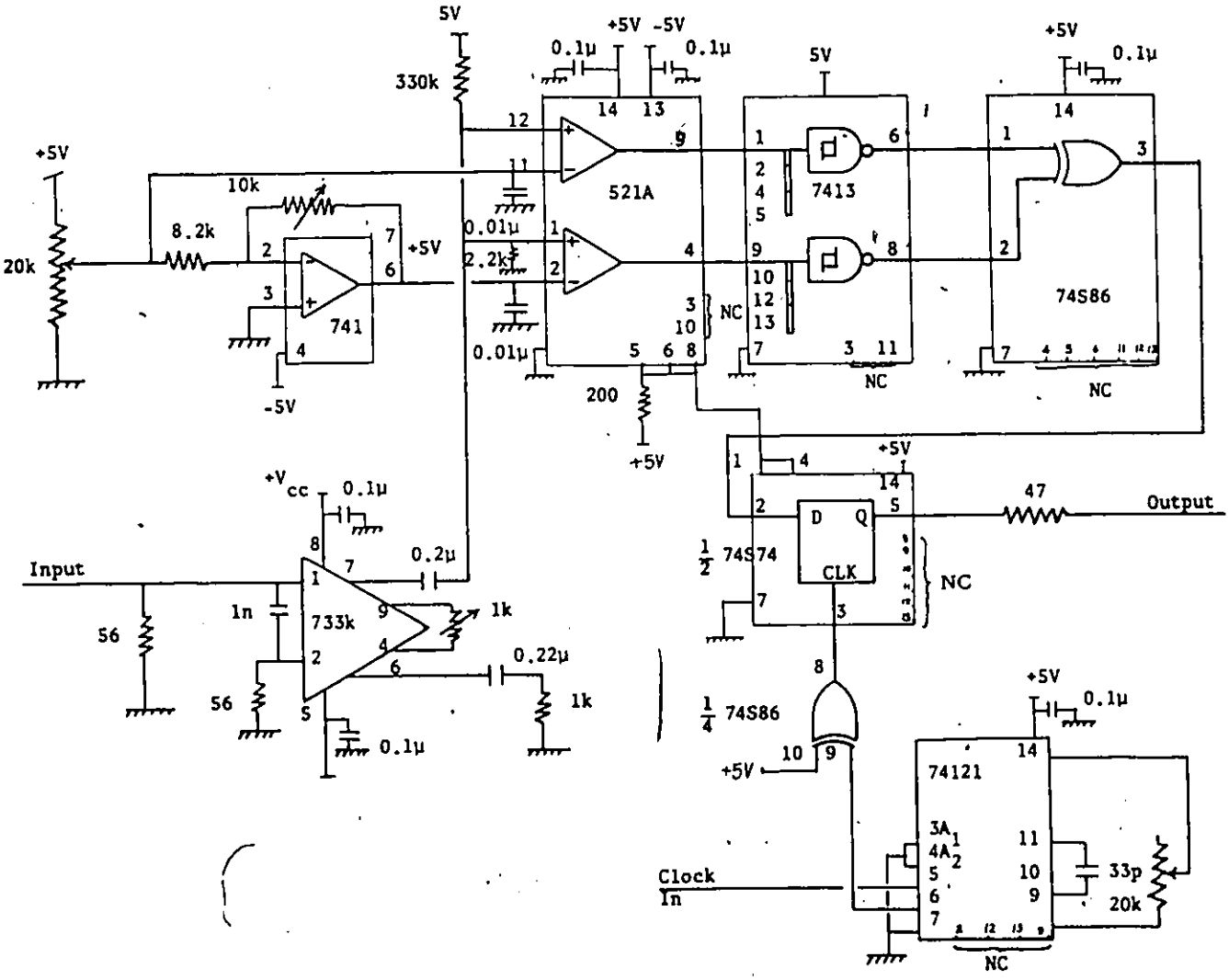

Figure 5-9. The circuit diagram of a three-level Class I decoder.

input appearing at C, and so on. For example, if the word 1 1 1 1 0 0 0 1 0 0 1 1 0 1 0 0 is present at the input A, 1 1 0 0 0 1 0 0 will appear at output B, and 1 1 0 1 0 1 1 0 will appear at output C.

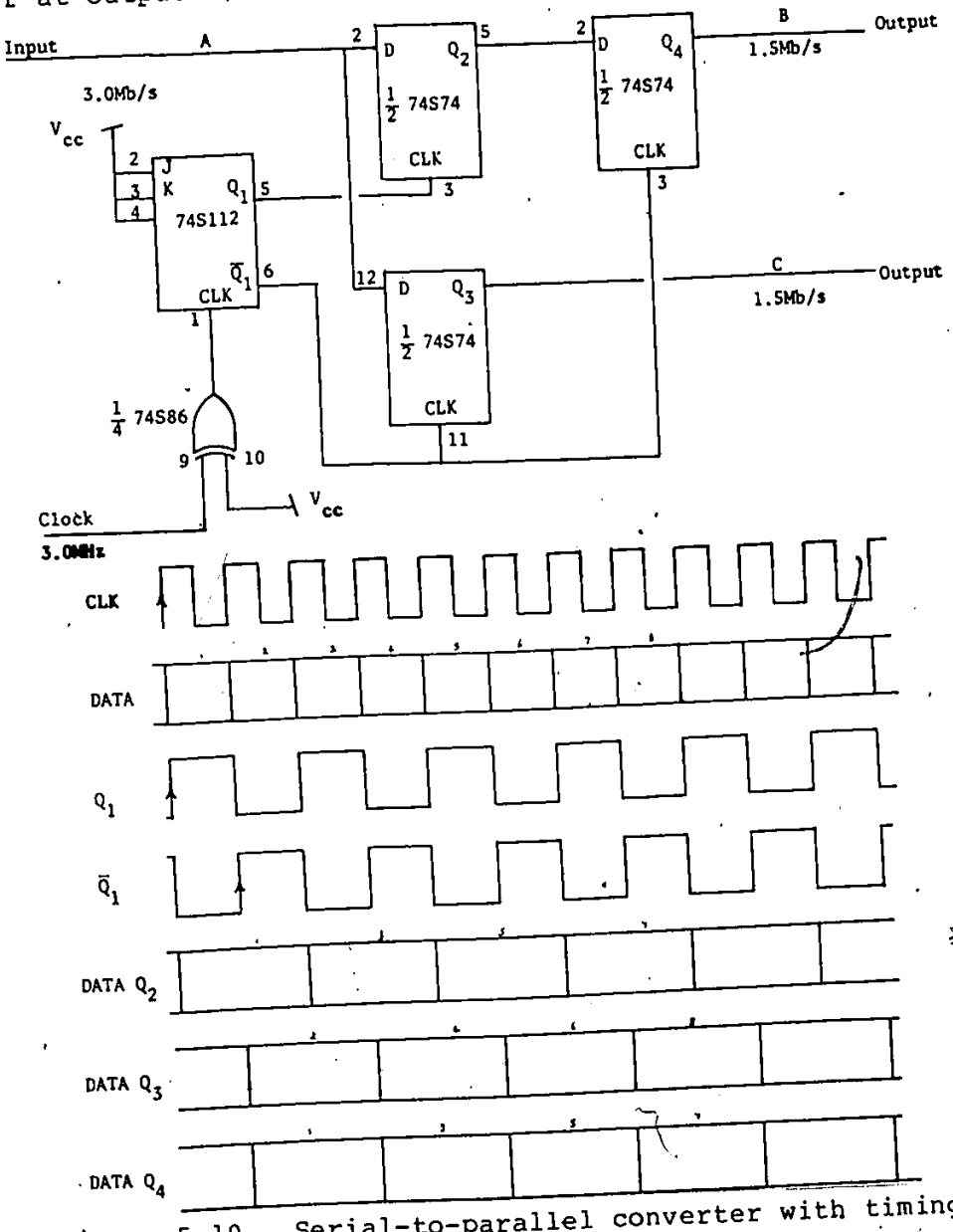

Figure 5-10. Serial-to-parallel converter with timing diagram.

For test purposes, an ordinary sine-wave generator (such as HP 3312A) may be used as the carrier or local oscillator source. The 90° phase-shifting circuit used is shown in Fig. 5-11 below. The outputs to the mixers are taken at the points marked V_1 and V_2. The phases of these two signals differ by 90°.

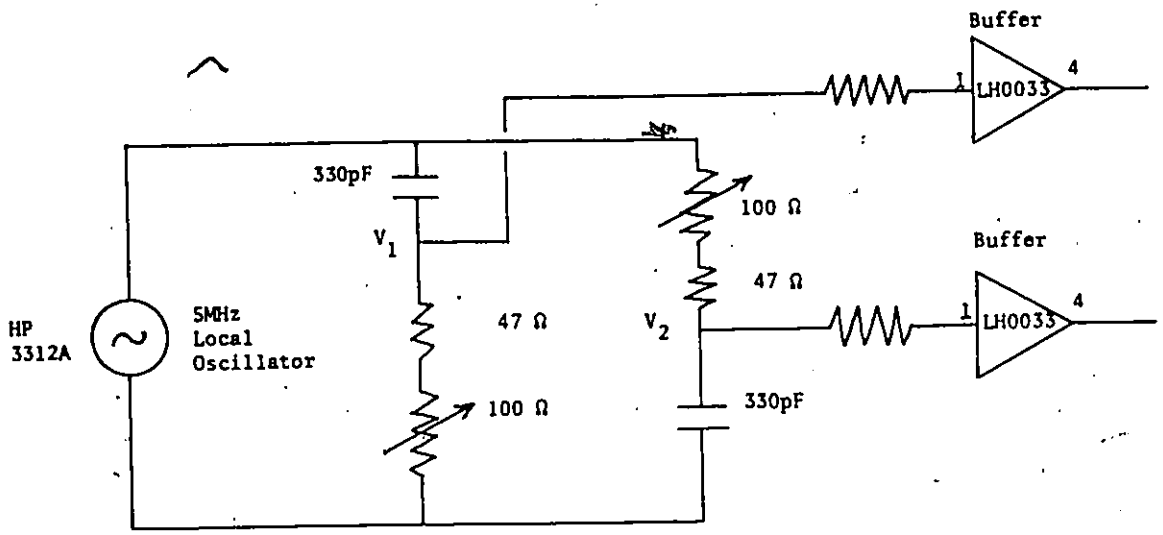

Figure 5-11. 90° phase-shifting network.

The outputs are applied to two double-balanced mixers (Mini-Circuits SRA-1) via buffers which also act as current drivers. The two modulated outputs are added using a 2-way 0° power combiner (Mini-Circuit MCL PSC2-1) resulting in a QPRS signal. Fig. 5-12 shows a circuit diagram of the QPRS modulator.

In the demodulator, the incoming QPRS signal is applied to a two-way 0° power splitter (Mini-Circuit MCL-PSC2-1), which produces two outputs each 3 dB lower than the input signal level, otherwise

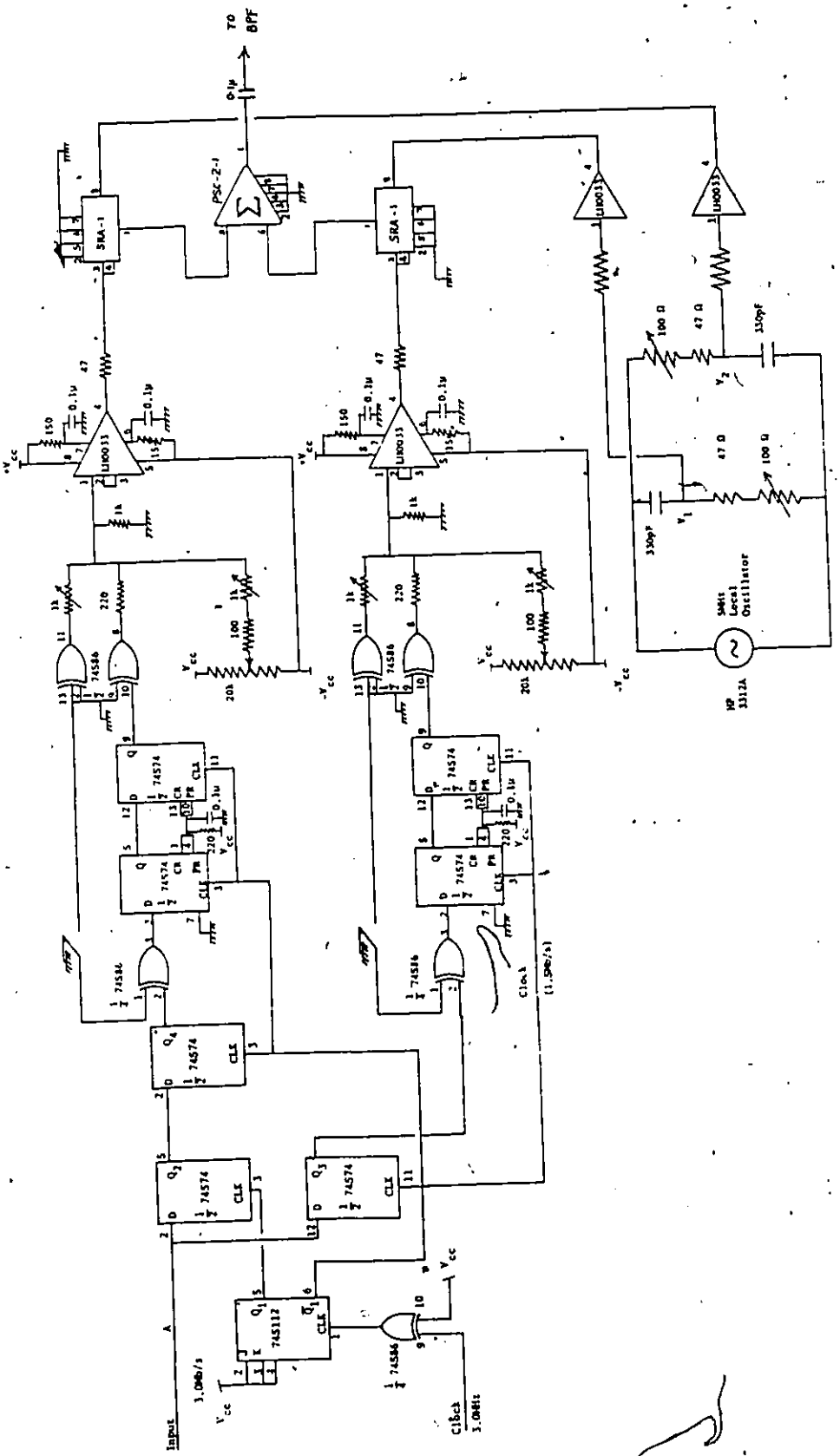

Figure 5-12. The Circuit Diagram of a QPRS Modulator

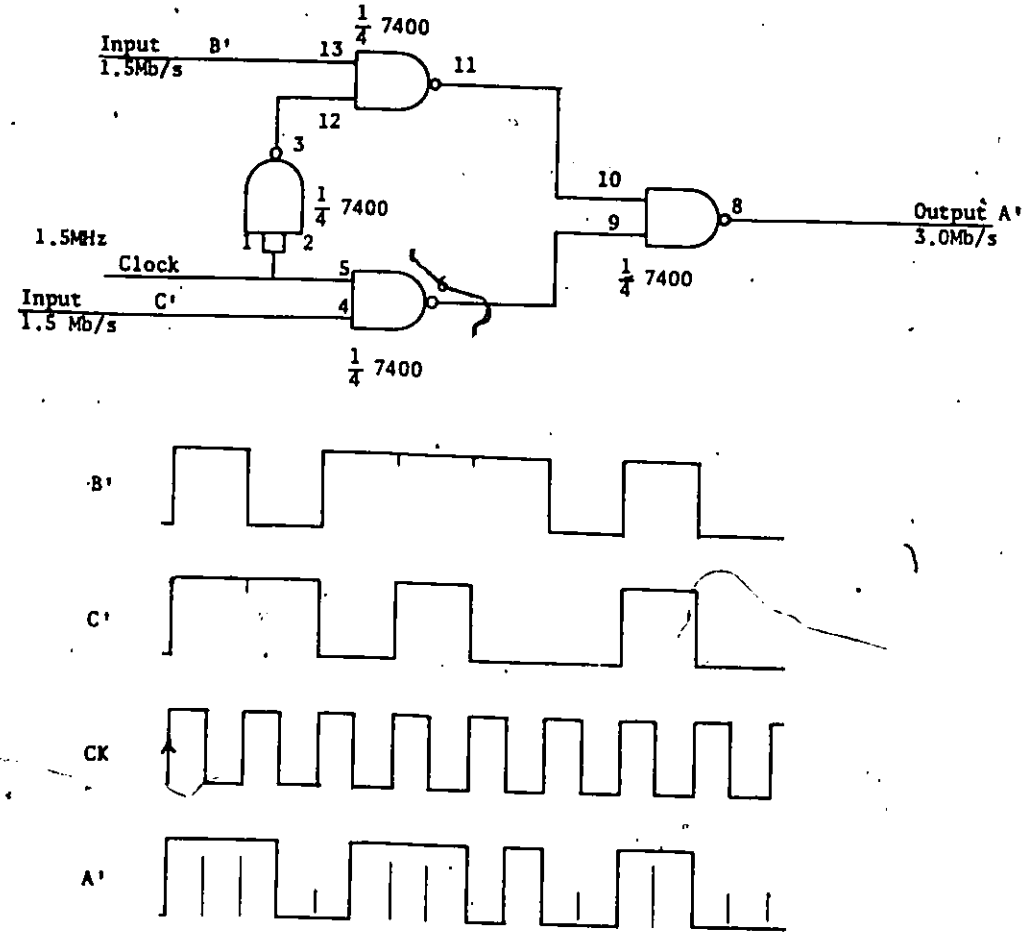

Figure 5-13. A circuit for a parallel-to-serial converter, and its timing diagram.

identical to the input signal. Each of these outputs is applied to a double-balanced mixer which is identical to the mixers in the modulator. The other input of the mixer is fed with a carrier signal.

The carriers feeding the two mixers are 90° out of phase. For test purposes in the laboratory, these carriers may be hard-wired (or "stolen") from the modulator. This avoids the trouble of carrier recovery and synchronisation. The PRS/NRZ decoder of Fig. 3-3 is identical to that described in Section 5.2 above.

The parallel-to-serial (P/S) converter recombines the two 1.5 Mb/s streams into a single 3.0 Mb/s stream. Fig. 5-13 shows the circuit diagram together with a timing diagram of the P/S converter used. The ouput A' alternates between the digits of the two serial inputs. For example, if the two bit streams B' and C' are 1 0 1 1 1 0 1 0 and 1 1 0 1 0 0 1 0 respectively the output A' will be 1 1 1 0 0 1 1 1 0 1 0 0 1 1 0 0. The circuit diagram of the whole demodulator is shown in Fig. 5-14.

5.4 Measurement Techniques and Test Results

This section describes the measurement techniques used in evaluating the PRS system. The test set-ups are described and the results given.

Fig. 5-15 shows the bench equipment for the system performance evaluation. A pseudo-random binary sequence (PRBS) generator provides binary NRZ data and clock. The eye pattern (or diagram) is used to evaluate intersymbol interference. To generate an eye diagram, the random data are fed to the vertical input of an oscilloscope which is

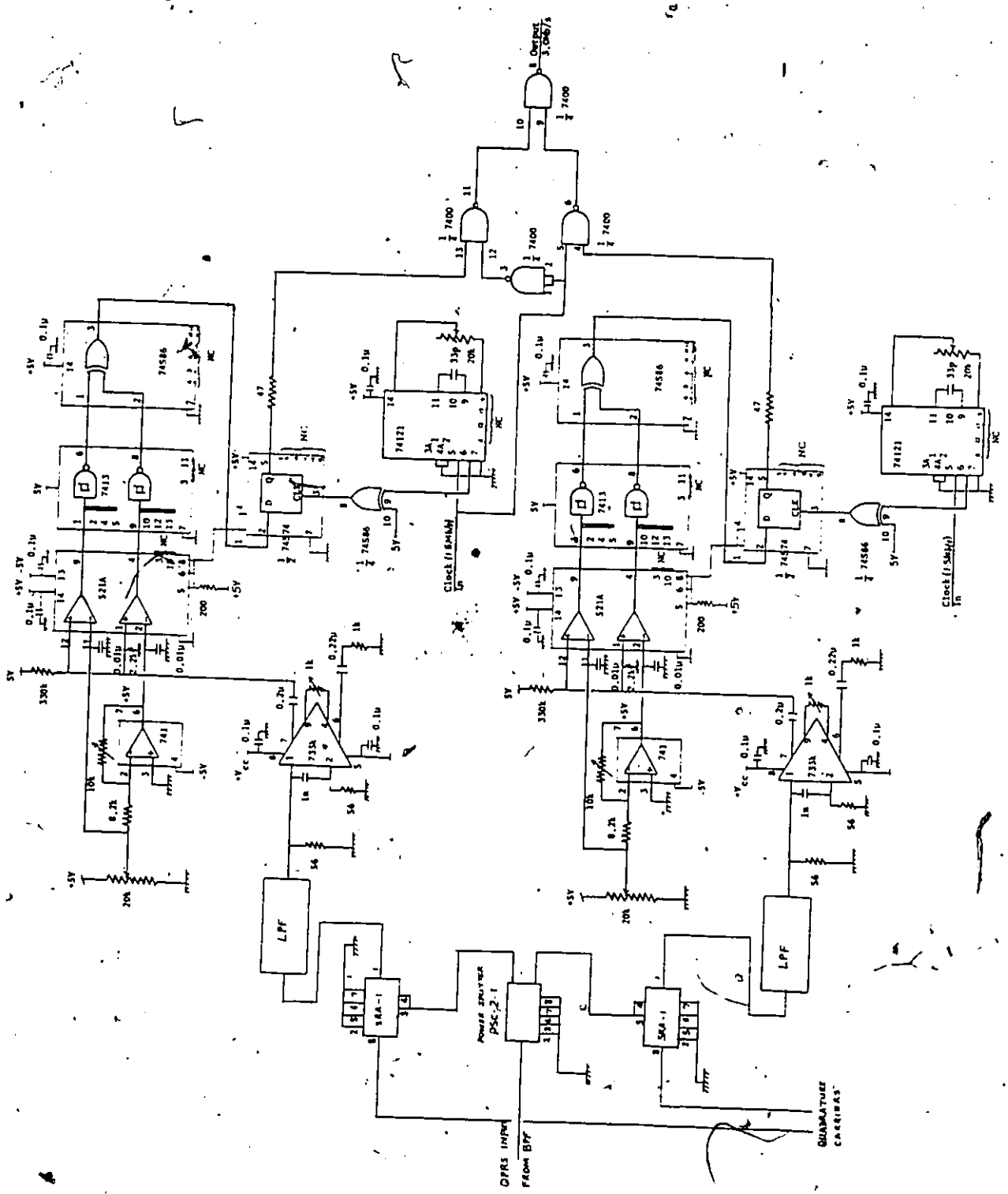

Figure 5-14. The QPRS Demodulator Circuit Diagram

externally triggered by the data clock. The PRBS sequence length should be as large as possible for a meaningful eye diagram. An n of 15 was used for these tests. The eye diagrams of a duobinary and modified duobinary systems are shown in Fig. 5-16 for a bit rate of 1.5 Mb/s.

To measure the power spectral density, a Hewlett-Packard Spectrum Analyser with a HP 141T display unit and a HP 8553B RF-Section plug-in unit were used. An XY plotter was used to record the spectra. The power spectral densities for binary NRZ, 3-level Class I (unfiltered and filtered), and Class IV PRS are shown in Figs. 5-17 to 5-20 for a bit rate is 1.5 Mb/s. Note that the first spectral null for binary NRZ is at 1.5 Mb/s while it is at 750 kHz for both 3-level Class I and Class IV PRS. Note also that for Class IV a spectral null also appears at dc.

The most important criterion of performance of a data transmission system is the probability of error. The detailed laboratory set-up for the measurement is depicted in Fig. 5-21. The HP 3310A function generator is used to clock the Hewlett-Packard HP 3760A PRBS generator. The latter provides NRZ data and clock. This data stream is converted by the PRS encoder into a three-level PRS signal. The channel is simulated by an attenuator in the signal path and linear adders which add noise and interference. I_1 and I_2 are two independent function generators (Wavetek Model 142) which can provide either a square wave or a sine wave. The resistive adders have the resistors chosen such that the input and output terminals have 50 ohms impedance.

Figure 5-15. Bench equipment for the system performance evaluation. Photo taken by Jean-François Meunier.

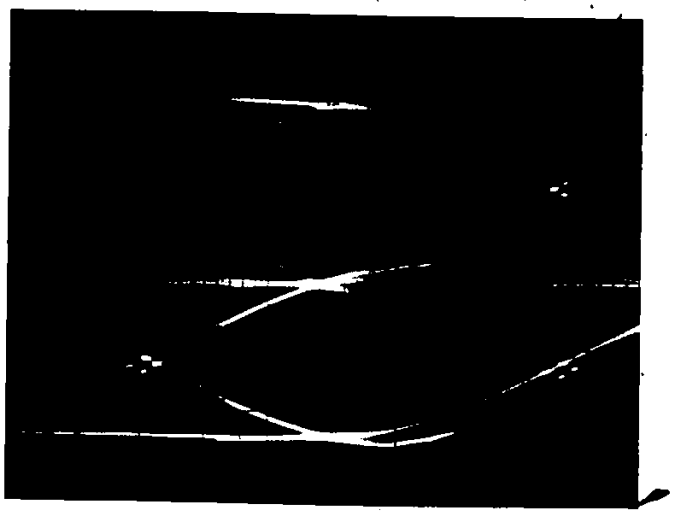

Data rate 1.5Mb/s

Filter cut off 900kHz

0.1 μsec/division

(a)

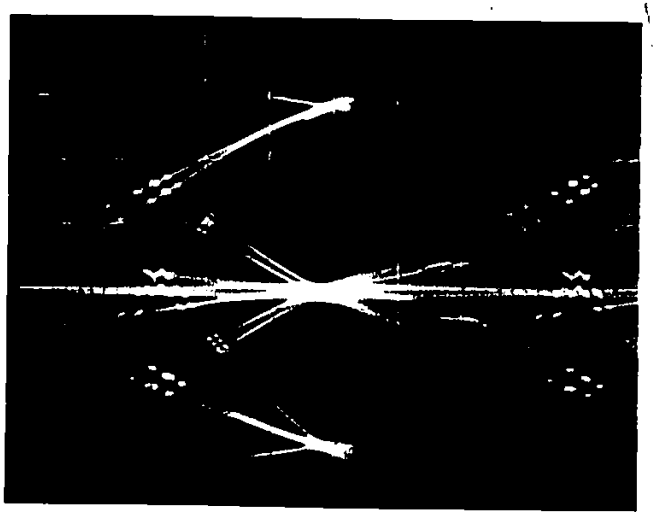

Data rate 1.5 Mb/s

Filter cut off 900kHz

0.1μ sec/division

(b)

Figure 5-16. Eye diagram for (a) duobinary system (b) modified duobinary system.

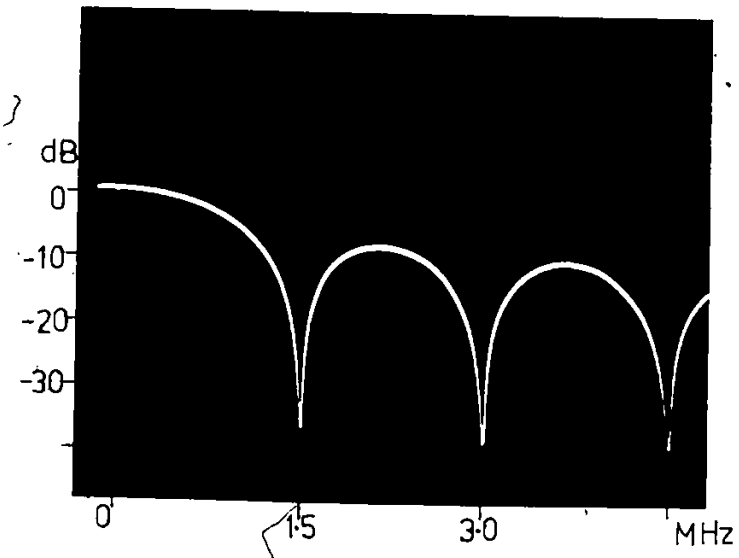

Data rate 1.5Mb/s

Figure 5-17. Power spectral density for a binary NRZ signal.

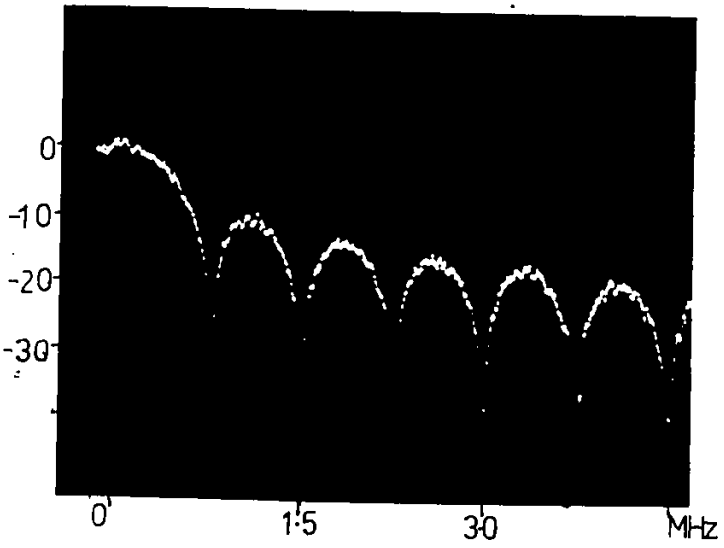

Data rate 1.5Mb/s

Figure 5-18. Power spectral density for a 3-level Class I PRS signal (unfiltered).

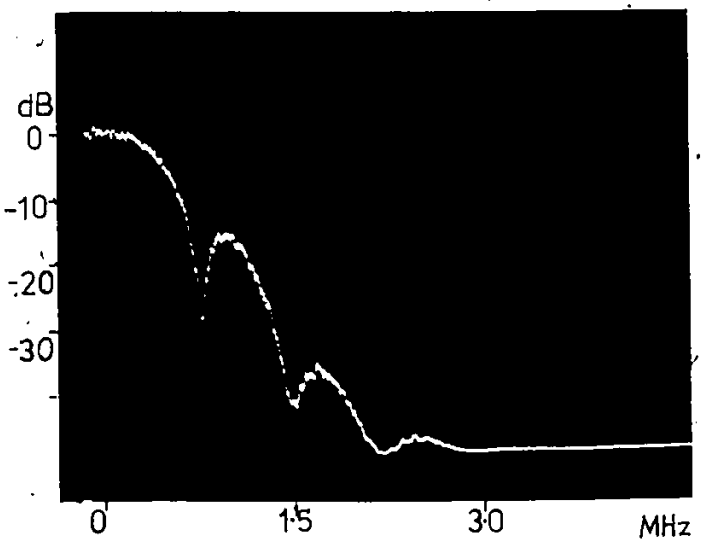

Data rate 1.5Mb/s

Figure 5-19. Power spectral density for a filtered Class I PRS signal.

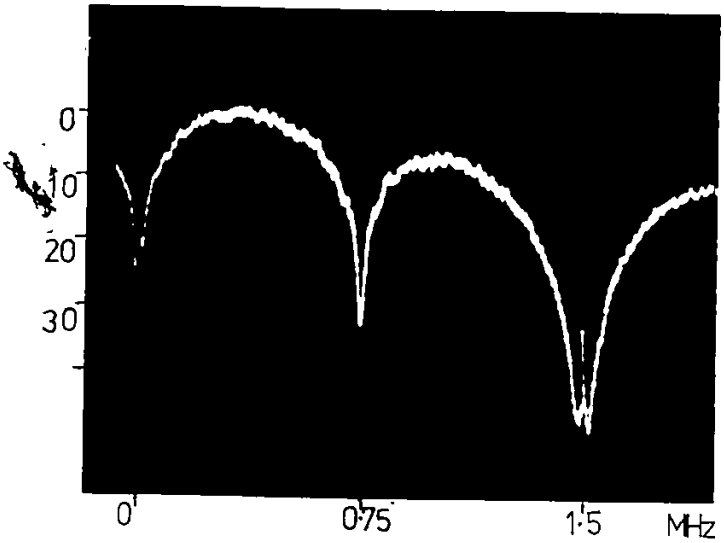

Data rate 1·5Mb/s

Figure 5-20. Power spectral density for a Class IV PRS signal.

The white noise is generated by a General Radio GR 1383 instrument which has a 20 Hz to 20 MHz bandwidth. A noise filter is needed to bandlimit this noise because of the frequency-dependent inaccuracy of the voltmeters for low signal levels. The composite signal (data plus noise and/or interference) passes through a fourth-order, low-pass filter, Krohn-Hite Model 3202, to the partial-response decoder which regenerates the data. The regenerated data (some of which are in error because of the corruption by noise etc.) are fed into the error detector, HP3761A, where they are compared bit by bit with a copy of the original data and the number of disagreements gives an indication of the bit error rate or probability of error. Throughout the measurements, no path is disconnected in order to maintain stable impedance characteristics.

A true rms voltmeter, HP3403C, is used at the input of the decoder to measure the signal, noise, and interference rms voltages. To measure the signal, all noise and interference paths are attenuated by at least 50 dB. To measure the noise, the signal and interference are attenuated, and for interference measurement, signal, noise and other interference sources are attenuated.

The probability of error is affected by the threshold levels at the decoder and the sampling instant. To experimentally optimise the P(e), a "screw-driver" algorithm was used; the thresholds were adjusted until the lowest error count was observed. The clock delay was also adjusted so as to sample at the centre of the eye, hence obtain the best P(e) possible. For very low BER measurements, extreme care has to be taken to avoid interference from external sources. For instance, during the course of one measurement, it was noticed that an electric

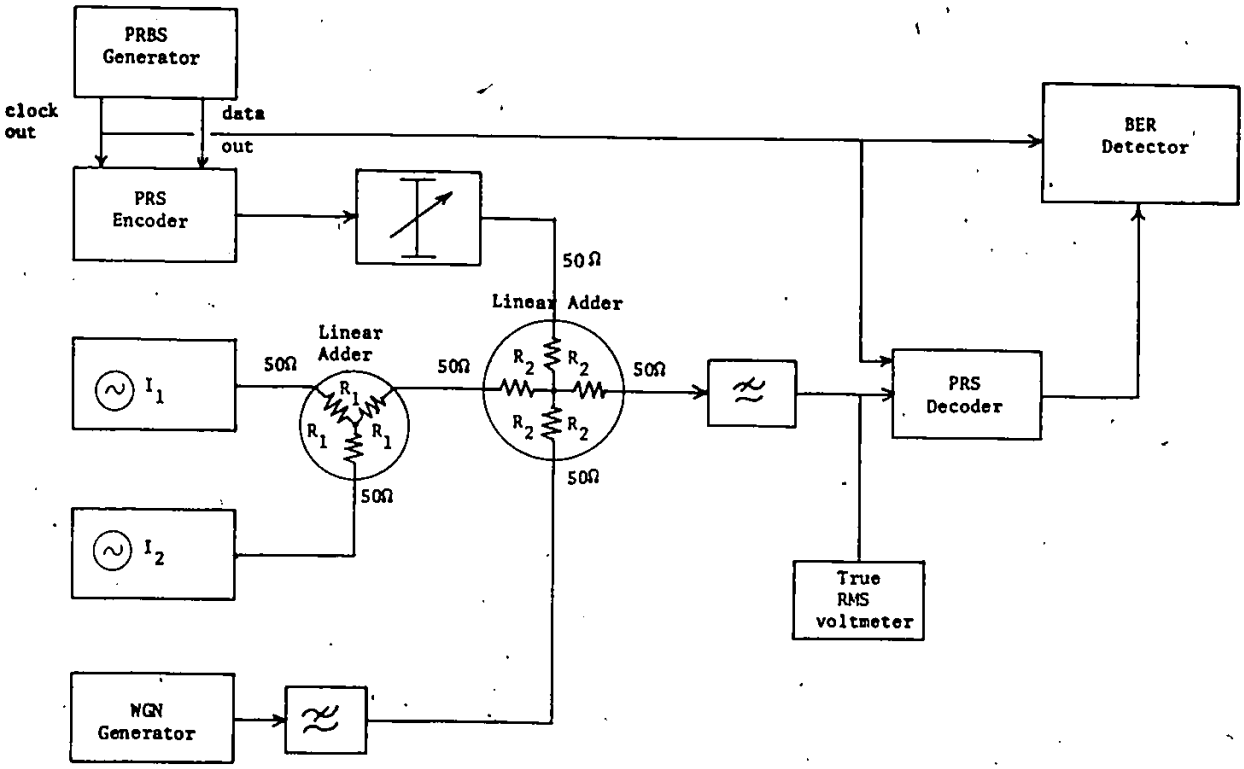

Figure 5-21. Laboratory set-up for measurement of the probability of error.

wire-wrap gun operated five meters away increased the number of errors from about 4 to 200 during one 10^7 bits interval. Switching on power supplies, oscilloscopes or even the lights near the test set-up introduces a handful of errors.

In Fig. 5-22 the performance of the experimental system in the presence of only white gaussian noise is shown together with the theoretical curve based on (4-33). The experimental curve is seen to differ from the theoretical one by about 1.5 dB. This is mainly due to hardware limitations of the coder/decoder used; for instance the actual uppermost and lowermost levels were not completely symmetrical about zero as assumed in the theoretical evaluation.

In Fig. 5-23 the laboratory measured results of the performance of the PRS system in the presence of square-wave interference alone are shown together with the theoretical curve. The low-pass filter just before the decoder in Fig. 5-21 was set at 2MHz cut off i.e. the square wave was virtually unaffected by it. By using square waves of 3kHz, 30kHz, and 100kHz, it was verified that, as would be expected from (4-35), the probability of error does not depend on the frequency of the interfering square wave since the pdf is independent of frequency. Using a 60 kb/s random binary sequence it was also verified that it does not matter whether the interfering signal is a periodic square wave or random data. The measured curve is seen to agree with the theoretical curve to within 2dB. No measurements were taken for SIR $\leq$ 3dB because the standard bit error rate (BER) instruments cannot measure any error rates above about 0.2. (However as pointed out earlier, these values would be of no practical interest anyway.)

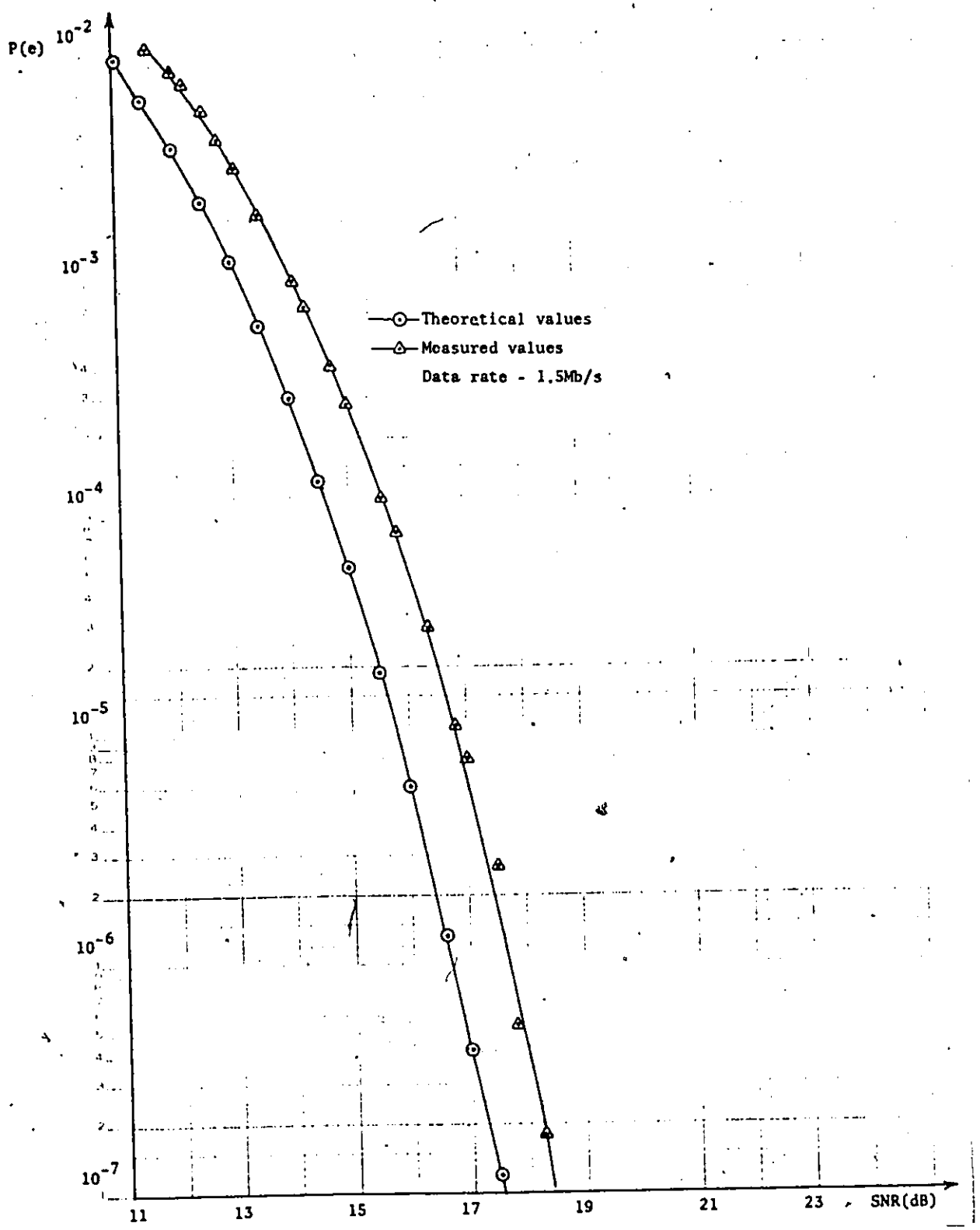

Figure 5-22. P(e) versus SNR in an AWGN environment, for a 3-level PRS system.

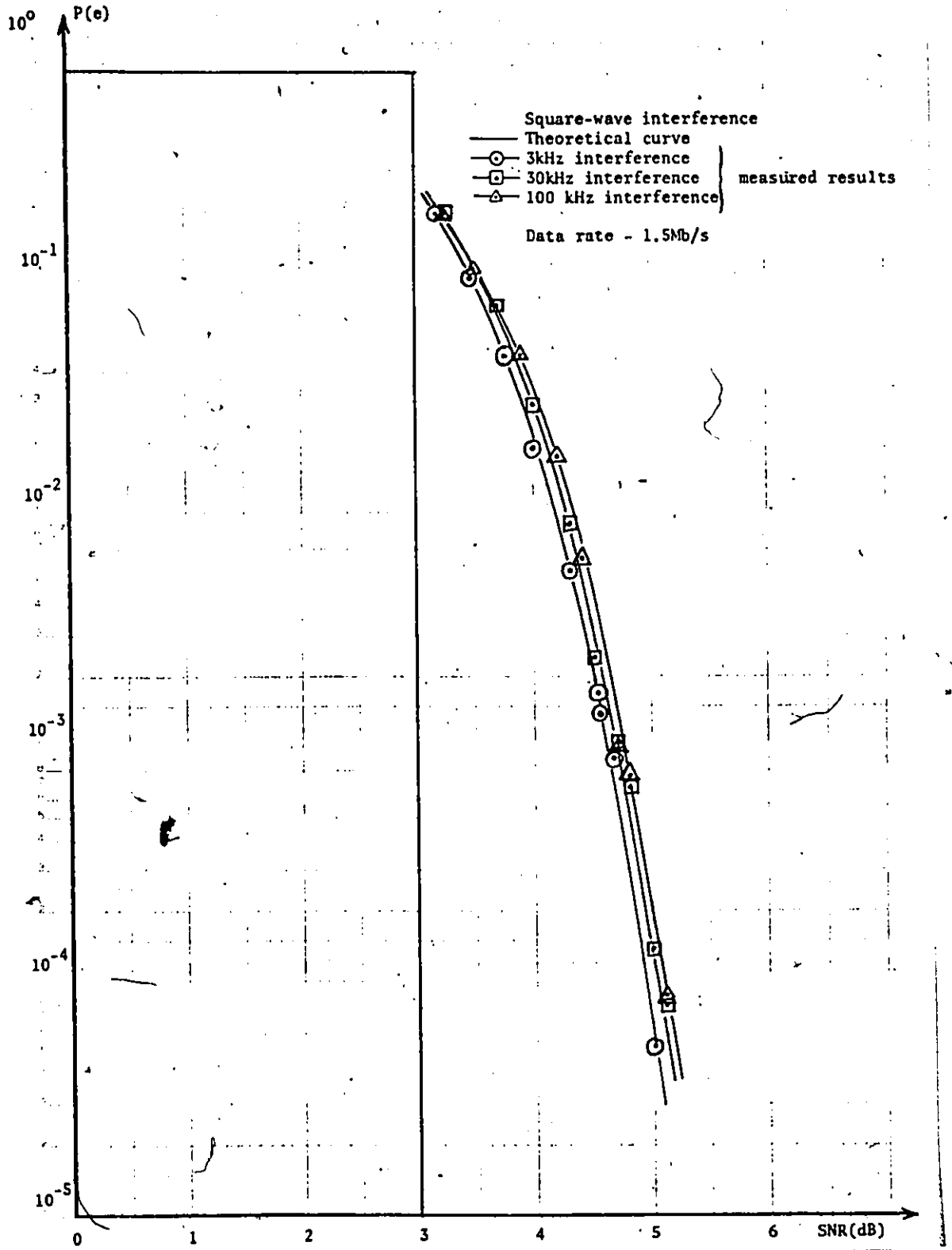

Figure 5-23. P(e) versus average SIR in a square-wave interference environment only, for a 3-level PRS system.

To be noted here also is the steepness of this curve; in fact the measured curve would be steeper were it not for the set-up limitations. This implies that a slight change in the signal would correspond to a drastic increase in the probability of error.

The theoretical performance of a binary NRZ system in the presence of sinusoidal interference alone was given by equation (4-41) in Section 4.3.2. The curve represented by this equation is plotted in Fig. 5-24. Also plotted in Fig. 5-24 is the measured results for the P(e) versus SIR performance of a binary system in a sinusoidal interference environment. This is for a 1.5 Mb/s data and 3 KHz and 100 KHz interfering sinusoids. It is seen that the frequency of the interference has little bearing on the probability of error.

Fig. 5-25 shows the measured results of the performance of the laboratory PRS system alongside of the theoretical values from (4-44). The region in which equation (4-45) applies is of no practical interest for data transmission. It is observed from this figure that the measured results are within about 1dB of the calculated values. One notes that for the laboratory system considered, the signal-to-sinusoidal interference ratio need to be maintained above 7dB. As mentioned earlier, in most digital transmission systems, this ratio is at least 20dB with the exception of deep fades. Note also the steepness of the curve in the neighbourhood of 7dB SIR. Comparing Figures 5-23 and 5-25, the threshold occurs at 3dB for the square-wave interference only case (Fig. 5-23) and at 6dB for the sinusoidal interference only case (Fig. 5-25). This 3dB difference is due to the 3dB difference in the peak-to-rms ratios of the sine wave and the

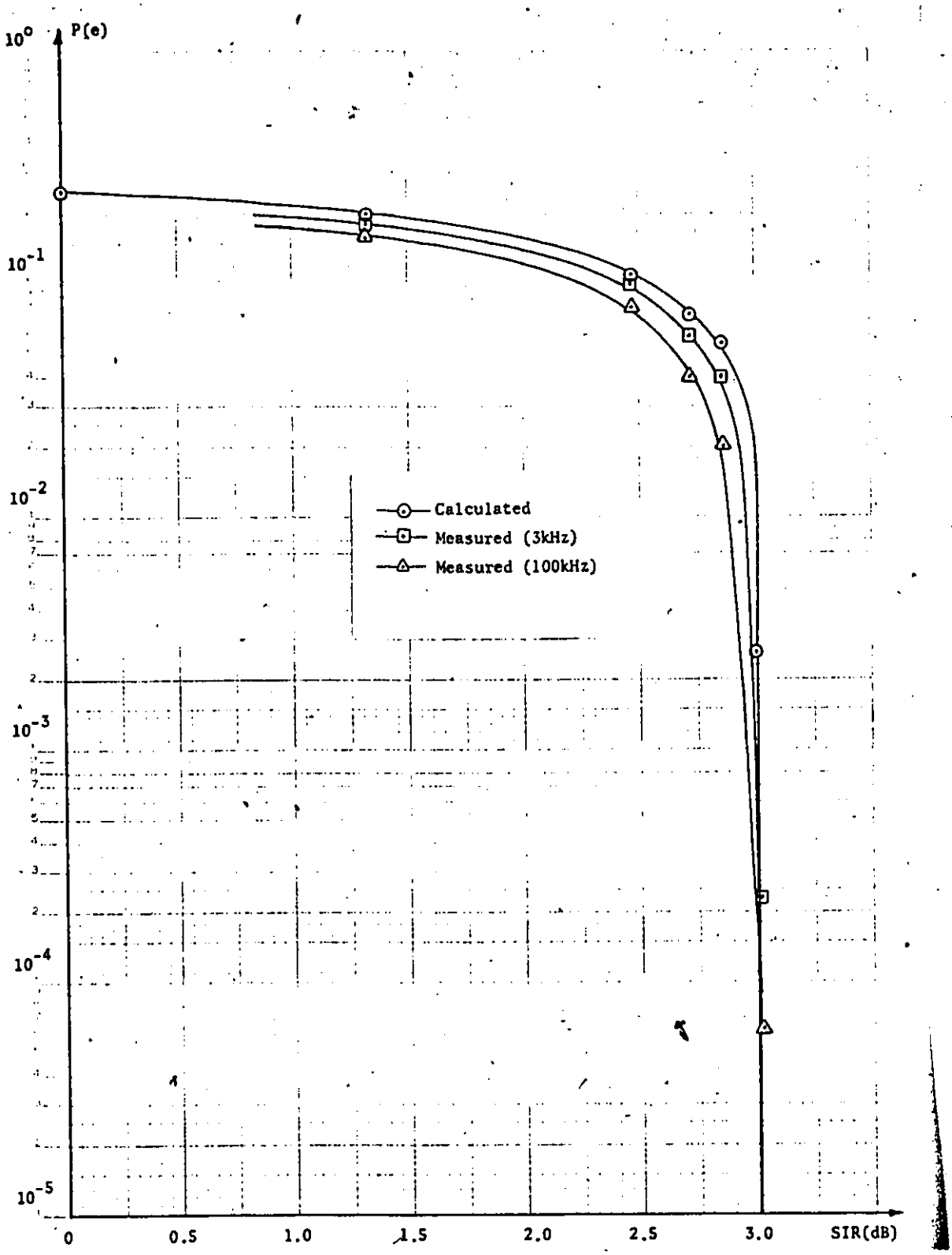

Figure 5-24. P(e) performance in a sinusoidal interference only environment for an NRZ signal.

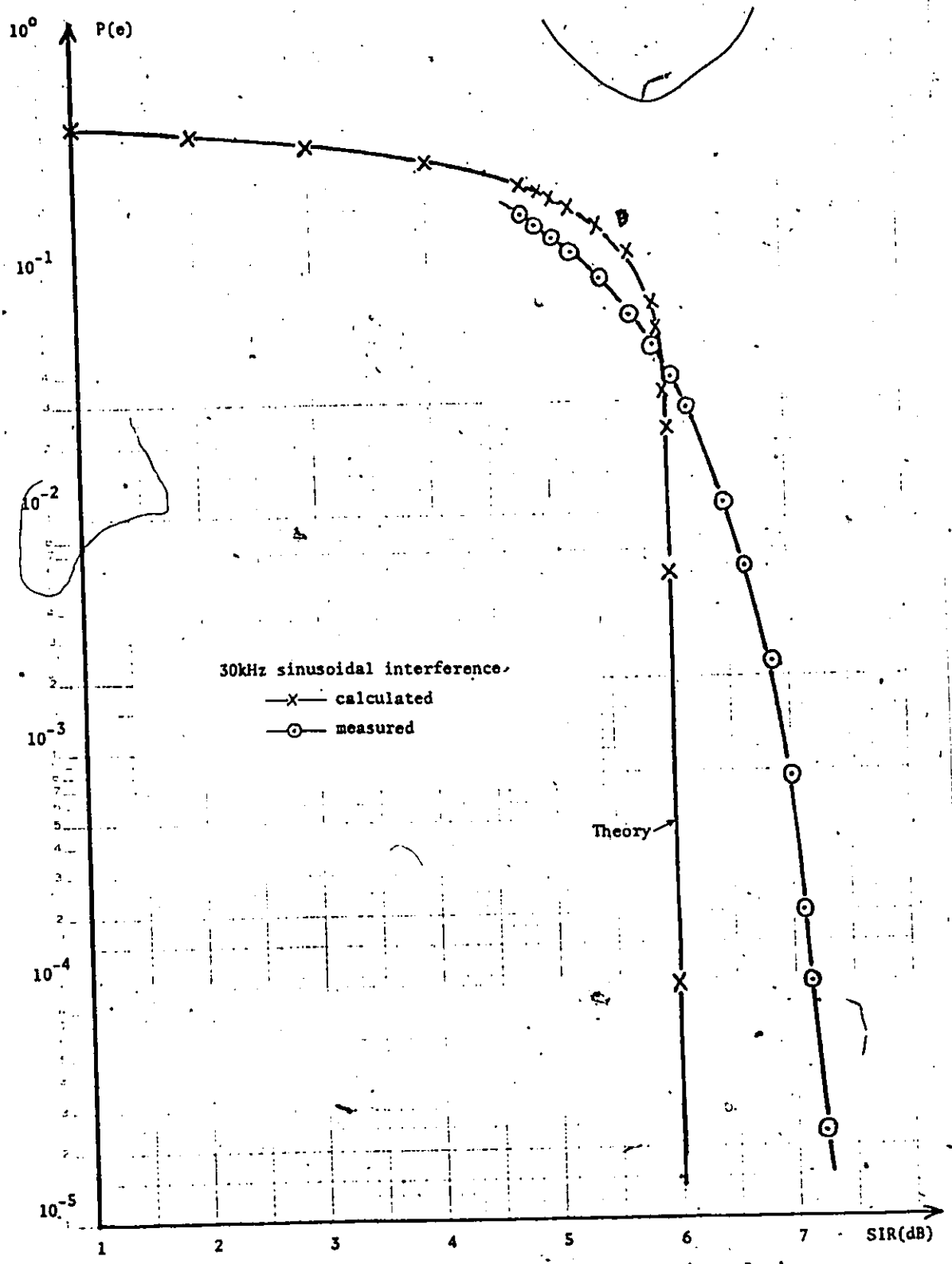

Figure 5-25. P(e) performance of a PRS signal in a sinusoidal interference only environment.

square wave. Fig. 5-26 shows the measured results, for a system perturbed by both AWGN and sinusoidal interference of 30KHz. The signal-to-interference ratio is used as a parameter. The results are for a wideband case i.e. the PRS signal is practically unfiltered. The leftmost curve gives the theoretical performance of the system in the presence of AWGN alone while the curve marked SIR = ∞ is the measured curve for AWGN alone. From these results, it may be concluded that PRS would not be severely degraded if the signal-to-interference ratio is maintained above 25dB. It was also experimentally verified that changing the frequency of the interference from 30kHz to 3kHz, 60kHz and 100 kHz respectively, the results did not differ from those in Fig. 5-26 by more than about 0.1dB which is within experimental error. Thus performance is independent of the interfering frequency as expected from theory.

The above results were taken with only one interfering sinusoid. The experiment was repeated with two interfering sinusoids, this time such that the total power (of both sinusoids) equals that in the previous experiment (one sinusoid). The two sinusoids were from two independent generators. The results obtained are shown in Fig. 5-27. The continuous curve indicates performance with all the power in one sinusoid, and the dotted curve is for the case when the power was divided equally between the two interferers. One notes that the P(e) curve is degraded the least when all the power is concentrated in one sinusoid. It is to be observed also that the difference between the two cases increases as the SIR ratio decreases. Any other case where the power is unequally divided between the two interferers would be

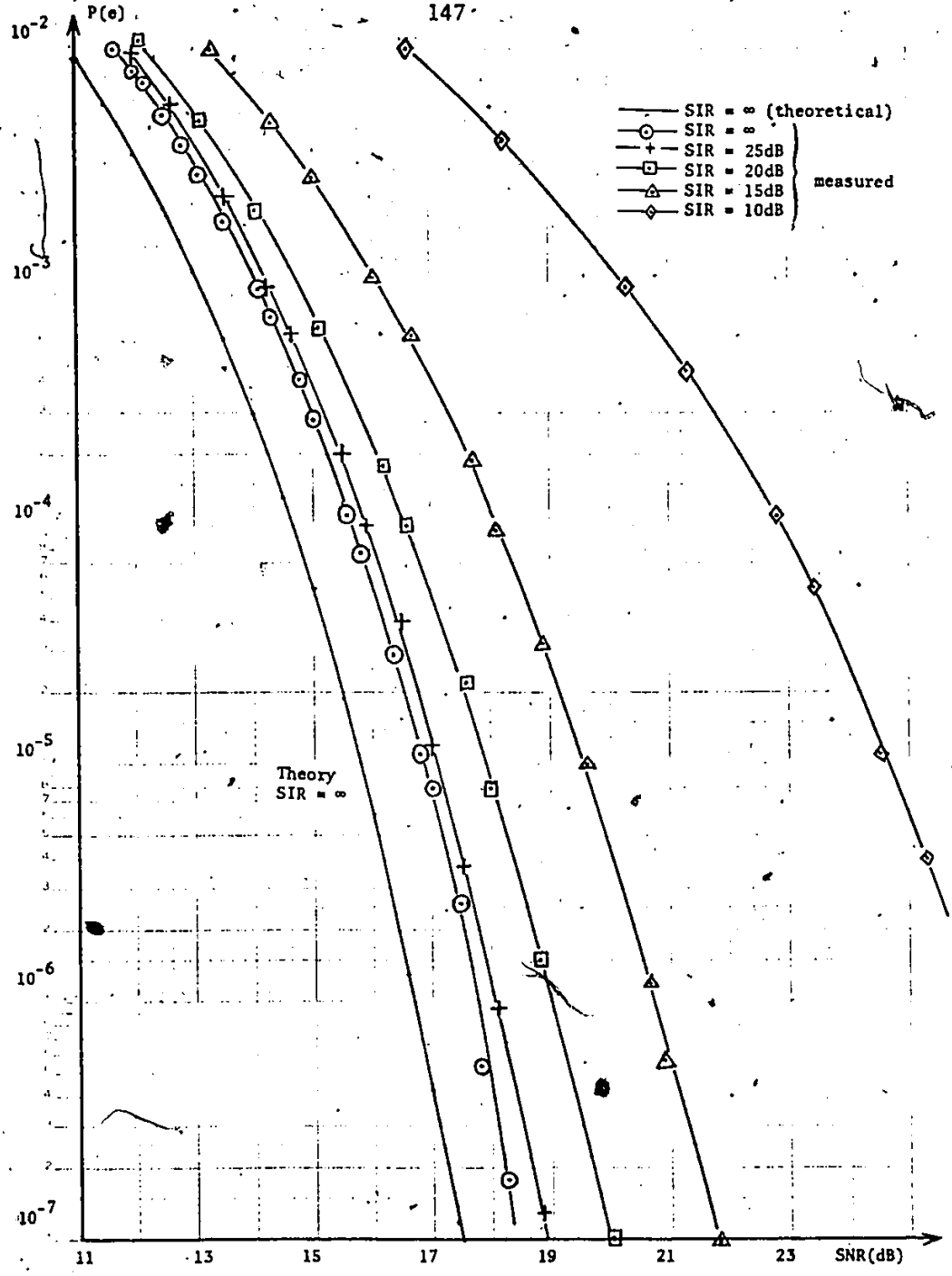

Figure 5-26. Performance of a PRS system in the presence of both sinusoidal interference (30KHz) and gaussian noise, for various interference levels.

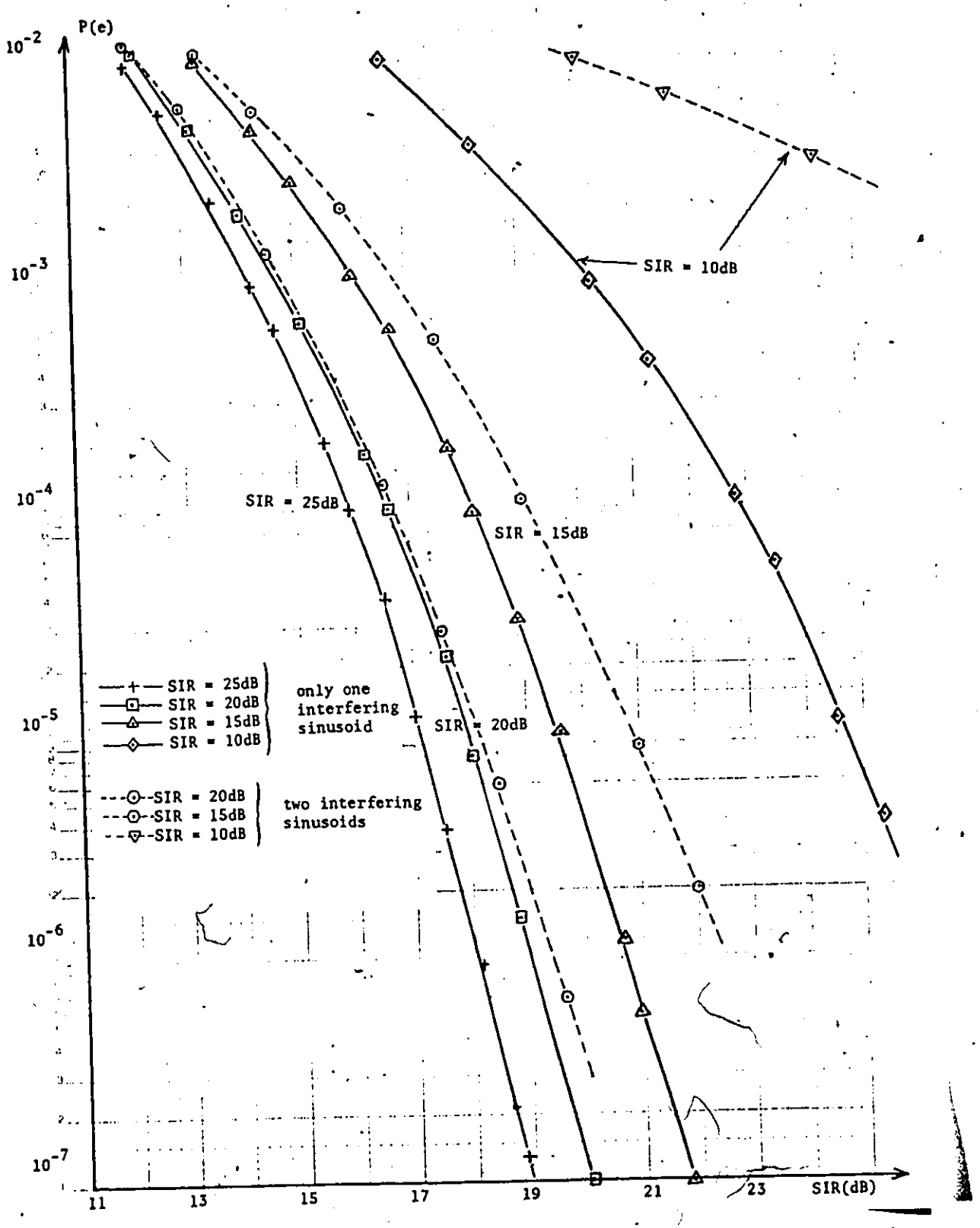

Figure 5-27. The effect of two interfering sinusoids on the performance of a PRS when AWGN is also present.

expected to lie between the cases considered here. If one permits himself to extrapolate on these results, he may conclude that the performance becomes progressively worse as power is equally divided among an increasing number of sinusoidal interferers. This is reasonable because as the number of sinusoidal interferers increase so does the peak-to-rms ratio [3].

Fig. 5-28 gives a comparison of square-wave interference and sinusoidal interference in the presence of random gaussian noise. A signal-to-interference ratio of SIR = 15dB is considered typical and is treated here. Square-wave interference seems to be slightly less degrading to the system. This is because the peak-to-rms ratio of a square wave is less than that of a sine-wave. The difference between the two is however only about 0.5dB.

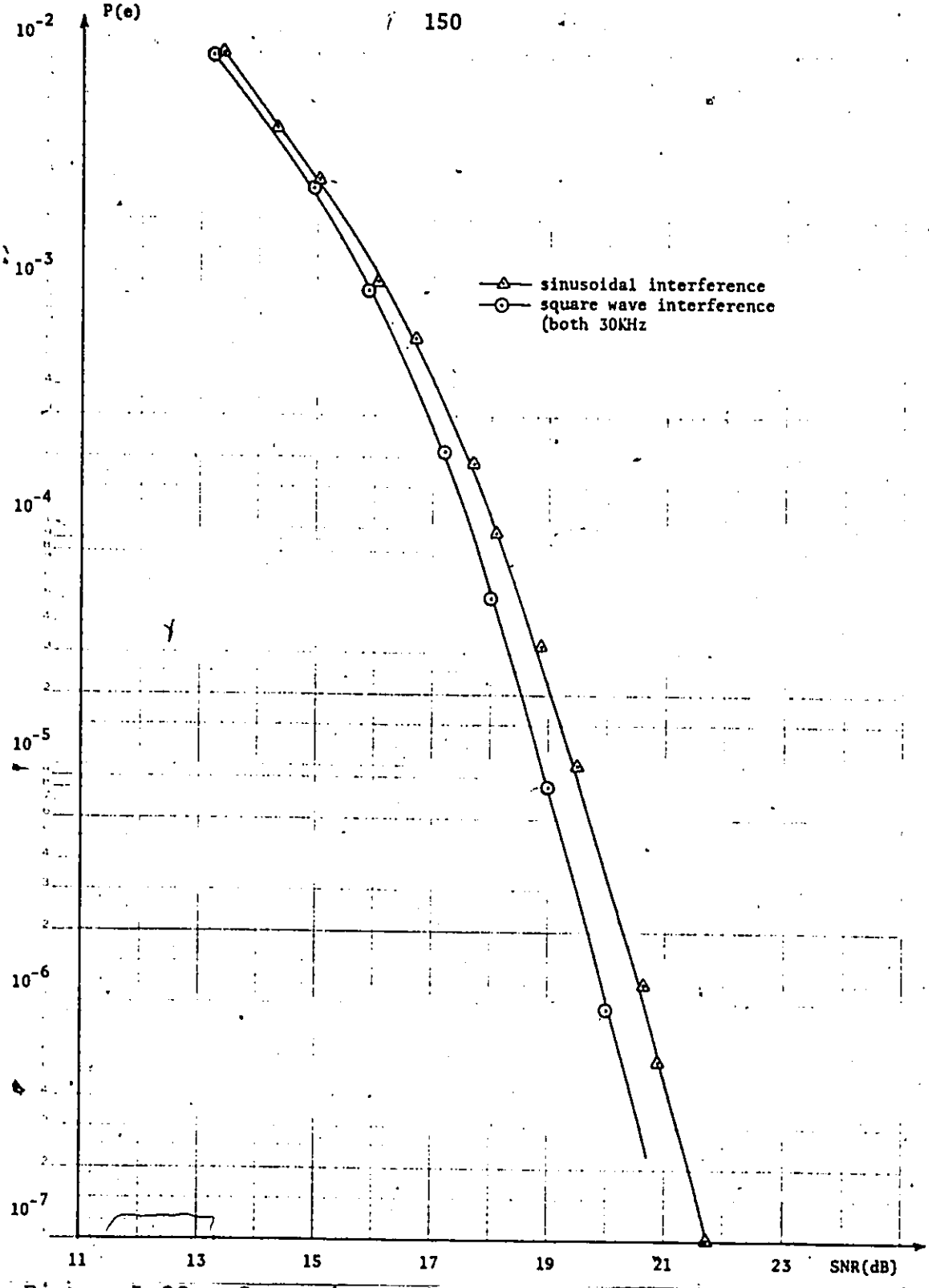

Figure 5-28. Comparison of square-wave and sinusoidal interferences in the presence of AWGN. A SIR = 15dB applies for both.

CHAPTER SIX

CONCLUSION

Partial-response signalling is becoming more popular as a method for data transmission. The basic concepts of PRS were thoroughly explored in this thesis, and presented in a form that is felt gives a good understanding of PRS. The bandwidth efficiency of PRS is a key factor in its popularity, this topped by the fact that this efficiency is achieved using practically realisable and perturbation tolerant filters. The relatively simple hardware realisation of PRS and its inherent capability of detecting errors without using redundant bits, are added advantages. Classes I and IV were given special attention as they are the ones most often used. The autocorrelation function of the duobinary system, not found in the literature perused, was derived and from this the corresponding spectral density expression developed.

A brief comparison of QPRS and 8-ϕ PSK modulation methods was made. It was found that QPRS is quite comparable to 8- ϕ PSK if the partial-response filtering is done after the final (nonlinear) power amplifier. In linear applications, QPRS is better from an E_b/N_0 point of view, but 8- ϕ PSK is more bandwidth efficient. Cost considerations would presumably favour QPRS since its hardware is simpler. A number of existing digital microwave radio systems, using either of these two methods, were compared in the form of two tables. Such a comparison (although it does not point at one preferred system) may be useful in selecting a digital microwave radio

system. It shows what is currently available and gives some, albeit limited analysis.

The probability of error performance of a Class I partial-response system in a random gaussian noise environment was derived in detail and measured for an experimental three-level system. Performances in the presence of square wave only and an interfering sinusoidal wave alone, respectively, were derived and compared to experimental results. Experimental results of the performance of the PRS system in the presence of both sinusoidal interference and random gaussian noise were presented and were found to be in good agreement with the theoretical ones. Finally sinusoidal interference was briefly compared to square-wave interference when both are accompanied by gaussian noise. It was seen that as long as the interference level is maintained about 25 dB below the signal level, performance of PRS is not seriously impaired. For QPSK, about 20 dB of CIR ratio is needed.

Although gaussian noise is the theoretician's dream, because of the ease with which it can be treated mathematically, noise in a practical operational environment often differs from this. Impulse ("popcorn") or burst noise, consisting of irregular bursts of short duration but of relatively high amplitudes, is often encountered in actual systems. It may originate from lightning, power lines, car ignition systems, switching transients, dialling and supervision in telephone switching centres, etc. Further work can be done on the effect of impulse noise on partial-response systems. A more complex interference environment than considered here may be considered in evaluating PRS systems. For example, AWGN, impulse noise, and sinusoidal interference may all be considered.

Another possible extension of this work could be the application of soft decoding techniques such as ambiguity-zone detection, maximum likelihood decoding, and matched-transmission techniques to PRS systems. The effect of the various interferences considered in this thesis, plus impulse noise, on PRS systems using these techniques, may be explored.

APPENDIX I

IMPULSE RESPONSE OF AN EQUIVALENT NYQUIST FILTER WITH SINUSOIDAL ROLL-OFF

The transfer function H(f) of the equivalent Nyquist filter is given by (2-6). The impulse response is

$$h(t) = \int_{-\infty}^{\infty} H(f) e^{j2\pi ft} df$$

$$= 2T \int_{0}^{\frac{1}{2T}(1-\alpha)} \cos 2\pi ft \, df + T \int_{\frac{1}{2T}(1-\alpha)}^{\frac{1}{2T}(1-\alpha)} [1-\sin\tfrac{\pi T}{\alpha}(f-\tfrac{1}{2T})]\cos 2\pi ft \, df$$

$$= 2T \frac{\sin 2\pi ft}{2\pi t} \Bigg|_{0}^{\frac{1}{2T}(1-\alpha)} + T \frac{\sin 2\pi ft}{2\pi t} \Bigg|_{\frac{1}{2T}(1-\alpha)}^{\frac{1}{2T}(1+\alpha)}$$

$$- \frac{T}{2} \int_{\frac{1}{2T}(1-\alpha)}^{\frac{1}{2T}(1+\alpha)} \left\{ \sin[(2\pi t + \tfrac{\pi T}{\alpha})f - \tfrac{\pi}{2\alpha}] + \sin[(\tfrac{\pi T}{\alpha} - 2\pi t)f - \tfrac{\pi}{2\alpha}] \right\} df$$

$$= T \frac{\sin \frac{\pi t}{T}(1-\alpha)}{2\pi t} + T \frac{\sin \frac{\pi t}{T}(1+\alpha)}{2\pi t}$$

$$+ \frac{T}{2} \frac{\cos[(2\pi t + \pi T/\alpha) f - \pi/2\alpha]}{\pi T/\alpha + 2\pi t} \Bigg|_{\frac{1}{2T}(1+\alpha)}^{\frac{1}{2T}(1-\alpha)}$$

$$+ \frac{T}{2} \frac{\cos[(-2\pi t + \pi T/\alpha) f - \pi/2\alpha]}{\pi T/\alpha - 2\pi t} \Bigg|_{\frac{1}{2T}(1+\alpha)}^{\frac{1}{2T}(1-\alpha)}$$

$$h(t) = \frac{T \sin \frac{\pi t}{T} \cos \frac{\pi t\alpha}{T}}{\pi t}$$

$$+ \frac{T}{2(\frac{\pi T}{\alpha} + 2\pi t)} \left\{ \cos[\frac{1}{2T}(2\pi t + \frac{\pi T}{\alpha})(1+\alpha) - \frac{\pi}{2\alpha}] \right.$$

$$\left. - \cos[\frac{1}{2T}(2\pi t + \frac{\pi T}{\alpha})(1-\alpha) - \frac{\pi}{2\alpha}] \right\}$$

$$+ \frac{T}{2(\frac{\pi T}{\alpha} - 2\pi t)} \left\{ \cos[\frac{1}{2T}(\frac{\pi T}{\alpha} - 2\pi t)(1+\alpha) - \frac{\pi}{2\alpha}] \right.$$

$$\left. - \cos[\frac{1}{2T}(\frac{\pi T}{\alpha} - 2\pi t)(1-\alpha) - \frac{\pi}{2\alpha}] \right\}$$

$$h(t) = \frac{\sin\frac{\pi t}{T}\cos\frac{\pi t\alpha}{T}}{\frac{\pi t}{T}}$$

$$- \frac{2T}{2(\frac{\pi T}{\alpha}+2\pi t)}\sin[\frac{1}{2T}(\frac{\pi T}{\alpha}+2\pi t) - \frac{\pi}{2\alpha}]\sin[\frac{1}{2T}(\frac{\pi T}{\alpha}+2\pi t)\alpha]$$

$$- \frac{2T}{2(\frac{\pi T}{\alpha}-2\pi t)}\sin[\frac{1}{2T}(\frac{\pi T}{\alpha}-2\pi t) - \frac{\pi}{2\alpha}]\sin[\frac{1}{2T}(\frac{\pi T}{\alpha}-2\pi t)\alpha]$$

$$= \frac{\sin\frac{\pi t}{T}\cos\frac{\pi t\alpha}{T}}{\frac{\pi t}{T}} - \frac{1}{(\frac{\pi}{\alpha}+\frac{2\pi t}{T})}\sin\frac{\pi t}{T}\sin(\frac{\pi\alpha t}{T}+\frac{\pi}{2})$$

$$+ \frac{1}{(\frac{\pi}{\alpha}-\frac{2\pi t}{T})}\sin\frac{\pi t}{T}\sin(\frac{\pi}{2}-\frac{\pi t\alpha}{T})$$

$$= \frac{\sin\frac{\pi t}{T}\cos\frac{\pi t\alpha}{T}}{\frac{\pi t}{T}} + \sin\frac{\pi t}{T}\cos\frac{\pi t\alpha}{T}[\frac{1}{\frac{\pi}{\alpha}-\frac{2\pi t}{T}} - \frac{1}{\frac{\pi}{\alpha}+\frac{2\pi t}{T}}]$$

$$= \frac{\sin\frac{\pi t}{T}\cos\frac{\pi t\alpha}{T}}{\frac{\pi t}{T}} + \frac{\sin\frac{\pi t}{T}\cos\frac{\pi t\alpha}{T}}{\pi(\frac{1}{\alpha 2} - \frac{4t^2}{T^2})}[\frac{4t}{T}]$$

$$h(t) = \frac{\sin\frac{\pi t}{T}\cos\frac{\pi t\alpha}{T}}{\frac{\pi t}{T}}\left[1 + \frac{4}{\frac{T^2}{t^2\alpha^2} - 4}\right]$$

$$= \frac{\sin\frac{\pi t}{T}\cos\frac{\pi t\alpha}{T}}{\frac{\pi t}{T}} \cdot \frac{\frac{T^2}{t^2\alpha^2}}{\frac{T^2}{t^2\alpha^2} - 4} = \frac{\sin\frac{\pi t}{T}}{\frac{\pi t}{T}} \cdot \frac{\cos\frac{\pi t\alpha}{T}}{1 - 4\frac{\alpha^2 t^2}{T^2}}$$

i.e. $h(t) = \dfrac{\sin\frac{\pi t}{T}}{\frac{\pi t}{T}} \cdot \dfrac{\cos\frac{\alpha\pi t}{T}}{1 - 4\alpha^2\frac{t^2}{T^2}}$ which was stated in (2-7).

APPENDIX II

It is required to show that equation (4-20) is true, i.e.

$$\sum_{k=0}^{M-1}\binom{M-1}{k}\left[\sum_{i=1}^{M-1-k}\Lambda_i + \sum_{i=1}^{k}\Lambda_i\right] = 2\sum_{k=1}^{M-1}\binom{M-1}{k}\sum_{i=1}^{k}\Lambda_i$$

For ease of notation let M-1 = p, therefore it is required to show that

$$\sum_{k=0}^{p}\binom{p}{k}\left\{\tfrac{1}{2}\sum_{i=1}^{p-k}\Lambda_i + \tfrac{1}{2}\sum_{i=1}^{k}\Lambda_i\right\} = \sum_{k=1}^{p}\binom{p}{k}\sum_{i=1}^{k}\Lambda_i \qquad (*)$$

Take the first term $\frac{1}{2}\sum_{k=0}^{p}\left[\binom{p}{k}\sum_{i=1}^{p-k}\Lambda_i\right]$

Let k = p - m or m = p - k

One quickly gets $\frac{1}{2}\sum_{m=p}^{m=0}\binom{p}{p-m}\sum_{i=1}^{m}\Lambda_i \qquad (\diamond)$

m takes on values p, p-1, ..., 2, 1, 0.

The sum on m in ($\diamond$) can be reversed to get

$$\tfrac{1}{2}\sum_{m=0}^{p}\binom{p}{p-m}\sum_{i=1}^{m}\Lambda_i$$

Now $\binom{p}{p-m} = \frac{p!}{(p-m)!m!} = \binom{p}{m}$

Hence the first term in (*) becomes $\frac{1}{2} \sum_{m=0}^{p} \binom{p}{m} \sum_{i=1}^{m} \Lambda_i$ which is identical to the second term [m and k are dummy variables of summation].

Now, when m = 0, each term in (*) becomes

$$\binom{p}{0} \sum_{i=1}^{0} \Lambda_i = 0$$

Hence LHS of (*) becomes

$$\sum_{k=1}^{p} \binom{p}{k} \sum_{i=1}^{k} \Lambda_i$$

and thus (*) holds true. Therefore equation (4-20) is shown to be valid.

APPENDIX III

One wants to show that

$$\sum_{k=0}^{M-1} \left(\tfrac{1}{2}\right)^{M-1} \binom{M-1}{k} \left(\frac{2Vk}{M-1}\right)^2 = \frac{V^2 M}{(M-1)} \qquad (\heartsuit)$$

The LHS of ($\heartsuit$) may be rewritten as

$$\text{LHS} = \left(\tfrac{1}{2}\right)^{M-1} \frac{4V^2}{(M-1)^2} \sum_{k=0}^{M-1} \binom{M-1}{k} k^2 = \left(\tfrac{1}{2}\right)^{M-1} \frac{4V^2}{(M-1)^2} \sum_{k=1}^{M-1} \binom{M-1}{k} k^2$$

It is an easy task to show that $k\binom{N}{k} = N\binom{N-1}{k-1}$. ($\clubsuit$)

Hence the LHS of ($\heartsuit$) becomes

$$\text{LHS} = \left(\tfrac{1}{2}\right)^{M-1} \frac{4V^2}{(M-1)} \sum_{k-1}^{M-1} \binom{M-2}{k-1} k$$

Let $m = k - 1$,

$$\text{LHS} = \left(\tfrac{1}{2}\right)^{M-1} \frac{4V^2}{(M-1)} \sum_{m=0}^{M-2} \binom{M-2}{m} (m+1)$$

$$= \left(\tfrac{1}{2}\right)^{M-1} \frac{4V^2}{(M-1)} \left\{ \sum_{m=0}^{M-2} \binom{M-2}{m} + \sum_{m=0}^{M-2} \binom{M-2}{m} m \right\}$$

Using ($\clubsuit$) in the second term in bracket and changing the variable $n = m - 1$, yields

$$\text{LHS} = (\tfrac{1}{2})^{M-1} \frac{4V^2}{(M-1)} \left\{ \sum_{m=0}^{M-2} \binom{M-2}{m} + (M-2) \sum_{n=0}^{M-3} \binom{M-3}{n} \right\}$$

Now, it is well known that

$$\sum_{i=0}^{b} \binom{b}{i} = 2^b$$

Therefore,

$$\text{LHS} = (\tfrac{1}{2})^{M-1} \frac{4V^2}{(M-1)} [2^{M-2} + (M-2)^{M-3}]$$

$$= (\tfrac{1}{2})^{M-1} \frac{4V^2}{(M-1)} 2^{M-3} M$$

$$= \frac{V^2 M}{M-1}$$

$$= \text{RHS}$$

Hence relation (♡) holds true.

APPENDIX IV

It is required to prove that

$$\sum_{k=1}^{M-1} \binom{M-1}{k} \sum_{i=1}^{k} (-I)^i = -\,2^{M-2} \qquad (\xi)$$

Clearly the L.H.S. is

$$-\sum_{\substack{k=1 \\ k \text{ odd}}}^{M-1} \binom{M-1}{k}$$

Now consider the well-known binomial series

$$(a+b)^n = \sum_{k=0}^{n} a^{n-k} b^k \binom{n}{k}$$

Substituting $a = 1$, $b = -1$, and $n = M-1$ one obtains

$$\sum_{k=0}^{M-1} (-1) \binom{n}{k} = 0$$

$$\text{i.e.} \sum_{\substack{k=0 \\ k \text{ even}}}^{M-1} \binom{M-1}{k} - \sum_{\substack{k=1 \\ k \text{ odd}}}^{M-1} \binom{M-1}{k} = 0$$

$$\text{Hence} \sum_{\substack{k=0 \\ k \text{ even}}}^{M-1} \binom{M-1}{k} = \sum_{\substack{k=1 \\ k \text{ odd}}}^{M-1} \binom{M-1}{k}$$

But $\sum_{\substack{k=0 \\ k \text{ even}}}^{M-1} \binom{M-1}{k} + \sum_{\substack{k=1 \\ k \text{ odd}}}^{M-1} \binom{M-1}{k} = \sum_{k=0}^{M-1} \binom{M-1}{k} = 2^{M-1}$

$\therefore \sum_{\substack{k=1 \\ k \text{ odd}}}^{M-1} \binom{M-1}{k} = \frac{1}{2} \sum_{k=0}^{M-1} \binom{M-1}{k} = 2^{M-2}$

or $-\sum_{\substack{k=1 \\ k \text{ odd}}}^{M-1} \binom{M-1}{k} = -2^{M-1}$. Therefore ($\xi$) holds true.

REFERENCES

[1] S.W. Golomb et al., Digital Communications with Space Applications, Prentice-Hall, Inc., Englewood Cliffs, N.J., 1964.

[2] J.J. Spilker, Jr., Digital Communications by Satellite, Prentice-Hall, Inc., Englewood Cliffs, N.J., 1977.

[3] K. Feher, Digital Modulation Techniques in an Interference Environment, Vol. IX EMC Encyclopedia, Don White Consultants, Inc., Germantown, Md., 1977.

[4] W.R. Bennett and J.R. Davey, Data Transmission, McGraw-Hill Book Company, New York, 1965.

[5] A Lender, "The duobinary technique for high-speed data transmission," IEEE Trans. Commun. Electron., Vol. 82, p. 214-218, May 1963.

[6] _____, "Correlative digital communication techniques," IEEE Trans. Commun. Technol. Vol. COM-12, p. 128-135, Dec. 1964.

[7] E.R. Kretzmer, "Binary data communication by partial response transmission," Conf. Rec. 1965 IEEE Ann. Communications Conv., p. 451-455.

[8] _____, "Generalization of a technique for binary data communication," IEEE Trans. Commun. Technol., Vol. COM-14, p. 67-68, Feb., 1966.

[9] A.M. Gerrish and R.D. Howson, "Multilevel partial-response signalling," Conf. Rec., IEEE ICC-67, p. 186, Minneapolis, June 1967.

[10] J.W. Smith, "Error control in duobinary data systems by means of null zone detection," IEEE Trans. Commun. Technol., Vol. COM-16, p. 825-830, Dec. 1968.

[11] H. Kobayashi and D.T. Tang, "On decoding of correlative level coding systems with ambiguity zone detection," IEEE Trans. Commun. Technol., Vol. COM-19, p. 467-477, Aug. 1971.

[12] H. Kobayashi, "Correlative level coding and maximum-likelihood decoding," IEEE Trans. Inform. Theory, Vol. IT-17, p. 586-594, Sept. 1971.

[13] C.D. Forney, "Maximum-likelihood sequence estimation of digital sequences in the presence of intersymbol interference," IEEE Trans. Inform. Theory, Vol. IT-18, p. 363-378, May 1972.

[14] H. Harashima and H. Miyakawa, "Matched-transmission technique for channels with intersymbol interference," IEEE Trans. Commun., Vol. COM-20, p. 744-780, Aug. 1972.

[15] P. Kabal and S. Pasupathy, "Partial-response signalling," IEEE Trans. Commun., Vol. COM-23, p. 921-934, Sept. 1975.

[16] H. Kobayashi and D.T. Tang, "Application of partial-response channel coding to magnetic recording systems'" IBM J. Res. Dev., Vol. 14, p. 368-375, July 1970.

[17] R.W. Lucky, J. Salz, and E.J. Weldon, Jr., Principles of Data Communications, McGraw-Hill Book Company, New York, 1968.

[18] A. Lender, "Correlative level coding for binary-data transmission," IEEE Spectrum, Vol. 3., p. 104-115, Feb. 1966.

[19] H. Nyquist, "Certain topics in telegraph transmission theory," Trans. AIEE, Vol. 47, p. 617-644, Apr. 1928.

[20] A. Lender, "Seven level correlative digital transmission over radio," IEEE ICC-76, p. 18-22 - 18-26, Philadelphia, June 1976.

[21] _____, "A synchronous signal with dual properties for digital communications," IEEE Trans. Commun. Technol., Vol. COM-13, p. 202-208, June 1965.

[22] T.L. Swartz, "Performance analysis of a three-level modified duobinary digital FM microwave radio system," IEEE ICC-74, p. 50-1 - 50-4, Minneapolis, June 1974.

[23] R.D. Howson, "An analysis of the capabilities of polybinary data transmission," IEEE Trans. Commun. Technol., Vol. COM-13, p. 312-319, Sept. 1965.

[24] A Lender, "Nonbinary correlative techniques for high speed data transmission," NEREM Record 1968, Vol. 1, p. 190-191, Nov. 1968.

[25] G.J. Garrison, "A power spectral density analysis for digital FM," IEEE Trans. Commun., Vol. COM-23, p. 1228-1243, Nov. 1975.

[26] K.L. Seastrand and L.L. Sheets, "Digital transmission over analog microwave systems," Conf. Rec. IEEE ICC-72, p. 29-1 - 29-5, Philadelphia, June 1972.

[27] J.F. Gunn and J.A. Lombardi, "Error detection for partial-response systems," IEEE Trans. Commun. Technol., Vol. COM-17, p. 734-737, Dec. 1969.

[28] D.W. Jurling and A.L. Pachynski Jr., "Duobinary PCM system doubles capacity of T1 facilities," IEEE ICC-77, p. 32.2-297-32.2-301, Chicago, June 1977.

[29] H.W. Cheung, K.T. Tanaka, and J.A. Thomas, "48 channel duobinary PCM repeater," IEEE ICC-77, p. 32.3-302-32.3-305, Chicago, June 1977.

[30] A. Lender and V. Stalick, "Engineering of the duobinary repeatered line," IEEE ICC-77, p. 32.4-306-32.4-309, Chicago, June 1977.

[31] A. Lender, "Correlative data transmission with coherent recovery using absolute reference," IEEE Trans. Comm. Techn., Vol. COM-16, No. 1, p. 108-115, Feb. 1968.

[32] F.K. Becker, E.R. Kretzmer, and J.R. Sheehan, "A new signal format for efficient data transmission," NEREM Record 1966, Vol. 8, p. 240-241, Nov. 1966.

[33] A Lender, A. Rogers and H. Olszanski, "4 bits per hertz correlative single-sideband digital radio at 2 GHz," IEEE ICC-79, Boston, June 1979.

[34] W.J. Melvin and R.W. Middlestead, "Power density spectrum of m-ary correlative encoded MSK," IEEE ICC-77, p. 3.7-60-3.7-63, Chicgo, June 1977.

[35] Avantek, "Data Sheet, ADS-1141-11-76."

[36] H. Kurematsu, K. Ogawa, and T. Katoh, "The QAM2G-10R digital radio equipment using a partial-response system," FUJITSU Sci. & Tech. J., p. 27-48, June 1977.

[37] R.H. Rearwin and M. Crandall, "Field performance of a 79 Mb/s, 11 GHz system," IEEE ICC-75, p. 21-10 - 21-14, San Francisco, June 1975.

[38] S.C. Barber and C.W. Anderson, "Modulation considerations for the DRS-8 91 Mb/s digital radio," IEEE ICC-77, p. 5.6-111-5.6-115, Chicago, June 1977.

[39] B. Godfrey, Q. Chow, and F. Halsey, "Practical considerations in the design of the DRS-8 system," IEEE ICC-77, p. 5.5-106-5.5-110, Chicago, June 1977.

[40] Y. Tan, et al., "The 8-level PSK modem with cosine roll-off spectrum for digital microwave communications," IEEE ICC-76, p. 29-13 - 29-18, Philadelphia, June 1976.

[41] K. Feher, M. Wachira, H. Yazdani, and W. Steenaart, "Bandwidth efficient 90 Mb/s digital radio systems," Proceedings of the INTELCOM-79, Dallas, Texas, Feb. 1979.

[42] M. Ramadan, "Practical considerations in the design of minimum bandwidth, 90 Mb/s, 8-PSK digital microwave systems," IEEE ICC-76, p. 29-1 - 29-6, Philadelphia, June 1976.

[43] W.A. Wood, "Modulation and filtering techniques for 3 bits/hertz operation in the 6 GHz frequency band," IEEE ICC-77, p. 5.3-97 - 5.3-101, Chicago, June 1977.

[44] C.R. Cahn, "Combined digital phase and amplitude modulation communication systems," IRE Trans. Commun. Systems, Vol. CS-8, p. 150-155, Sept. 1960.

[45] M. Wachira, H. Yazdani, K. Feher, and W. Steenaart, "A survey of eight-phase PSK and QPRS digital radio systems," Proceedings of the 1978 IEEE Canadian Communications and Power Conference, Montreal, Oct. 1978.

[46] S. Yokoyama, et al., "An eight-level PSK microwave radio for long-haul data communications," IEEE ICC-75, p. 21-15 - 21-19, San Francisco, June 1975.

[47] E. Takeuchi and P. Tobey, "A 6 GHz radio for telephony applications," IEEE ICC-76, p. 18-27 - 18-32, Philadelphia, June 1976.

[48] P.R. Hartmann and J.A. Crossett, "A 90 Mb/s digital transmission system at 11 GHz using 8-PSK Modulation," IEEE ICC-76, p. 18-8 - 18-13, Philadelphia, June 1975.

[49] R.J. Tracey, "A 90 megabit per second modem for microwave radio links," IEEE ICC-77, Chicago, June 1977.

[50] P.R. Hartmann and E.W. Allen, "Design considerations for a 3 bit/hertz digital radio at 6 GHz," IEEE ICC-78, p. 33.1.1 - 33.1.3, Toronto, June 1978.

[51] J. Huang and K. Feher, "On partial response transmission systems," IEEE ICC-77, p. 3.3-47 - 3.3-51, Chicago, June 1977.

[52] S.U.H. Qureshi and E.E. Newhall, "An adaptive receiver for data transmission over time-dispersive channels," IEEE Trans. Inform. Theory, vol. IT-19, p. 448-457, July 1973.

[53] M. Wachira, K. Feher, and W. Steenaart, "Noise and interference in partial-response systems," 9th Biennial Conference on Communications, Kingston, Ont., Aug. 1978.

[54] A. Papoulis, Probability, Random Variables, and Stochastic Processes, McGraw-Hill Book Company, New York, 1965.

[55] C. Anderson, and S. Barber, "Modulation Considerations for a 91 Mbit/s Digital Radio," IEEE Trans. Commun., Vol. COM-26, p. 523-527, May 1978.

VITAE

NAME: Mūriūki Muya Wachira

DATE OF BIRTH: July 12, 1951

PLACE OF BIRTH: Nyeri, Kenya

EDUCATION: University of Cambridge

Advanced Level H.S.C. 1970

Thika High School, Thika, Kenya

B.A.Sc. (Elect. Eng.)
(Summa Cum Laude)
May 1975

University of Ottawa,

OTTAWA, Ontario, Canada.